UNIVERSITA' DEGLI STUDI

DI MODENA E REGGIO EMILIA

International Doctorate School in Clinical and Experimental Medicine (CEM)

Cycle XXXII

AUTOFLUORESCENCE SPECTROPHOTOMETRIC QUANTIFICATION AS POTENTIAL DIAGNOSTIC TOOL FOR MALIGNANT LESIONS OF SKIN AND ORAL MUCOSA

Candidate: **Ilaria Giovannacci**

Tutor: **Prof.ssa Cristina Magnoni**

Co-tutor: **Prof. Marco Meleti**

PhD Program Coordinator: **Prof. Giuseppe Biagini**

Table of contents

List of abbreviations

AF: autofluorescence

AGEs: advanced glycation end products

BCC: basal cell carcinoma

CEBM: centre for evidence-based medicine

COE: conventional oral examination

cSCC: cutaneous squamous cell carcinoma

DB: data-base

DRS: diffused reflectance spectroscopy

FAD: flavin adenine dinucleotide

H&E: hematoxylin and eosin

HW: hardware

ID: unique identifier

laBCC: locally advanced BCC

LAF: loss of autofluorescence

LED: light emitting diode

LIF: light-induced fluorescence

MAV: mean area of blood vessels

mBCC: metastatic BCC

MCS: micrographically controlled surgery

MDI: mean depth of inflammatory infiltrate

MDV: mean diameter of blood vessels

MLT: multiphoton laser tomography

MMS: Moh's microsurgery

MWE: mean width of the entire epithelium

MWK: mean width of the keratin layer

NADH: nicotinamide adenine dinucleotide

NADPH: nicotinamide adenine dinucleotide phosphate

NIH: national institutes of health

NMSC: non-melanoma skin cancer

NPV: negative prognostic value

OAE: overall area of the epithelium

OAV: overall area of blood vessels

OCT: optical coherence tomography

OED: oral epithelial dysplasia

OFI: optical fluorescence imaging

OPMD: oral potentially malignant disorders

OSCC: oral squamous cell carcinoma

PNI: perineural invasion

PpIX: protoporphyrin IX

PPV: positive prognostic value

PRISMA: preferred reporting Items for systematic reviews and meta-analysis

sBCC: superficial BCC

SCC: squamous cell carcinoma

SD: standard deviation

SW: software application

TNM: tumor-node-metastasis

UV: ultra-violet

VC: verrucous carcinoma

WHO: world health organization

List of Figures

List of tables

Abstract

Autofluorescence (AF) is defined as an emission of light by some tissues, associated with the concentration and distribution of specific fluorophores, so molecules that can absorb and re-emit light of specific wavelengths.

Cells and extracellular compartments within dysplastic and malignant lesions may display modifications of the amount, distribution and chemical–physical properties of some endogenous fluorophores. Malignant and potentially malignant changes may therefore result in AF variations, potentially useful for diagnostic purposes.

AF evaluation might improve sensitivity and specificity of cancer diagnosis and it has been tested on several organs, such as colon, lung, cervix and oesophagus. Evidences have recently emerged, supporting the usefulness of AF for head and neck cancer diagnosis, both at mucosal and cutaneous level.

The aim of this research program was to study the efficacy of AF in identifying malignant and pre-malignant lesions of the oral mucosa and skin. In the first studies the tissue AF was studied using the VELscope ® system (LED Medical Diagnostics Inc., Barnaby, Canada) from a qualitative point of view, while in the last study carried out *ex vivo* on the non-melanoma skin cancers (NMSCs) an experimental setup was developed in order to evaluate the fluorescence in a quantitative and objective way.

The studies that were carried out are during the research program are the following:

- A systematic review was performed with the aim of identifying which molecules show evidence of being the main fluorophores in skin and oral mucosa, together with their excitation and emission wavelengths and the devices used for inducing fluorescence, as well as a discussion of clinical applications of AF.
- A clinical trial (ethical committee code: FLISTO - n°46556/17) was developed in order to describe the most relevant clinicopathological features associated with

AF alteration in a cohort of patients with oral squamocellular carcinoma and potentially malignant oral disorders (SCC and PMODs). Lesions included in this study were 108. For each case, the following variables were recorded and compared to the AF pattern: a) Clinical appearance (white, red and white/red); b) Histological diagnosis (no dysplasia, mild/moderate dysplasia, severe dysplasia/in situ carcinoma, invasive carcinoma and verrucous carcinoma) and c) Clinicopathological diagnosis. Binomial logistic regression was performed to investigate whether clinical appearance and/or histological diagnosis were significant in determining the degree of AF.

- A histopathological study (ethical committee code: FLISTO - n°46556/17) was carried out in order to identify which are the main histopathological features possibly related to variations of AF patterns in a set of oral SCC and verrucous carcinoma (VC). Twenty oral lesions (SCC or VC) were evaluated. AF features were compared to 8 histologic categories, including a) width of the epithelium; b) width of the keratin layer; c) width of the epithelium without keratin; d) overall area of the epithelium; e) depth of inflammatory infiltrate and f) area of blood vessels.
- A pre-clinical *ex vivo* study (ethical committee code: 1167.2018) was performed in order to investigate the correlation between the intensity of cutaneous AF and the histopathological characteristics of malignant and potentially malignant lesions of the skin included the group of NMSC. An experimental spectrophotometric setup was developed to evaluate the intensity of fluorescence in a quantitative and objective way. The fluorescence intensity was compared with different histopathological variables (diagnosis, hyperkeratosis, epithelial thickening, fibrosis, elastosis, neovascularization and cellular atypia) in order to identify which were most relevant in influencing the fluorescence pattern of the lesion and to establish the histopathological basis of skin fluorescence.

Abstract italiano

L'autofluorescenza (AF) è definita come un'emissione di luce da parte di alcuni tessuti, associata alla concentrazione e distribuzione di fluorofori specifici, quindi molecole in grado di assorbire e riemettere luce di lunghezze d'onda specifiche.

Le cellule e i compartimenti extracellulari all'interno di lesioni displastiche e maligne possono mostrare modifiche della quantità, della distribuzione e delle proprietà chimico-fisiche di alcuni fluorofori endogeni. Lesioni maligne e potenzialmente maligne possono quindi comportare variazioni dell'AF, potenzialmente utili a fini diagnostici.

La valutazione dell'AF potrebbe migliorare la sensibilità e la specificità della diagnosi del cancro ed è stata testata su diversi organi, come colon, polmone, cervice ed esofago. Recentemente sono emerse prove a supporto dell'utilità dell'AF per la diagnosi dei tumori del distretto testa-collo, sia a livello mucoso che cutaneo.

Lo scopo di questo programma di ricerca è stato quello di studiare l'efficacia dell'AF nell'identificazione di lesioni maligne e pre-maligne della mucosa orale e della cute. Nei primi studi esposti l'AF tissutale è stata studiata utilizzando il sistema VELscope ® (LED Medical Diagnostics Inc., Barnaby, Canada) da un punto di vista qualitativo, mentre nell'ultimo studio, condotto ex vivo sui tumori cutanei diversi dal melanoma (NMSC), è stata sviluppato un setup sperimentale per valutare la fluorescenza in modo quantitativo e oggettivo.

Gli studi effettuati durante questo programma di ricerca sono i seguenti:

- È stata eseguita una revisione sistematica allo scopo di identificare quali molecole mostrano evidenza di essere i principali fluorofori della cute e delle mucose orali, insieme alle loro lunghezze d'onda di eccitazione ed emissione e ai dispositivi utilizzati per indurre la fluorescenza, nonché una discussione delle applicazioni cliniche dell'AF.

- È stato sviluppato un trial clinico (codice comitato etico: FLISTO - n ° 46556/17) al fine di descrivere le caratteristiche clinicopatologiche più rilevanti associate

all'alterazione dell'AF in una coorte di pazienti con carcinoma squamocellulare orale e lesioni orali potenzialmente maligne (SCC e PMODs). Le lesioni incluse in questo studio erano 108. Per ogni caso, le seguenti variabili sono state registrate e confrontate con il pattern di AF: a) aspetto clinico (bianco, rosso e bianco/rosso); b) Diagnosi istologica (nessuna displasia, displasia lieve/moderata, displasia grave/carcinoma in situ, carcinoma invasivo e carcinoma verrucoso) e c) Diagnosi clinicopatologica. Una regressione logistica binomiale è stata eseguita per capire se l'aspetto clinico e/o la diagnosi istologica erano significativi nel determinare il grado di AF.

- È stato condotto uno studio istopatologico (codice comitato etico: FLISTO - n ° 46556/17) al fine di identificare quali sono le principali caratteristiche istopatologiche possibilmente correlate alle variazioni dei pattern di AF in un gruppo di SCCs orali e carcinomi verrucosi (VC). Sono state valutate 20 lesioni orali (SCC o VC). Le caratteristiche dell'AF sono state confrontate con 8 categorie istologiche, tra cui a) profondità dell'epitelio; b) profondità dello strato di cheratina; c) profondità dell'epitelio senza cheratina; d) area complessiva dell'epitelio; e) profondità dell'infiltrato infiammatorio e f) area dei vasi sanguigni.

- È stato condotto uno studio preclinico *ex vivo* (codice del comitato etico: 1167.2018) al fine di studiare la correlazione tra l'intensità dell'AF cutanea e le caratteristiche istopatologiche delle lesioni maligne e potenzialmente maligne della cute incluse nel gruppo dei NMSC. È stato messo a punto un setup sperimentale spettrofotometrico per valutare l'intensità della fluorescenza in modo quantitativo e oggettivo. L'intensità della fluorescenza è stata confrontata con diverse variabili istopatologiche (diagnosi, ipercheratosi, ispessimento epiteliale, fibrosi, elastosi, neovascolarizzazione e atipia cellulare) al fine di identificare quali erano più rilevanti nell'influenzare il modello di fluorescenza della lesione e stabilire le basi istopatologiche della fluorescenza cutanea.

1 Physical and biological bases of fluorescence

1.1 Phenomena of fluorescence

Luminescence is the emission of light from any substance, and occurs from electronically excited states. Luminescence is formally divided into two categories—**fluorescence** and **phosphorescence**, depending on the nature of the excited state.

For a long time after the introduction of the term fluorescence by G. G. Stokes in the middle of the 19th century, the distinction between fluorescence and phosphorescence was based on the duration of emission after the end of excitation: fluorescence was considered as an emission of light that disappears simultaneously with the end of excitation, whereas in phosphorescence, the emitted light persists after the end of excitation (Stokes, 1852). But this criterion is insufficient because there are long-lived fluorescences (e.g., divalent europium salts) and short-lived phosphorescences (e.g., violet luminescence of zinc sulfide) whose durations are comparable (several hundreds of nanoseconds). The usual condition for observing phosphorescence is that the excited species passes through an intermediate state before emission, as stated for the first time by Francis Perrin in 1929 (Perrin, 1929). More precisely, in the frame of molecular photochemistry, we now say that the spin multiplicity is retained in the case of fluorescence, whereas phosphorescence involves a change in spin multiplicity, typically from triplet to singlet or *vice versa* (Figure 1.1) (Valeur & Berberan-Santos, 2011).

An important feature of fluorescence is high sensitivity detection. The sensitivity of fluorescence was used in 1877 to demonstrate that the rivers Danube and Rhine were connected by underground streams. This connection was demonstrated by placing 10 kg of fluorescein into the Danube. Some sixty hours later its characteristic green

fluorescence appeared in a small river that led to the Rhine (Figure 1.2). Nowadays, fluorescence tracing is currently used in hydrogeology, especially to simulate and trace the discharge of pollutants.

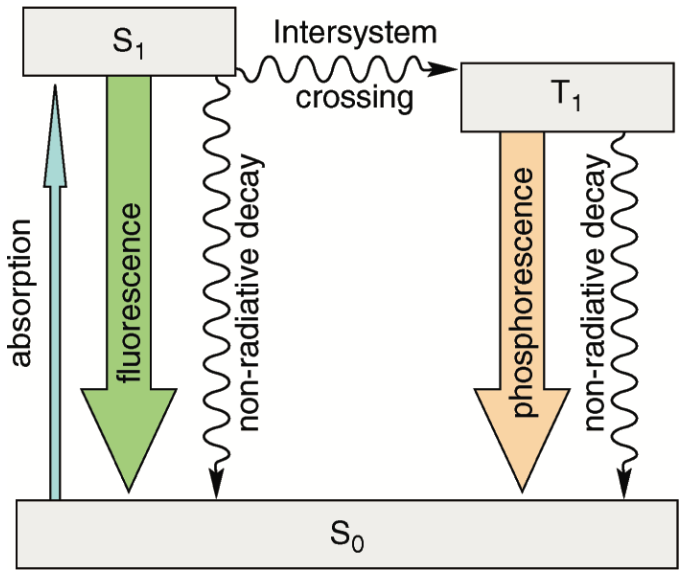

Figure 1.1 Simplified Perrin Jablonski diagram showing the difference between fluorescence and phosphorescence. Fluorescence occurs when radiation is emitted from the first excited singlet state S_1 that is reached by previous absorption of a photon. Phosphorescence occurs when radiation is emitted from the triplet state T_1 after intersystem crossing from S_1. (Valeur & Berberan-Santos, 2011)

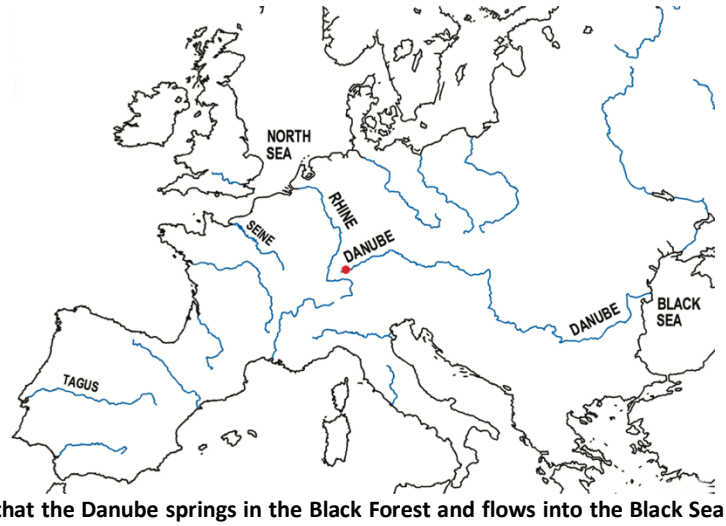

Figure 1.2 Map showing that the Danube springs in the Black Forest and flows into the Black Sea. By means of uranin as a fluorescent tracer, it was demonstrated that most of the spring water flows into the North Sea. The red point indicates the location of Immendingen. (Valeur & Berberan-Santos, 2011)

1.2 History of fluorescence

Nicolás Monardes, a Spanish physician and botanist publishes in 1565 the *Historia medicinal de las cosas que se traen de nuestras Indias Occidentales* in which he describes the bluish opalescence of the water infusion from the wood of a small Mexican tree (Figure 1.3). This wood (later called *Lignum nephriticum*), whose peculiar color effect and diuretic properties were already known to the Aztecs, was a scarce and expensive medicine. This detection could be considered as the first observation of the phenomenon that would be later called fluorescence. Extracts of the wood were further investigated by Boyle, Newton, and others, but the phenomenon was not understood at the time (Figure 1.4). The chemical species responsible for the intense blue fluorescence was recently identified in an infusion of *L. nephriticum* (*E. polystachya*): it is called *matlaline* (from Matlali, the Aztec word for blue). This compound is not present in the plant but results from an unusual spontaneous oxidation of at least one of the tree's flavonoids (Valeur & Berberan-Santos, 2011).

Figure 1.3 Portrait of Nicol as Monardes. From the front page of the book Dos Libros, el Vno Qve Trata de Todas las Cosas que traen de nuestras Indias Occidentales, que siruen al vso de la Medicina, y el otro qve trata de la Piedra Bezaar, y de la Yerva Escuer-conera, Seville, Spain, 1569.

Figure 1.4 *Lignum nephriticum* cup of made from the wood of the narra tree (*Pterocarpus indicus*), and a flask containing its fluorescent solution. Safford, William Edwin (1916). "Lignum nephriticum". Annual report of the Board of Regents of the Smithsonian Institution. Washington: Government Printing Office. p. 271–298.

Robert Boyle in 1664 was inspired by Monardes' report and investigated this system more fully. He discovered that after many infusions the wood lost its power to give colour to the water and concluded that there was some "essential salt" in the wood responsible for the effect. He also discovered that addition of acid abolished the colour and that addition of alkali brought it back.

In 1819, a peculiar property of some crystals of fluorite (calcium fluoride, then called fluated lime, spath fluor, or fluor spar) from Weardale, Durham, England, was reported by Edward D. Clarke, Professor of Mineralogy at the University of Cambridge (Clarke, 1819).

In 1833, David Brewster, the well-known Scottish physicist, described the beautiful red fluorescence of chlorophyll in the article "On the Colour of Natural Bodies", where it is reported that a beam of sunlight passing through a green alcoholic extract of leaves (mainly a chlorophyll solution) appears to be red when observed from the side. He pointed out the similarity with the blue light coming from a light beam when entering some fluorite crystals (Brewster, 1834).

In 1845 John Herschel (Figure 1.5) made the first observation of fluorescence from quinine sulfate and he termed this phenomenon "epipolic dispersion". He prepared an acid solution of quinine sulfate and stated (Herschel, 1845):

"*Though perfectly transparent and colorless when held between the eye and the light, it yet exhibits in certain aspects, and under certain incidences of the light, an extremely vivid and beautiful celestial blue color*"

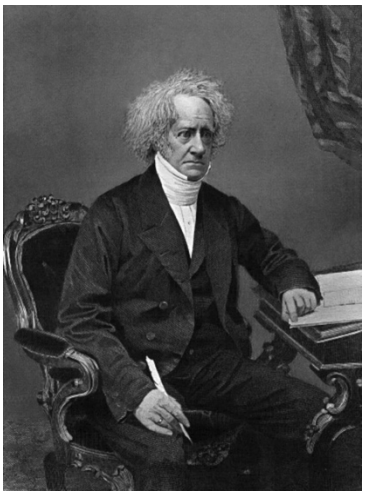

Figure 1.5 Portrait of John Frederick William Herschel (1792-1871)

1.2.1 The origin of the word "fluorescence"

Sir George Gabriel Stokes (Figure 1.6), physicist and professor of mathematics at Cambridge, published in 1852 his famous paper entitled "On the Refrangibility of Light" (Stokes, 1852). He reported detailed experimental studies on several samples, both organic (e.g. quinine) and inorganic (e.g. fluorite crystal), in which was identified a common phenomenon he called "*dispersive reflection*": the wavelengths of the dispersed light are always longer than the wavelength of the original light (Valeur & Berberan-Santos, 2011).

In particular, Stokes used a prism to disperse the solar spectrum and illuminate a solution of quinine. He noted that there was no effect until the solution was placed in the ultraviolet region of the spectrum (Figure 1.7). This observation led Stokes to proclaim that fluorescence is of longer wavelength than the exciting light, which led to this displacement being called the *Stokes Shift*.

He wrote:

"*I confess that I do not like this term. I am almost inclined to coin a word, and call the appearance* ***fluorescence****, from fluor-spar, as the analogous term opalescence is derived from the name of a mineral*."

However, 10 years before Stokes's first paper, the French physicist Edmond Becquerel (Figure 1.6) published an original paper in which he described the emission of light by calcium sulfide deposited on paper when exposed to solar light beyond the violet part of the spectrum. Therefore, he was the first to state that the emitted light is of longer wavelength than the incident light. Stokes's paper led Becquerel to a priority claim for this result. The difference between the Stokes and Becquerel experiments is that, according to the definitions given in the preceding section, quinine is fluorescent whereas calcium sulfide is phosphorescent, but both species are relevant to photoluminescence (Becquerel, 1867) (Valeur & Berberan-Santos, 2011).

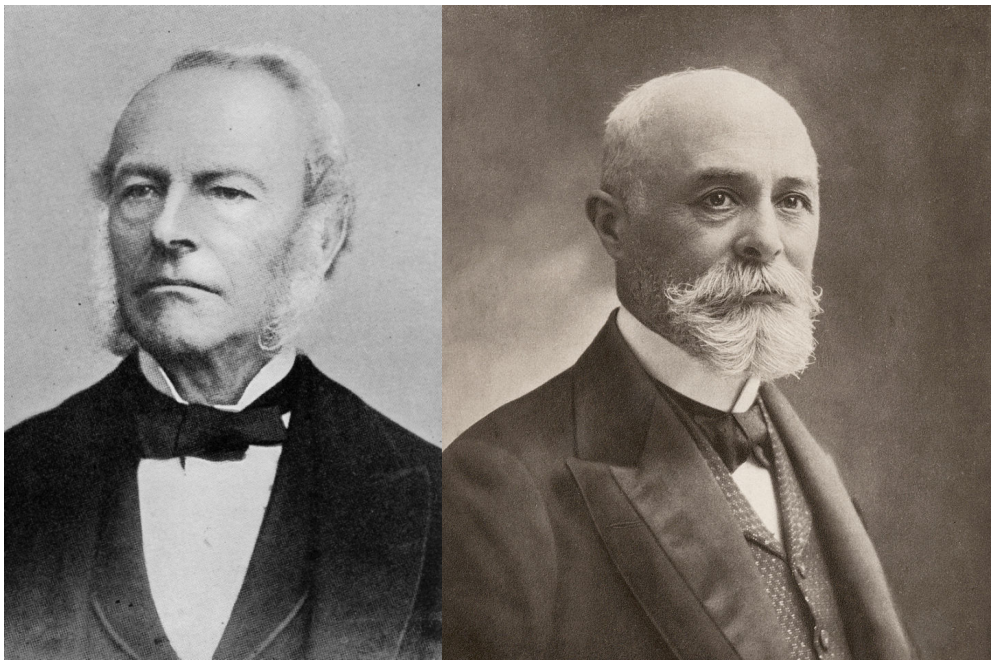

Figure 1.6 Left: Portrait of George Gabriel Strokes (Skreen 1819 – Cambridge 1903) – Right: Portrait of Antoine Henri Becquerel (Paris 1852 – La Croisic 1908)

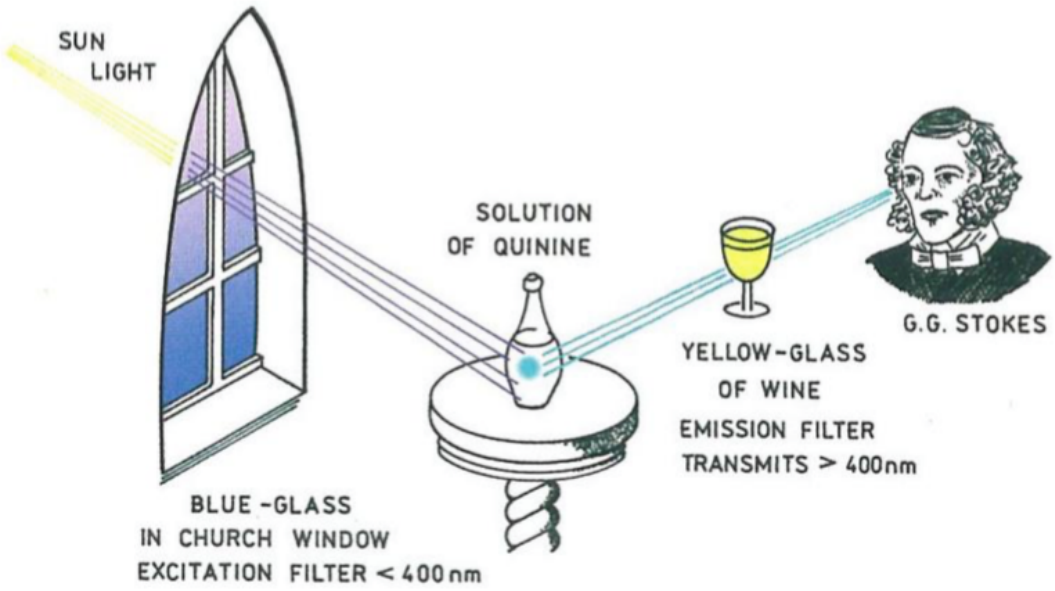

Figure 1.7 Experimental set-up used by GG Stokes (Lakowicz, 1999).

1.3 Jablonski diagram

Aleksander Jablonski was a Polish academic who devoted his life to the study of molecular absorbance and emission of light. He developed a written representation (Jablonski diagram) that generally shows a portion of the possible consequences of applying photons from the visible spectrum of light to a molecule.

A typical Jablonski diagram is shown in Figure 1.8. The singlet ground, first, and second electronic states are depicted by S_0, S_1, and S_2, respectively. At each of these electronic energy levels the fluorophores can exist in a number of vibrational energy levels, depicted by 0, 1, 2, etc. The transitions between states are depicted as vertical lines. Transitions occur in about 10^{-15} s, a time too short for significant displacement of nuclei. This is the Franck-Condon principle (Lakowicz, 1999).

Following light absorption, several processes usually occur. A fluorophore is usually excited to some higher vibrational level of either S_1 or S_2. With a few rare exceptions, molecules in condensed phases rapidly relax to the lowest vibrational level of S1. This process is called *internal conversion* and generally occurs within 10^{-12} s or less. Since fluorescence lifetimes are typically near 10^{-8} s, internal conversion is generally

complete prior to emission. Hence, fluorescence emission generally results from a thermally equilibrated excited state, that is, the lowest energy vibrational state of S_1 (Lakowicz, 1999).

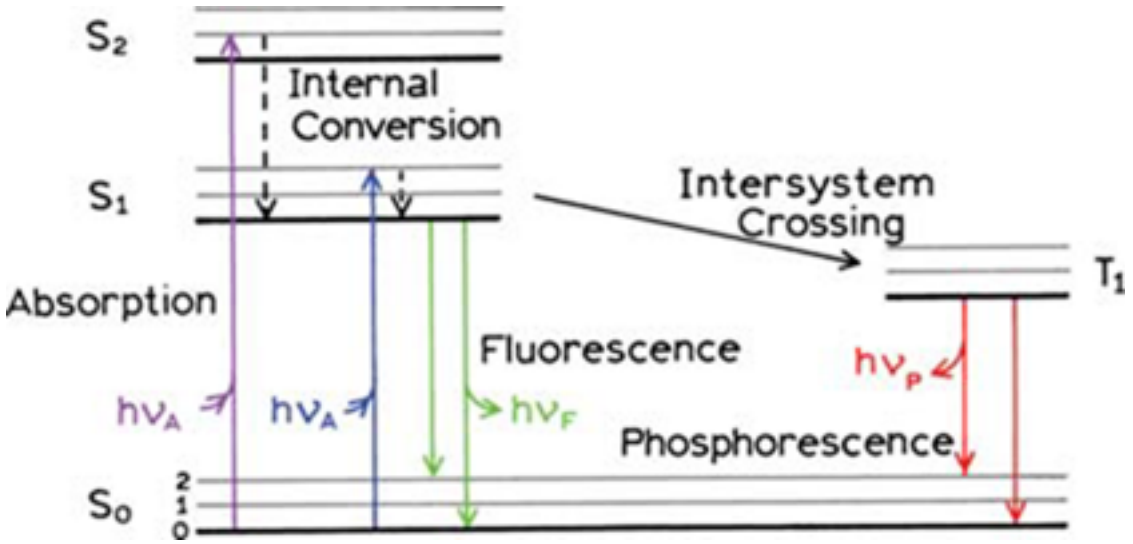

Figure 1.8 Jablonski diagram (adapted from J. R. Lakowicz, Principles of Fluorescence Spectroscopy, 3rd Ed., Springer, 2006)

Molecules in the S_1 state can also undergo a spin conversion to the first triplet state T_1. Emission from T_1 is termed **phosphorescence** and is generally shifted to longer wavelengths (lower energy) relative to the fluorescence. Conversion of S_1 to T_1 is called *intersystem crossing*. Transition from T_1 to the singlet ground state is forbidden, and as a result the rate constants for triplet emission are several orders of magnitude smaller than those for fluorescence (Lakowicz, 1999).

1.4 Excitation and emission spectra

All fluorescent molecules can be characterized by two types of spectra: the **excitation spectrum** and the **emission spectrum**. The excitation spectrum is a plot of emitted fluorescence as a function of the excitation wavelength at a fixed emission wavelength. The excitation spectrum represents the relative probability that a fluorescent molecule will be excited by a given wavelength of incident light. If the excitation energy is constant, the fluorescence excitation spectrum is very similar to the **absorption spectrum**. The photon energy at the maximum of the excitation peak

equals the energy difference between the ground state (S_0) and a favored vibrational level of the first excited state (S_1) of the molecule.

In some cases, the excitation spectrum shows a second peak at a shorter wavelength (higher energy) that indicates transition of the molecule from the ground state to the second excited state (S_2) (Fig. 1.9) (Díaz-García & Badía-Laíño, 2019).

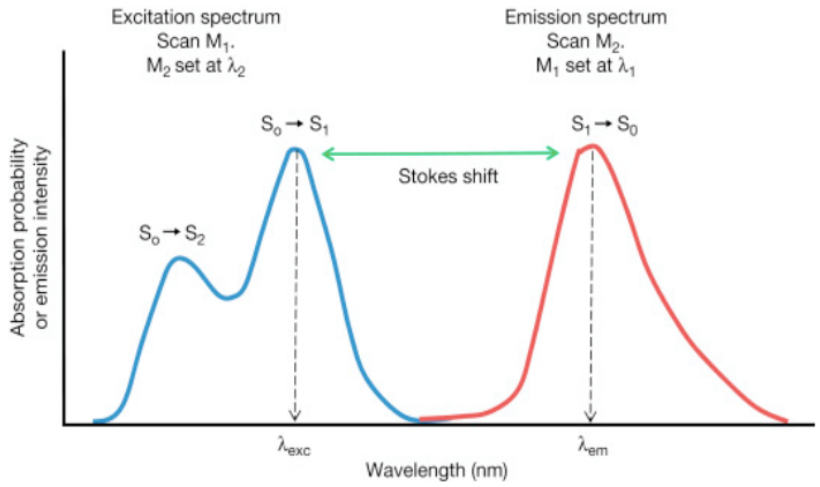

Figure 1.9 Features of excitation and emission fluorescence spectra (Díaz-García & Badía-Laíño, 2019)

A plot of the relative intensity of emitted light as a function of the emission wavelength at a fixed excitation wavelength is termed **fluorescence emission spectrum**. The fluorescence emission is characterized by the transition from the lowest vibrational mode of the electronically excited state (S1) to the ground state. Therefore, **the shape of the emission spectrum is always the same and is independent of the wavelength of the exciting radiation**.

The shape of the emission spectrum is approximately a mirror image of the longest-wavelength excitation band. The emission spectrum is always shifted toward a longer wavelength relative to the excitation spectrum, as shown in Fig. 1.9. This difference between the excitation and emission maxima is termed the **Stokes shift** and it represents the energy lost whilst the molecule was in the excited state. From a practical point of view, Stokes shift allows the excitation and emission peaks to be spectrally separated and easily distinguished.

The emission wavelength and the fluorescence intensity are determined by the structure of the molecule. In principle, any molecule that absorbs radiation of adequate energy could fluoresce. However, many molecules exhibit very weak fluorescence and only a small fraction of molecules exhibit analytically useful fluorescence (Díaz-García & Badía-Laíño, 2019).

The quantification of the emissivity of a sample is far from trivial. The area underneath the emission band is proportional to the number of emitted photons, but also to the intensity of the excitation light, to the absorbance of the sample at the excitation wavelength, as well as it depends on the sensitivity of the detecting system. To quantify the fluorescence capability, the fluorescence quantum yield is introduced, defined as the fraction of emitted photon per each absorbed photon. Its determination can be done in an absolute way, with an integrating sphere, or in a relative way, through the use of fluorescence standards.

In this thesis, the fluorescence quantum yield was not determined, yet the emission intensities can be compared with each other since all the emission spectra were obtained using a single setup, configured as to always deliver the same excitation intensity, illuminating the sample and collecting the emitted light from a fixed distance and orientation.

2 Fluorophores of skin and oral mucosa: systematic review of the literature

2.1 Background

Fluorophores are molecules that can absorb and re-emit light of specific wavelengths and are therefore responsible for the phenomenon of fluorescence.

Fluorophores can be classified into endogenous, when produced within the body, and exogenous, if they originate from outside the organism. Endogenous fluorophores are either intracellular or extracellular, both the cause of biological tissue autofluorescence (AF). AF is defined as a peculiar visual property of some tissues directly associated with the concentration and distribution of specific fluorophores.

Cells and extracellular compartments within dysplastic and malignant lesions may display modifications of the amount, distribution and physicochemical properties of some endogenous fluorophores (Monici, 2005). Malignant and potentially malignant changes may therefore result in AF variations, potentially useful for diagnostic purposes.

AF evaluation might improve the sensitivity and specificity of cancer diagnosis, having been tested on several organs, such as colon, lung, cervix and esophagus (Schantz, Savage, Sacks, & Alfano, 1997). Evidence has recently emerged that supports the usefulness of AF for head and neck cancer diagnosis, at both the mucosal and cutaneous levels (Monici, 2005) (Schantz, Savage, Sacks, & Alfano, 1997).

However, even though some fluorophores have been identified and described in detail, there is currently a gap of knowledge about other specific molecules responsible for tissue AF as well as about the mechanisms through which they cease to emit fluorescence in cases of malignant or pre-malignant lesions (Schantz, Savage, Sacks, & Alfano, 1997). (Moher, Liberati, Tetzlaff, & Altman, 2009)

The present review provides information about which molecules show evidence of being the main fluorophores in skin and oral mucosa, together with their absorption and emission wavelengths and the devices used for inducing fluorescence, as well as a discussion of clinical applications of AF.

2.2 Methods for the literature search

The MEDLINE database was searched, using "oral mucosa AND fluorophores", "skin AND fluorophores", "epidermal AND fluorophores", "dermal AND fluorophores" and "cutaneous AND fluorophores" as entry terms.

To avoid accidental loss of relevant studies, we searched the literature following the Preferred Reporting Items for Systematic Reviews and Meta-Analysis (PRISMA) statement published in 2009 (Moher, Liberati, Tetzlaff, & Altman, 2009). (Gurushankar, Nazeer, Jayasree, & Krishnakumar, 2015) (Nazeer, Asish, Venugopal, Anita, & Gupta, 2014) (Vedeswari, Jayachandran, & Ganesan, 2009) (Jayanthi, et al., 2009)

Reference lists of reviews were screened to identify papers potentially not identified in the database search.

Study selection and data extraction

Inclusion criteria

- Papers focused on identification and characterization of endogenous fluorophores, reporting studies performed in *in vivo* (humans, animals), *ex vivo* and *in vitro* models
- No time limits

Exclusion criteria

- Papers with unavailable abstract
- Papers not in English language
- Congress proceedings
- Review papers

- Papers not clearly detailing the fluorophores investigated
- Papers not indicating excitation wavelength used for inducing fluorescence
- Studies evaluating fluorescence induced by exogenous fluorophores

A PRISMA flow diagram was used to summarize the study selection process. The flowchart followed for selection of studies of oral mucosa is shown in Figure 2.1. The flowchart for selection of studies on fluorophores in skin is shown in Figure 2.2

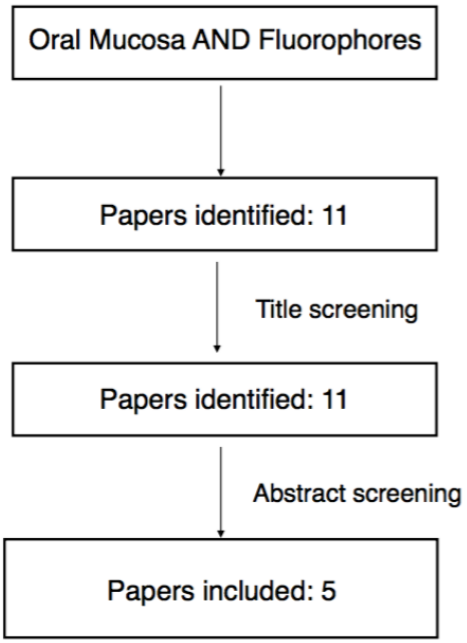

Figure 2.1 Flowchart reporting the selection procedures for papers on oral mucosa.

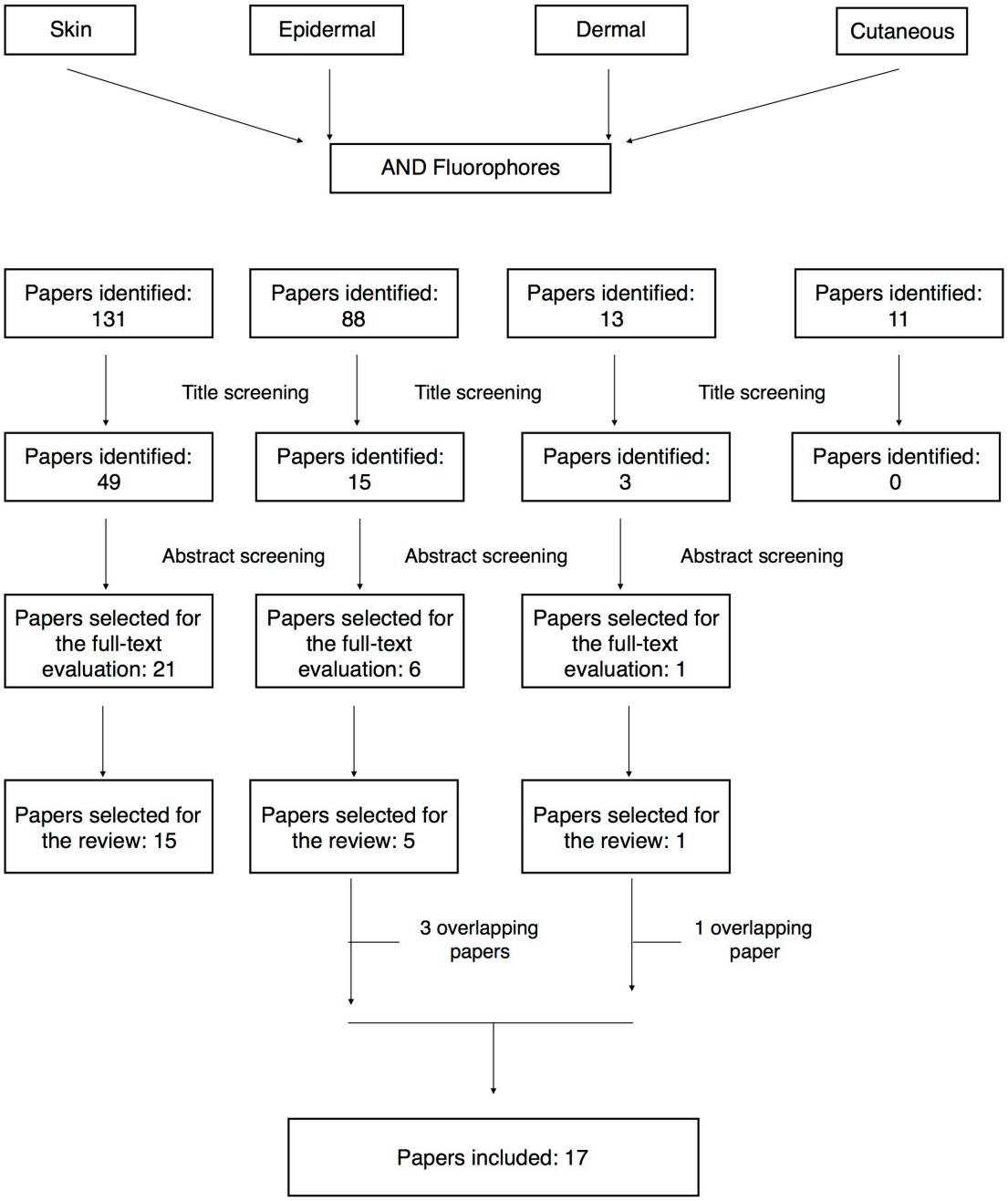

Figure 2.2 Flowchart reporting the selection procedures for papers on skin.

The level of evidence in the studies was assessed using the Classification of the Oxford Centre for Evidence-based Medicine (CEBM) Levels for Diagnosis, updated in March 2009.

2.3 Results regarding oral mucosa

2.3.1 Fluorophores

Five papers evaluating fluorophores in oral mucosa were identified (Figure 3) (Gurushankar, Nazeer, Jayasree, & Krishnakumar, 2015) (Nazeer, Asish, Venugopal, Anita, & Gupta, 2014) (Vedeswari, Jayachandran, & Ganesan, 2009) (Jayanthi, et al., 2009) (Lane, et al., 2006).

Molecules identified as fluorophores of the oral mucosa are: collagen, the reduced form of nicotinamide, adenine dinucleotide (NADH), flavin, adenine dinucleotide (FAD), porphyrins, elastin and keratin. Specific data extracted from each study is shown in Figure 2.3.

Collagen, NADH and FAD were indicated as fluorophores in four studies, porphyrins in two studies and elastin and keratin in one study.

Excitation wavelengths used for the identification of the presumptive fluorophores ranged from 320 to 460 nm (including ultra-violet [UV] radiations). Instead, the emission spectra ranged from 350 to 750 nm.

Author	Year	Type of paper	Fluorophores	Excitation wavelength	Emission wavelength	Device (excitation source)	Application fields or conclusions
K. Gurushankar et al	2015	Animal scientific study (hamster)	- Collagen - nicotinamide adenine dinucleotide (NADH) - flavin adenine dinucleotide (FAD)	320 nm	ranging from 350 to 550 nm	Datamax software (Datamax, Round Rock, Texas) and the inbuilt double-grating monochromator.	Fluorescence spectroscopy for monitoring or potentially predicting response to cancer therapy.
SS. Nazeer et al	2014	Clinical cohort study	- FAD - Porphyrins - Hemoglobin (chromophore)	410 nm	ranging from 450 to 750 nm	Instruments consists of a 450-W Xenon arc lamp, a double excitation monochromator, a double emission monochromator, and a photomultiplier tube.	The study demonstrated a variation in auto-fluorescence spectra from the oral mucosa of habitual tobacco users with that of a group of volunteers without any habits in a clinical setup.
CP. Vedeswari et al	2009	Clinical cohort study	- Collagen - NADH	330 nm	ranging from 350 to 600 nm * emission spectra in normal mucosa different from oral submucous fibrosis and different after treatment	A monochromator with a 150 W ozone-free Xenon lamp	Autofluorescence spectroscopy for monitoring the therapeutic response and characterize the tissue transformation after treatment of oral submucous fibrosis.
JL. Jayanthi et al	2009	Clinical cohort study	- Collagen - NADH - Elastin - Keratin - FAD - Porphyrins	404 nm	- peak in healthy patient: 500 nm - peaks in malignant lesions: 635, 685 and 705 nm	A 404 nm, 50 mW diode laser (Stocker Yale, Montreal, Canada)	Autofluorescence can improve diagnostic accuracy.
PM. Lane et al	2006	Clinical pilot study	- Collagen - NADH - FAD	400-460 nm	> 475 nm	The light source: X-Cite 120, EXFO used a 120-W metal-halide arc lamp with integral elliptical reflector optimized for near- UV/blue reflection.	Direct fluorescence visualization device has potential as a simple, cost-effective screening device for the early detection of oral premalignant lesions.

Figure 2.3 Outline of papers investigating fluorophores in oral mucosa.

2.3.2 Reported clinical applications

Data on clinical applications was available in all five of the studies selected for the present review.

In two studies AF was investigated as a potential aid for improving cancer diagnostic accuracy (excitation wavelength used: 400–460 nm) (Jayanthi, et al., 2009) (Lane, et al., 2006). In one study, AF spectroscopy was used for monitoring the therapeutic response and for characterizing tissue reaction after treatment of oral submucous fibrosis (excitation wavelength used: 330 nm) (Vedeswari, Jayachandran, & Ganesan, 2009). Another study demonstrated a variation in AF spectra between the oral mucosa of habitual tobacco users and the oral mucosa of a group of volunteers without any habits (excitation wavelength used: 410 nm) (Nazeer, Asish, Venugopal, Anita, & Gupta, 2014).

In the only animal study identified, fluorescence spectroscopy was proposed for monitoring or potentially predicting response to cancer therapy (excitation wavelength used: 320 nm) (Gurushankar, Nazeer, Jayasree, & Krishnakumar, 2015).

2.3.3 Level of evidence

Four out of the five studies on oral mucosa and fluorophores were *in vivo* studies, performed on humans. One study was a randomized trial in an animal model (Gurushankar, Nazeer, Jayasree, & Krishnakumar, 2015). The Oxford CEBM and National Institutes of Health (NIH) Quality Assessment classifications were therefore applicable for four studies (Nazeer, Asish, Venugopal, Anita, & Gupta, 2014) (Vedeswari, Jayachandran, & Ganesan, 2009) (Jayanthi, et al., 2009) (Lane, et al., 2006). Level of evidence was 2b for all studies evaluated.

2.4 Results regarding skin

2.4.1 Fluorophores

Fifteen papers were identified by using “Skin AND Fluorophores” as entry terms, five papers by using “Epidermal AND Fluorophores” and one paper by using “Dermal AND Fluorophores”. Four papers were repetitions. The database search using “Cutaneous AND Fluorophores” as entry terms did not identify papers dealing with the topic of the present review. Seventeen papers were eventually included (Figure 2.2) (Richter, Trojahn, Dobos, Blume-Peytavi, & Kottner, 2016) (Eny, et al., 2015) (Zhao, et al., 2016) (Miyamoto & Kudoh, 2013) (Krasieva, et al., 2013) (Yu, et al., 2012) (McMullen, Chen, & Moore, 2012) (Patalay, et al., 2011) (Leupold, et al., 2011) (Breunig, Studier, & König, 2010) (Stirban, Nandrean, Negrean, Koschinsky, & Tschoepe, 2008) (Laiho, Pelet, Hancewicz, Kaplan, & So, 2005) (Sandby-Møller, Thieden, Philipsen, Heydenreich, & Wulf, 2004) (Na, Stender, Henriksen, & Wulf, 2011) (Gillies, Zonios, Anderson, & Kollias, 2000) (Dimitrow, et al., 2009a) (Dimitrow, et al., 2009b).

Molecules identified as possible fluorophores in the skin were porphyrins, advanced glycation end products (AGEs), flavins, lipopigment, the reduced form of nicotinamide adenine dinucleotide (NADH), flavin adenine dinucleotide (FAD), pheomelanin, eumelanin, collagen, elastin, tryptophan, components of lipofuscin and keratin. Details of studies and molecules are shown in Figures 2.4 and 2.5.

Excitation wavelengths used for inducing AF ranged from 260 to 1000 nm (including UV). Wavelengths used with two-photon tomography and femtosecond laser ranged from 720 to 1000 nm. Wavelengths used with other devices ranged from 260 to 488 nm.

Figure 2.4 Outline of papers investigating fluorophores in oral mucosa.

Author	Year	Type of paper	Fluorophores	Excitation wavelength	Emission wavelength	Device (excitation source)	Application fields or conclusions
Richter C et al	2016	Clinical study	Porphyrins	UVA light (about 400 nm)	Red fluorescence	Visiopor PP 34 (Courage + Khazaka Electronic GmbH)	Fluorescence quantity for measuring acne severity
Eny KM et al	2015	Clinical study	Advanced glycation end products (AGEs)	SIF 1: 375 nm; SIF 14: 456 nm	SIF 1: 435-655 nm; SIF 14: 491-655 nm	SCOUT DS SF spectrometer (VeraLight, Inc., Albuquerque, NM)	Skin intrinsic fluorescence is associated with caffeine consumption
Zhao HL et al	2015	Ex vivo study	Flavin; Lipopigment	488 nm	2 peaks: 530 nm and 590 nm	Olympus Microscope IX71, OLYMPUS CORPORATION, Tokyo, Japan	Autofluorescence for diagnosis and therapy of eccrine sweat glands disease
Miyamoto K et al	2013	Clinical study	NADPH	near-infrared (760 nm)	–	Two-photon tomography (DermaInspect/ MPTflex, JenLab GmbH, Jena, Germany)	NADPH visualization and quantification in living keratinocyte for evaluating skin aging and its progression
Krasieva TB et al	2013	In vitro scientific study	Pheomelanin; Eumelanin	900-1000 nm	Pheomelanin: 615-625 nm Eumelanin: 640-680 nm	Meta detector of the Zeiss LSM 510 Meta NLO microscopy system; Chameleon-Ultra femtosecond pulsed tunable laser (Coherent Inc.)	Two-photon excited fluorescence (TPF) spectral index and phasor fluorescence lifetime imaging microscopy (FILM) used for rapid melanin ratio characterization boh in vivo and in vitro.
Yu Y et al	2012	In vitro + ex vivo scientific study	Keratin; NADH; FAD; Melanin; Collagen; Elastin	ranging from 730 to 920 nm	Keratin: 485-525 nm NADH: 460 nm FAD: 550-543 nm Melanin: 579 nm Collagen: 458-475-510 nm Elastin: 454-472-508 nm	720-950 nm femto-second laser (Chameleon, Coherent Inc., Santa Clara, CA)	Imaging guided TPF excitation-emission-matrix (EEM) spectroscopy provides useful information for developing clinical devices for skin disease diagnosis
McMullen RL et al	2012	Ex vivo animal study + in vivo human study	(human skin) - Collagen - Tryptophan	ranging from 270 to 450 nm	(human skin) - Collagen: 466 nm - Trp: 350 nm	UVA lamp	Collagen fluorescence has different characteristics depending on type of skin tissue investigated.
Patalay R et al	2011	Ex vivo scientific study	Collagen; Elastin; Melanin; Keratin; Porphyrins; NADPH; Flavins	760 nm	NADPH: 450-460 nm (main fluorophore in the blue channel) Melanin: 550 nm Flavins: 525 nm (main fluorophores in the green channel)	(modified) Two-photon tomography (DermaInspect/MPTflex, JenLab GmbH, Jena, Germany)	Fluorescence for differential diagnosis from dysplastic nevi and malignant nodular basal cell carcinoma.
Leupold D et al	2010	Ex vivo scientific study	Pheomelanin; Eumelanin	810 nm	Common melanocytic nevi: band peaking 590 nm Melanoma: band peaking 640 nm	2.5 ns-pulsed via 810 nm wo-photon	Two-photon excited fluorescence is a possible new diagnostic tool on the basis of the red-shift of melanin fluorescence in melanoma.
Breunig HG et al	2010	Clinical study	Keratin; NADH; FAD; Melanin; Collagen; Elastin	ranging from 710 to 920 nm	–	Sapphire laser (Mai Tai XF, Spectra Physics)	–
Dimitrow E et al.	2009	In vivo + ex vivo scientific study	- FAD - NAD(P)H - -metal-free porphyrins - components of lipofuscin - melanin - elastin - collagen - keratin	760 nm and 800 nm	–	Two-photon tomography (DermaInspect/ MPTflex, JenLab GmbH, Jena, Germany)	Early detection of black skin cancer.

Author	Year	Type of paper	Fluorophores	Excitation wavelength	Emission wavelength	Device (excitation source)	Application fields or conclusions
Dimitrow E et al.	2009	In vivo + ex vivo scientific study	- NAD(P)H - metal-free porphyrins - components of lipofuscin - melanin - elastin - collagen - keratin	750 nm - 850 nm	–	Two-photon tomography (DermaInspect/ MPTflex, JenLab GmbH, Jena, Germany)	Multiphoton laser tomography for malignant melanoma diagnosis
Stirban A et al	2008	Clinical study	AGEs	ranging from 300 to 420 nm	–	AGE Reader (Diagnoptics BV, Groningen, The Netherlands)	Skin Autofluorescence as a non-invasive tool for screening people for undetected diabetes or cardiovascular risk.
Laiho LH et al	2005	ex vivo study	Tryptophan; NADPH; Melanin; Elastin; Collagen.	ranging from 375 to 600 nm	Collagen: peak 400-425 nm Tryptophan: peak 425 nm NADPH: peak 475 nm Elastin: peak475 nm Melanin: peak 550nm	Ti:sapphire laser (Tsunami,Spectra Physics, Palo Alto, California))	Basis for future in vivo skin spectroscopy studies and clinical examinations.
Sandby-Møller J et al	2004	Clinical study	Collagen	EX1 370 nm EX 2: 330 nm	EM 1: 455 nm EM 2: 455 / 370nm	Quarz Y-fiber (wavelenght allowance range: 120-1600 n. Volpi AG, Zurich, Switzerland)	Collagen-linked autofluorescence decreased with UVR exposure. F ratio might be the best measure of individual photodamage and a marker of individual cumulative UVR dose.
Na R et al	2001	Clinical study	–	EX1 330 nm EX 2: 370 nm	EM 1: 375 nm; EM 2: 455 nm	Quarz Y-fiber (wavelenght allowance range: 120-1600 n. Volpi AG, Zurich, Switzerland)	375 nm skin autofluorescence as a biologic marker of skin aging in vivo.
Gillies R et al	2000	In vivo + ex vivo scientific study	Tyrosine; Tryptophan; Collagen; Elastin	ranging from 260 to 480 nm	Tyrosine: EX 270 EM: 320 nm Tryptophan: EX:295 EM: 345 nm Pepsin digestible collagen cross-link: EX: 335 EM: 390 nm Collagenase digestible collagen cross-link: EX: 370 EM: 460 nm Elastin: EX: 440 EM: 520 nm	–	Tryptophan fluorescence is potentially associated with proliferation and may be a useful marker in assessing the effectiveness of anti-proliferative agents or treatment.

Figure 2.5 Outline of papers investigating fluorophores in oral mucosa (continuation).

2.4.2 Reported clinical applications

Clinical applications of skin AF displayed a great heterogeneity.

In four of the selected studies, skin AF was proposed as a possible new diagnostic tool for malignant melanoma. In all these papers, a two-photon tomography instrument was the device used for investigation (Miyamoto & Kudoh, 2013) (Krasieva, et al., 2013) (Dimitrow, et al., 2009a) (Dimitrow, et al., 2009b).

In two out of 17 papers, skin AF was investigated as a marker for photo-aging, using UV wavelengths (330 and 370 nm) (Sandby-Møller, Thieden, Philipsen, Heydenreich, & Wulf, 2004) (Na, Stender, Henriksen, & Wulf, 2011).

Other applications reported for skin AF were measurement of acne severity (excitation wavelength: 400 nm) (Richter, Trojahn, Dobos, Blume-Peytavi, & Kottner, 2016) diagnosis and therapy of eccrine sweat gland disease (excitation wavelength: 488 nm) (Zhao, et al., 2016); screening for patients with undetected diabetes or cardiovascular risk (excitation wavelength used: 300–420 nm) and assessment of the effectiveness of anti-proliferative agents (excitation wavelength used: 260–480 nm) (Stirban, Nandrean, Negrean, Koschinsky, & Tschoepe, 2008) (Gillies, Zonios, Anderson, & Kollias, 2000).

2.4.3 Level of evidence

Seven out of 17 studies on skin/epidermal fluorophores were *in vivo* studies performed on humans; four out of 17 studies selected were *ex vivo* and *in vivo* studies, and six out of 17 studies were *ex vivo* or *in vitro* studies (Richter, Trojahn, Dobos, Blume-Peytavi, & Kottner, 2016) (Eny, et al., 2015) (Zhao, et al., 2016) (Miyamoto & Kudoh, 2013) (Krasieva, et al., 2013) (Yu, et al., 2012) (McMullen, Chen, & Moore, 2012) (Patalay, et al., 2011) (Leupold, et al., 2011) (Breunig, Studier, & König, 2010) (Stirban, Nandrean, Negrean, Koschinsky, & Tschoepe, 2008) (Laiho, Pelet, Hancewicz, Kaplan, & So, 2005) (Sandby-Møller, Thieden, Philipsen, Heydenreich, & Wulf, 2004)

(Na, Stender, Henriksen, & Wulf, 2011) (Gillies, Zonios, Anderson, & Kollias, 2000) (Dimitrow, et al., 2009a) (Dimitrow, et al., 2009b).

The Oxford CEBM guidelines were applicable in 11 studies (Richter, Trojahn, Dobos, Blume-Peytavi, & Kottner, 2016) (Eny, et al., 2015) (Miyamoto & Kudoh, 2013) (McMullen, Chen, & Moore, 2012) (Breunig, Studier, & König, 2010) (Stirban, Nandrean, Negrean, Koschinsky, & Tschoepe, 2008) (Sandby-Møller, Thieden, Philipsen, Heydenreich, & Wulf, 2004) (Gillies, Zonios, Anderson, & Kollias, 2000) (Dimitrow, et al., 2009a) (Dimitrow, et al., 2009b) (Na, Stender, Henriksen, & Wulf, 2011).

The level of evidence was 1b for one study, 2b for six studies and 3b for four studies.

2.5 Commercial devices used to induce and visualize fluorescence

Commercial devices reported in the literature are usually based on simple setups, (e.g., peculiar excitation and emission wavelength bands, obtained by using excitation light sources [light emitting diode LED]). Such devices have been optimized for specific applications, (e.g., Visiopor© (Courage + Khazaka Electronic GmbH, Germany), including the quantitative measurement of the AF emitted by bacterial porphyrins in patients with acne (Richter, Trojahn, Dobos, Blume-Peytavi, & Kottner, 2016).

A qualitative analysis of tissue AF is possible through devices similar to those described. The VELscope™ system (LED Medical Diagnostics Inc., Barnaby, Canada) has been widely employed for diagnostic purposes, particularly for oral mucosa.

Other devices are based on multi-photon tomography (e.g., DermaInspec© [JenLab GmbH, Germany]). The technique, used for *in vivo* non-invasive tomography of human skin (Miyamoto & Kudoh, 2013) (Patalay, et al., 2011) (Breunig, Studier, & König, 2010) (Dimitrow, et al., 2009a) (Dimitrow, et al., 2009b) is based on the near-infrared femto laser beam scanning technology. Devices employing multi-photon tomography allow optical biopsies with subcellular spatial resolution. The technology generates an image

based on the AF intensity and time decay of fluorophores, including NADH, flavins, porphyrins and elastin at different tissue depths.

For more specific *ex vivo* or *in vitro* AF measurements, particular microscopes (e.g., Olympus IX71©) are used. Depending on their setup, such microscopes allow high-resolution imaging of reflected or transmitted fluorescence, by selecting the chosen excitation and emission bands, followed by digital image processing (Ericson, et al., 2008).

Scout DS© (Veralight) performs a non-invasive automatic quantitative fluorescence spectroscopy to detect the levels of advanced glycation end products (AGEs) in the skin of patients with diabetes (Eny, et al., 2015).

Among the optical components more frequently used in clinical settings, the monochromator is a tunable optical filter that enables selection and transmission of wavelengths of only a specific, narrow band of the incident light (Gurushankar, Nazeer, Jayasree, & Krishnakumar, 2015) (Nazeer, Asish, Venugopal, Anita, & Gupta, 2014) (Vedeswari, Jayachandran, & Ganesan, 2009). Such a device can be used to filter narrow-band light, starting from a wide-band source to elicit tissue AF (Gurushankar, Nazeer, Jayasree, & Krishnakumar, 2015) (Nazeer, Asish, Venugopal, Anita, & Gupta, 2014) (Vedeswari, Jayachandran, & Ganesan, 2009) (Lane, et al., 2006) (Breunig, Studier, & König, 2010) (Sandby-Møller, Thieden, Philipsen, Heydenreich, & Wulf, 2004) (Na, Stender, Henriksen, & Wulf, 2011) (Drakaki, Dessinioti, Stratigos, Salavastru, & Antoniou, 2014) (Yaroslavsky, Neel, & Anderson, 2004).

A dichroic filter can be used to select the wanted emission narrow-band light by removing the unwanted reflected excitation light. In some cases, photomultiplier tubes, which are extremely sensitive detectors of light signals, can be used (Gurushankar, Nazeer, Jayasree, & Krishnakumar, 2015) (Nazeer, Asish, Venugopal, Anita, & Gupta, 2014) (Vedeswari, Jayachandran, & Ganesan, 2009) (Krasieva, et al., 2013) (Yu, et al., 2012) (Leupold, et al., 2011) (Breunig, Studier, & König, 2010) (Dimitrow, et al., 2009a) (Dimitrow, et al., 2009b).

2.6 Discussion

Innovative, non-invasive visual tools, possibly improving diagnostic accuracy, have recently gained interest. Among these, devices evaluating tissues' autofluorescence (AF) are emerging (Giovannacci, Vescovi, Manfredi, & Meleti, 2016).

It seems likely that malignant or potentially malignant changes in soft tissues may induce variations of the tissue AF spectra, which can be visualized in real time by non-invasive methods.

On the basis of the present literature review, some evidence exists that endogenous fluorophores of skin, stimulated by ultraviolet or blue excitation wavelengths, are proteins such as collagen, elastin, keratin and the amino acid tryptophan. On the other hand, as the number of papers investigating fluorophores of the oral mucosa is very low, it is difficult to draw solid conclusions regarding this anatomical district. Data on AF molecules in oral mucosa should, therefore, be considered preliminary and presumptive, and they should be confirmed by further research.

Even though skin and oral mucosa share some similarities in terms of overall histological architecture and molecule distribution, it should be borne in mind that specific features (e.g., depth of the keratin layer, presence of peculiar glands, *etc.*) may be associated with different behaviors in terms of AF (light absorption and emission). Nevertheless, it would seem that both in skin and oral mucosa, dysplastic and neoplastic processes induce some alteration of fluorophores' structure and/or concentration, thus producing a variation of normal AF (Jayanthi, et al., 2009).

Among fluorophores identified in the present review, localized either in the oral mucosa or skin, there are molecules involved in tissue metabolism such as the reduced forms of NAD (NADH) and NAD phosphate (NADPH) and FAD. Metabolic activity of the relative amounts of NADH, NADPH and FAD and the microenvironment of these metabolic electron carriers can apparently be used to monitor changes in metabolism non-invasively, which is one of the hallmarks of carcinogenesis (Gurushankar, Nazeer,

Jayasree, & Krishnakumar, 2015) (Skala, et al., 2007). Such coenzymes are the main ones responsible for AF rising from cell cytoplasm, with their amount, redox and bound-free state in close relationship with their engagement in energetic metabolism, cell oxidative defence, reductive biosynthesis, and signal transduction (Croce & Bottiroli, 2014).

Particularly, NADH is more fluorescent than the oxidised form, NAD^+ (Miyamoto & Kudoh, 2013). Depending on the metabolic status of cells (e.g., prevalence of reactions of oxidation or reduction), the oxidised or reduced form of the coenzyme will be prevalent in the cytoplasm, thus leading to a higher or lower degree of fluorescence (Croce & Bottiroli, 2014). It has been widely demonstrated that neoplastic cells display an increase in oxidative processes, and it is therefore reasonable to hypothesize a shift in the NAD^+/NADH equilibrium toward a predominance of NAD^+ (Gào & Schöttker, 2017) (Drakaki, Dessinioti, Stratigos, Salavastru, & Antoniou, 2014).

In addition, Drakaki et al., in their review on laser-induced fluorescence for diagnosis of basal cell carcinoma, confirmed that AF variation in malignant tissues was caused by decreased NADH levels and by a shifted equilibrium between the highly fluorescent NADH and the less-fluorescent oxidised-form NAD+ (Drakaki, Dessinioti, Stratigos, Salavastru, & Antoniou, 2014).

Similar to NAD, NADP is fluorescent in its reduced form (NADPH); the AF emission properties were strictly dependent on the bound/free condition (Miyamoto & Kudoh, 2013). The typical energetic anaerobic metabolism was observed in most neoplastic cells results, in general, in lower values in the NADPH bound/free ratio with respect to non-neoplastic cells (Salmon, et al., 1982).

Such a low value of the bound/free ratio is, most probably, one of the biological features associated to the loss of AF observed in tumor cells.

As part of the group of flavin *free derivatives*, FAD exhibits absorption/excitation and emission properties at 440–450 nm and 525 nm (Penzer, 1980) (Wolfbeiss, 1985). The fluorescence emission from FAD has been reported to be strongly affected by the

nature of the protein to which the prosthetic group is bound (Kunz & Kunz, 1985). Interestingly, the first description of FAD fluorescence was performed in 1962, in intracellular granules of eosinophils (Grossi & Zaccheo, 1963). It seems worthy to mention here that further studies demonstrated an increase in AF intensity and a shift from the blue to the yellow region when the circulating cells settled in the tissues

(Mayeno, Hamann, & Gleich, 1992) (Barnes, Aggarwal, Thomsen, Fitzmaurice, & Richards-Kortum, 1992).

Porphyrins are indicated as fluorophores both in oral mucosa and in skin tissues, with an excitation wavelength of about 400 nm and emission wavelength around 630–690 nm. Variation in porphyrin concentration is considered an important marker for differentiating malignant disorders from healthy tissues (Jayanthi, et al., 2009).

According to Bagri-Manjrekar et al., the mechanism responsible for such a phenomenon seems to depend on one or more of the following possibilities: (1) porphyrins of host origin and excreted from the circulating blood by the tumor; (2) the tumor itself produces porphyrins and (3) porphyrins are the product of microbial activity restricted to the ulcerated surface of the tumor (Bagri-Manjrekar, et al., 2018).

In particular, Nazeer et al. demonstrated a more elevated level of porphyrins in the tissues of patients with oral leukoplakia and among tobacco users compared to non-tobacco users. Jayanthi et al. reported that the level of porphyrins increases with the increase in pathological grading, and Croce et al. reported that an excess of protoporphyrin IX (PpIX) occurs naturally in cancers and their metastases (Jayanthi, Subhash, Stephen, Philip, & Beena, 2011).

Interestingly, Inaguma et al. demonstrated that when exposed to 410 nm wavelength light, 85% of oral carcinomas returned porphyrin-like fluorescence spectra, whereas the normal mucosa of the oral cavity did not display such a feature (Inaguma & Hashimoto, 1999).

Moreover, the Mallia et al. study highlighted that the peak observed at 685 nm, especially in neoplastic and dysplastic tissues, could depend on the accumulation of

the endogenous fluorophore coproporphyrin III, which is a precursor of PpIX in the heme synthesis. This peak was absent in tissues from healthy volunteers, which confirmed such findings (Mallia, et al., 2008).

Among less-reported fluorophores, the present review identified flavin, lipopigment, advanced glycation end products (AGEs), pheomelanin and eumelanin.

Zhao et al. reported flavin and lipopigment as endogenous fluorophores of eccrine sweat glands. Following irradiation with a 488 nm wavelength, a single eccrine sweat gland isolated from normal skin tissue under a microscope showed AF with two peaks: 530 and 590 nm, corresponding to flavin and lipopigment peaks. Such molecules are coenzymes in many metabolic pathways. AF measurement could therefore be performed to monitor cells and tissue energy metabolism (Zhao, et al., 2016).

AGEs are a heterogeneous group of molecules resulting from non-enzymatic glycation of proteins, lipids, and nucleic acids. The measure of AGE residues provides information on glycemic control in diabetic patients (Eny, et al., 2015) (Stirban, Nandrean, Negrean, Koschinsky, & Tschoepe, 2008). It would seem that their concentration can be indirectly measured by evaluating skin AF. Stirban et al., using an excitation light source between 300 and 420 nm, demonstrated that skin AF increases after lunch in both healthy and diabetic patients (Stirban, Nandrean, Negrean, Koschinsky, & Tschoepe, 2008).

Light absorption behavior of melanin is completely different from the absorption of other organic fluorophores (Hoffmann, Stucker, Altmeyer, Teuchner, & Leupold, 2001). In fact, melanin AF in the spectral region of 450–650 nm is extremely weak in human skin tissue and is completely hidden from the main endogenous fluorophores (e.g., NADPH e flavins) (Teuchner K, Volkmer, Birch, Altmeyer, & al., 1999) (Zeng, MacAulay, McLean, & Palcic, 1995). Such a disadvantage has been overcome only recently, by using special techniques such as two-photon excitation (Teuchner K, Volkmer, Birch, Altmeyer, & al., 1999). In particular, upon irradiation with 800-nm laser

pulses, melanin absorbs two photons through an intermediate excited electronic state (Teuchner K, Volkmer, Birch, Altmeyer, & al., 1999).

Investigation of melanin fluorescence, within a different set of pigmented lesions of the skin, showed a marked difference in AF behavior of benign pigmentations (e.g., melanocytic nevi) with respect to melanoma (Hoffmann, Stucker, Altmeyer, Teuchner, & Leupold, 2001). Leupold et al. confirmed that through the use of a two-photon excitation technology with 2.5-ns pulses, melanin fluorescence peak is 590 nm in all types of benign melanocytic nevi, although it shifts to red light with 640 nm in melanoma (Leupold, et al., 2011). Such observation led to the hypothesis that malignant transformation of melanocytes is associated with changes in melanogenesis and in the amounts of cellular eumelanin and pheomelanin (Leupold, et al., 2011).

The reason for the red-shift of melanin fluorescence in melanoma is the modification of the eumelanin/pheomelanin ratio with an higher concentration of pheomelanin in malignant lesions (Leupold, et al., 2011) (Yaroslavsky, Neel, & Anderson, 2004) (Simon, Peles, Wakamatsu, & Ito, 2009).

Dimitrow et al. further demonstrated that MLT can differentiate between benign and malignant melanocytic lesions both *in vivo* and *ex vivo*. In fact, among 83 pigmented lesions of the skin, the authors highlighted distinct morphological differences in melanoma compared with melanocytic nevi. In particular, six characteristic features of AF malignant melanoma were specified (architectural disarray, pleomorphic cells, poorly defined keratinocyte cell borders, large intercellular distance, ascending melanocytes and dendritic cells). The technique showed an overall sensitivity of 75% *in vivo* and 93% *ex vivo* (Dimitrow, et al., 2009a).

All clinical applications of oral mucosal AF reported in the papers included in the present review were related to the diagnosis and follow-up of malignant and potentially malignant lesions (Gurushankar, Nazeer, Jayasree, & Krishnakumar, 2015) (Vedeswari, Jayachandran, & Ganesan, 2009) (Jayanthi, Subhash, Stephen, Philip, & Beena, 2011) (Lane, et al., 2006).

It should be borne in mind that a potential risk of malignant transformation associated with the use of UV-emitting devices exists (D'Orazio, Jarrett, Amaro-Ortiz, & Scott, 2013). Therefore, caution should be used in clinical settings, when fluorescence is excited through UV wavelengths. It would, however, seem improbable that the limited time of exposure necessary in the reported techniques is sufficient to generate some damage at the cellular and tissue levels.

AF detection in skin seems to cover a wider range of applications than in oral mucosa. Several papers are focused on the diagnosis and follow-up of malignant and potentially malignant lesions, both non-melanoma skin cancers and melanoma. Skin AF has also been proposed for assessing the severity of acne, for the diagnosis of sweat gland pathologies, for monitoring glycemic control in diabetic patients and as a marker for skin aging.

2.7 Conclusion

Some evidence exists for the usefulness of AF in the management of potentially malignant and malignant lesions of the skin. On the other hand, the very limited number of papers (5) investigating fluorophores in oral mucosa, and their behavior in physiologic and pathologic conditions, does not allow any robust conclusions about such anatomical compartmentalization. Further to diagnosis of malignant lesions, potential fields of application of skin and mucosal AF have been explored. However, on the basis of the weak level of evidence, more well-designed studies are needed to confirm such potentialities.

The heterogeneity of AF devices as well as their applications makes it difficult to compare the results of the studies included in the present review.

3 Clinico-pathological features associated to fluorescence alteration. Analysis of 108 oral malignant and potentially malignant lesions.

3.1 Background

Oral squamous cell carcinoma (OSCC) is among the first 15 most common malignant tumors, with an incidence of more than 500.000 cases per year (Dissanayaka, et al., 2012). The main factor capable of modifying the prognosis of the disease is the stage of the tumor at the time of diagnosis. Five-year survival rate of patients with stage I tumors is 75%. It strongly decreases in patients affected by tumors with a higher stage. In particular, if the diagnosis occurs in stage II, the survival is of 49% and of 30% if it is in stage III (Dissanayaka, et al., 2012) (Sciubba, 2001).

OSCC can appear *ex novo* on oral mucosa or can be diagnosed on a specific group of lesions named oral potentially malignant disorders (OPMD). They are characterized by an increased risk of progressing to OSCC and include leukoplakia, erythroplakia and oral lichen planus (Ho, Wang, Huang, & Yang, 2019) (Shi, et al., 2019) (Speight, Khurram, & Kujan, 2018). OPMDs have a statistically increased risk of progressing to cancer, but predicting the risk in any individual patient is difficult because it varies according to a range of patient- or lesion-related factors (Speight, Khurram, & Kujan, 2018).

Several clinical parameters can help clinicians to assess an increased risk of progression to malignancy, such as the localization of a lesion within the mouth, the nonhomogeneous appearance, the size greater than 200 mm^2, the duration of the lesion, the patient age and habits (Speight, Khurram, & Kujan, 2018) (Holmstrup, Vedtofte, Reibel, & Stoltze, 2006) (Warnakulasuriya & Ariyawardana, 2016).

However, the biopsy and the histologic examination of the specimen are the gold standard for the diagnostic process. In fact, the most reliable prognostic factor for

progression to cancer is the histological presence of tissue changes (oral epithelial dysplasia - OED) (Speight, Khurram, & Kujan, 2018) (Warnakulasuriya, Reibel, Bouquot, & Dabelsteen, 2008).

Several non-invasive diagnostic tools have been developed to improve the effectiveness in the early detection of oral cancer and in the evaluation of the OPMDs before definitive biopsy (Giovannacci, Vescovi, Manfredi, & Meleti, 2016).

Among these, devices evaluating tissues autofluorescence (AF) are emerging. In particular, the most known is the VELscope® system (LED Medical Diagnostics Inc., Barnaby, Canada) that has an excitation source of 400-460 nm. Fluorophores of normal tissues, if stimulated, shows a bright green autofluorescence. In contrast, several Authors described that abnormal tissue has a reduction in fluorescence and appears dark brown or black (Rashid & Warnakulasuriya, 2015). This event is known as loss of AF (LAF) (Farah, Dost, & Do, 2019) (Yamamoto, et al., 2017) (Huang, et al., 2017).

Moreover, some lesions, especially those characterized by an increase in keratin, show an increase in AF and appear bright green or white. Less frequently than LAF, the hyper-fluorescence has been considered as an alteration of AF (Meleti, et al., 2020).

Data reported on the clinical applications of AF are extremely heterogeneous and difficult to compare. Recently, the diagnostic value of optical fluorescence imaging (OFI) has been reviewed by Tiwari et al. (Tiwari, Kujan, & Farah, 2019). The Authors highlighted that OFI demonstrated positive results, with higher sensitivity scores, increased lesion detection and visualization than comprehensive oral examination alone in the clinical evaluation of OSCC and OPMDs (Tiwari, Kujan, & Farah, 2019).

However, the weak point of the VELscope is the low specificity reported in the literature in agreement despite the heterogeneity of the studies (Shi, et al., 2019) (Tiwari, Kujan, & Farah, 2019) (Mascitti, et al., 2018).

The present study has been developed in order to describe the most relevant clinicopathological features associated to AF alteration in a cohort of patients with OSCC and PMDs.

3.2 Materials and Methods

Ethical Committee of the Academic Hospital of Parma approved the present study (Study code: FLISTO - n°46556/17).

One hundred and eight lesions from 60 patients with clinical diagnosis of PMDs and carcinomas were included in the study.

Epidemiological data of patients were as follows: 23 (38.3%) males, 37 (61.7%) females; mean age 69 years (minimum: 33; maximum: 95 years).

Eleven out of 60 (18.6%) patients were smokers and 18 (30%) ex-smokers. No patient declared current alcohol abuse and 3 patients (5%) were former alcoholics. Thirty-four (31.5%) lesions were localized on the borders of the tongue; in 23 cases (21.3%) localization was gingiva; in 16 cases (14.8%) lesions were on cheek mucosa, in 10 cases (9.3%) on the lower lip, in 8 cases (7.4%) on the floor of mouth, in 4 cases (3.7%) on the hard palate, in 4 cases (3.7%) on the ventral aspect of the tongue, in 3 cases (2.8%) on the soft palate, in 3 cases (2.8%) on the dorsum of the tongue and in 3 cases (2.8%) in the vestibular mucosa.

AF pattern of the lesions was analysed before surgery. Fluorescence was stimulated through irradiation with a blue-violet light (400-460 nm wavelength) using the Velscope® system (LED Medical Diagnostics, Inc, Barnaby, BC, Canada).

AF was assessed as follows: 1. Normo-fluorescence, when a lesion did not show fluorescence differences with regard to the surrounding tissues; 2. Hypo-fluorescence, when a lesion displayed a darker aspect; 3. Hyper-fluorescence, when a lesion showed

a white, shining appearance (Figure 3.1).

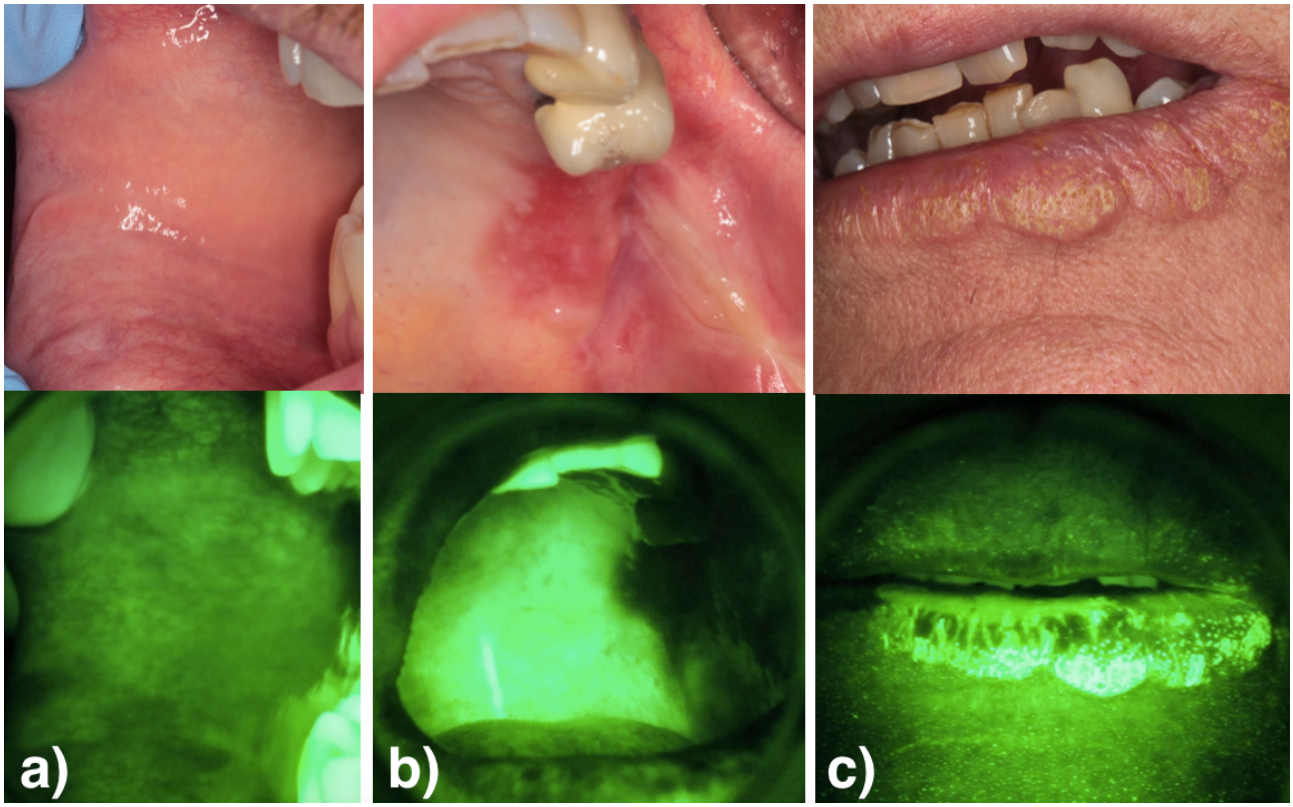

Figure 3.1 a) normo-fluorescence – b) hypo-fluorescence – c) hyper-fluorescence

Incisional or excisional biopsies were obtained in all cases (87 out of 108 (80.5%) incisional and 21 out of 108 (19.5%) excisional biopsies). For lesions with inhomogeneous AF pattern (e.g. presence in the same lesion of hypo- and hyperfluorescent areas) we obtained a specimen for each area.

All specimens were stained with haematoxylin and eosin (H&E). Histopathological evaluation was performed by an oral pathologist unaware of the AF pattern of the lesion.

For each case, the following variables were recorded and compared to the AF pattern:

1. clinical appearance of the lesion (subclassified as white, red and white/red);
2. histological diagnosis (including no dysplasia, mild/moderate dysplasia, severe dysplasia/in situ carcinoma, invasive carcinoma, verrucous carcinoma) and
3. clinicopathological diagnosis (including leukoplakia, lichenoid oral lesions, oral squamocellular carcinoma, verrucous carcinoma).

Moreover, a binomial logistic regression performed in order to investigate whether clinical appearance and/or histological diagnosis were significant in determining degree of AF.

3.2.1 Statistical analysis

Data analysis was performed using IBM-SPSS statistical package version 22.

Statistical analysis was obtained for the main descriptive indexes among which, mean, median, mode, 5% trimmed mean, variance, standard deviation, interquartile range, minimum, maximum, asymmetry, and kurtosis coefficients. Where relevant, standard errors and the corresponding 95% confidence intervals were also calculated. Qualitative characters have been reported in frequency tables and expressed as absolute frequencies, relative frequencies, cumulated frequencies and percentages. For the part of graphic analysis, histograms and box-plots were used. Histograms are useful to visualize the shape of the data distribution and to determine the presence of anomalous values, while the box-plots immediately make visible the differences in the central trend (median) between the different groups.

Pearson Chi-square test was used for groups comparisons between the continuous variables.

Binary logistic regression was used to test the possible association between fluorescence expression (hyper, hypo) and the main covariates and factors (clinical appearance of the lesion and histological diagnosis). The statistical significance has been established with a p-value less than 0.05.

3.3 Results

3.3.1 Comparison between AF degree and clinical appearance

Among white lesions, 66% resulted hyper-fluorescent, 29.8% normo-fluorescent and 4.3% hypo-fluorescent. Red lesions appeared hypo-fluorescent in 95.2% of cases and normo-fluorescent in 4.8% of cases.

Fifty percent of white/red lesions were hypo-fluorescent, 27.5% were hyper-fluorescent and 22.5% were normo-fluorescent.

The association resulted extremely statistically significant ($p<0.0001$). Details are shown in Table 3.1

3.3.2 Comparison between AF degree and histological diagnosis

When the degree of AF was considered in a binary way (normal AF or altered AF), the percentage of cases in which the fluorescence resulted altered (both hypo- and hyper-fluorescence) was increased with the increase of the histological invasiveness of the lesion. In particular, AF resulted altered in 36% of lesions without dysplasia; in 75.9% of lesions with mild or moderate dysplasia and in the totality of in situ, invasive and verrucous carcinomas (Figure 3.2).

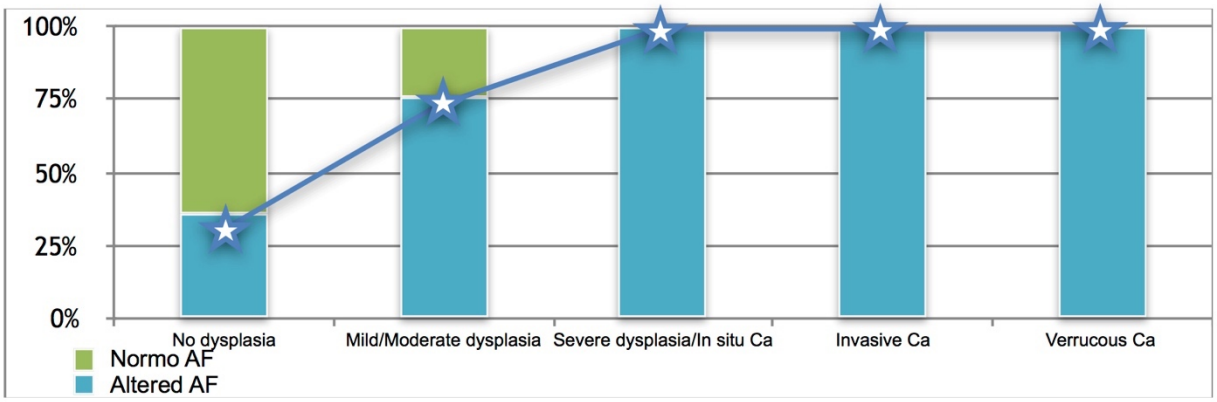

Figure 3.2 Percentage of cases in which the fluorescence resulted altered. The graph highlight that it was increased with the increase of the histological invasiveness of the lesion.

Specific data of comparison between AF degree and histological diagnosis considering fluorescence in 3-way (normal AF, hypo-fluorescence and hyper-fluorescence) are shown in Table 3.2. Statistical analysis showed a high significance ($p<0.0001$).

3.3.3 Comparison between AF degree and clinicopathological diagnosis

In the group of “leukoplakia” (homogeneous, non-homogeneous and proliferative verrucous leukoplakia)16 lesions (55.2%) were hyperfluorescent, 10 (34.5%) were normo-fluorescent and 3 (10.3%) were hypo-fluorescent.

Among “lichenoid oral lesions” (oral lichen planus and oral lichenoid lesions), 13 (50%) were normo-fluorescent, 8 (30.8%) were hyper-fluorescent and 5 (19.2%) were hypo-fluorescent.

In case of SCC or VC, any lesion was normo-fluorescent. Squamous cell carcinomas resulted more hypo-fluorescent (33 cases, 73.3%) than hyper-fluorescent (12 cases, 26.7%). On the contrary, verrucous carcinomas shown in the majority of cases a hyperfluorescent pattern (7 cases, 87.5%); only 1 case of VC resulted as hypo-fluorescent (12.5%).

Association between AF degree and clinicopathological diagnosis was extremely statistically significant ($p<0.0001$).

3.3.4 Binomial logistic regression

Binomial logistic regression was performed in order to investigate whether clinical appearance and/or histological diagnosis were significant in determining the degree of AF. In the case in which the variables “clinical appearance" and “histological diagnosis" were inserted pooled in the regression, it was not possible to perform a correct evaluation because the two variables showed a strong correlation.

As a consequence, the variables were separately considered in the regression and both resulted extremely significant in determining the degree of AF.

3.3.4.1 Clinical appearance

Clinical appearance has a p value <0.001 and specific model coefficients are shown in Table 3.3. Figure 3.3 highlights the predictive measures. In particular, AF degree of hypo-fluorescent lesions are predicted correctly in 95.2% of cases and hyper-fluorescent lesions in 72.1% of cases, with an accuracy of 83.5%.

3.3.4.2 Histological diagnosis

Also, the regression whit this variable resulted statistically significant (p=0.001). Specific model coefficients are shown in Table 3.4.

Regarding predictive measures, specificity was 76.7%, sensitivity was 81% and accuracy 78.8% (Figure 3.4).

Clinical appearance

Observed	Predicted		% Correct
	Hyper-fluorescent	Hypo-fluorescent	
Hyper-fluorescent	31	12	72.1
Hypo-fluorescent	2	40	95.2

Note. The cut-off value is set to 0.5

Predictive Measures

Accuracy	Specificity	Sensitivity	AUC
0.835	0.721	0.952	0.892

Note. The cut-off value is set to 0.5

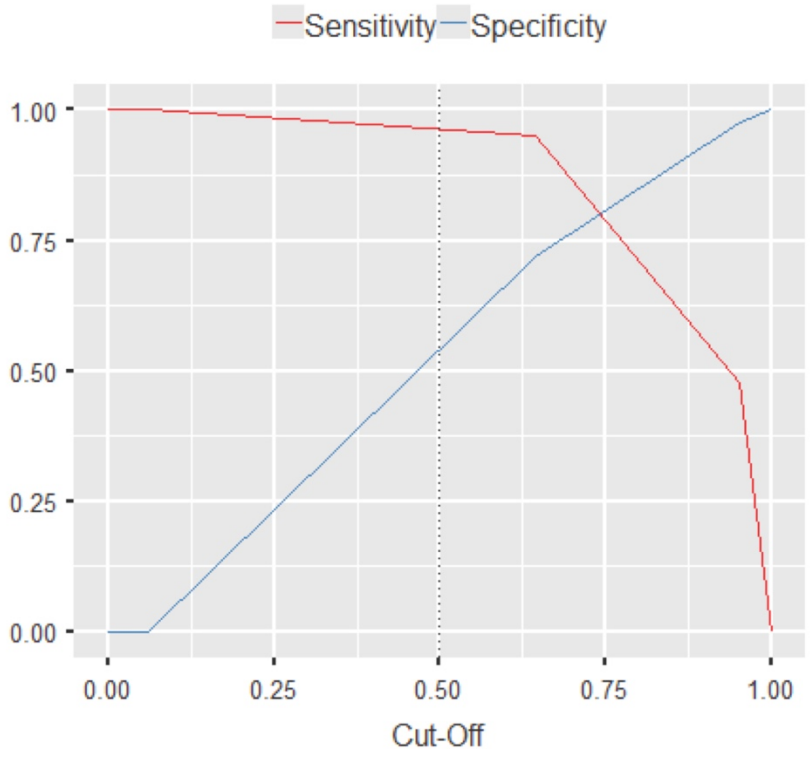

Figure 3.3 Predictive measures (specificity and sensitivity) with ROC curve related to the variable "Clinical appearance"

Histological diagnosis

Observed	Predicted		% Correct
	Hyper-fluorescent	Hypo-fluorescent	
Hyper-fluorescent	33	10	76.7
Hypo-fluorescent	8	34	81.0

Note. The cut-off value is set to 0.5

Predictive Measures

Accuracy	Specificity	Sensitivity	AUC
0.788	0.767	0.810	0.826

Note. The cut-off value is set to 0.5

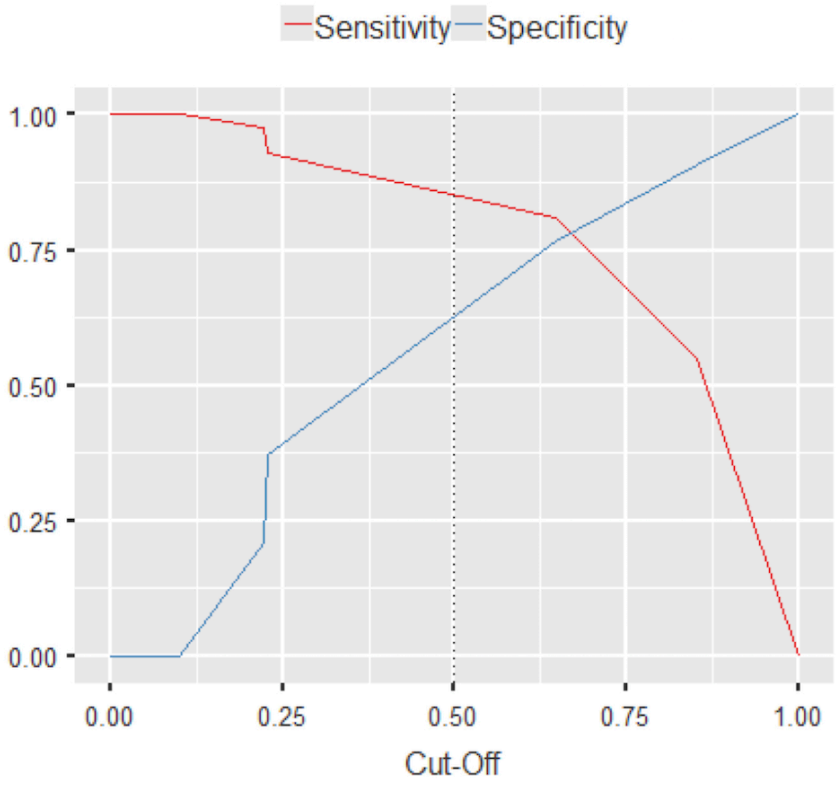

Figure 3.4 Predictive measures (specificity and sensitivity) with ROC curve related to the variable "Histological diagnosis"

Table 3.1 Specific data of association between AF degree and clinical

			AF degree			Total
			Hyper-fluorescent	Hypo-fluorescent	Normo-fluorescent	
Clinical appearance	White	Count	31	2	14	47
		% within Clinical appearance	66.0%	4.3%	29.8%	100.0%
		% within AF degree	72.1%	4.8%	60.9%	43.5%
		% of Total	28.7%	1.9%	13.0%	43.5%
	Red	Count	1	20	0	21
		% within Clinical appearance	4.8%	95.2%	.0%	100.0%
		% within AF degree	2.3%	47.6%	.0%	19.4%
		% of Total	.9%	18.5%	.0%	19.4%
	White/red	Count	11	20	9	40
		% within Clinical appearance	27.5%	50.0%	22.5%	100.0%
		% within AF degree	25.6%	47.6%	39.1%	37.0%
		% of Total	10.2%	18.5%	8.3%	37.0%
Total		Count	43	42	23	108
		% within Clinical appearance	39.8%	38.9%	21.3%	100.0%
		% within AF degree	100.0%	100.0%	100.0%	100.0%
		% of Total	39.8%	38.9%	21.3%	100.0%

Chi-Square Tests

	Value	df	Asymp. Sig. (2-sided)
Pearson Chi-Square	55.075a	4	.000
Likelihood Ratio	66.322	4	.000
N of Valid Cases	108		

a. 1 cells (11.1%) have expected count less than 5. The minimum expected count is 4.47.

Table 3.2 Specific data of comparison between AF degree and histological diagnosis considering fluorescence in 3-ways (normal AF, hypo-fluorescence and hyper-fluorescence)

			AF degree			Total
			Normal-AF	Hypo-AF	Hyper-AF	
Histological diagnosis	No Dysplasia	Count	16	2	7	25
		% within Histological diagnosis	**64.0%**	**8.0%**	**28.0%**	100.0%
		% within AF degree	69.6%	4.8%	16.3%	23.1%
		% of Total	14.8%	1.9%	6.5%	23.1%
	Mild / Moderate Dysplasia	Count	7	5	17	29
		% within Histological diagnosis	**24.1%**	**17.2%**	**58.6%**	100.0%
		% within AF degree	30.4%	11.9%	39.5%	26.9%
		% of Total	6.5%	4.6%	15.7%	26.9%
	Severe Dysplasia / In situ Ca	Count	0	11	6	17
		% within Histological diagnosis	**.0%**	**64.7%**	**35.3%**	100.0%
		% within AF degree	.0%	26.2%	14.0%	15.7%
		% of Total	.0%	10.2%	5.6%	15.7%
	Invasive Ca	Count	0	23	4	27
		% within Histological diagnosis	**.0%**	**85.2%**	**14.8%**	100.0%
		% within AF degree	.0%	54.8%	9.3%	25.0%
		% of Total	.0%	21.3%	3.7%	25.0%
	Verrucous Ca	Count	0	1	9	10
		% within Histological diagnosis	**.0%**	**10.0%**	**90.0%**	100.0%
		% within AF degree	.0%	2.4%	20.9%	9.3%
		% of Total	.0%	.9%	8.3%	9.3%
Total		Count	23	42	43	108
		% within Histological diagnosis	**21.3%**	**38.9%**	**39.8%**	100.0%
		% within AF degree	100.0%	100.0%	100.0%	100.0%
		% of Total	21.3%	38.9%	39.8%	100.0%

Chi-Square Tests

	Value	df	Asymp. Sig. (2-sided)
Pearson Chi-Square	76.690a	8	**.000**
Likelihood Ratio	80.610	8	**.000**
Linear-by-Linear Association	11.835	1	**.001**
N of Valid Cases	108		

a. 4 cells (26.7%) have expected count less than 5. The minimum expected count is 2.13.

Table 3.3 Binomial logistic regression related to the variable "clinical appearance"

Model Coefficients							
						95% Confidence Interval	
Predictor	Estimate	SE	Z	p	Odds ratio	Lower	Upper
Intercept	-2.74	0.730	-3.76	<.001	0.0645	0.0154	0.270
Clinical Appearance:							
White/red – White	3.34	0.820	4.07	<.001	28.1818	5.6440	140.717
Red – White	5.74	1.258	4.56	<.001	310.0000	26.3458	3647.644

Note. Estimates represent the log odds of "Hyper_Hypo = Hypo-fluorescent" vs. "Hyper_Hypo = Hyper-fluorescent"

Table 3.4 Binomial logistic regression related to the variable "Histological diagnosis"

Model Coefficients							
						95% Confidence Interval	
Predictor	Estimate	SE	Z	p	Odds ratio	Lower	Upper
Intercept	1.75	0.542	3.23	0.001	5.7500	1.98857	16.626
Histological-Diagnosis:							
No-Dysplasia – Invasive Ca	-3.00	0.968	-3.10	0.002	0.0497	0.00746	0.331
Mild / Moderate Dysplasia – Invasive Ca	-2.97	0.743	-4.00	<.001	0.0512	0.01192	0.220
Severe Dysplasia / In situ Ca – Invasive Ca	-1.14	0.742	-1.54	0.124	0.3188	0.07442	1.366
Verrucous Ca – Invasive Ca	-3.95	1.185	-3.33	<.001	0.0193	0.00189	0.197

Note. Estimates represent the log odds of "Hyper_Hypo = Hypo-fluorescent" vs. "Hyper_Hypo = Hyper-fluorescent"

3.4 Discussion

Velscope® system is a medical device approved in 2006 by the US Food and Drug Administration as a support tool for the implementation of the oral mucosa examination.

Biopsy and histopathological evaluation of the specimen are the gold standard for the diagnosis of oral suspicious lesions. However, promising evidence for the use of the autofluorescence (AF) visualization as an adjunctive tool to conventional oral examination (COE) have been demonstrated.

Tiwari et al. in their systematic review highlighted that the use of adjunctive optical fluorescence imaging (OFI) are able to increase the diagnostic accuracy of malignant and potentially malignant lesions in the oral cavity (Tiwari, Kujan, & Farah, 2019) (Bhatia, Matias, & Farah, 2014) (Farah, Dost, & Do, 2019) (Rana, Zapf, Kuehle, Gellrich, & Eckardt, 2012). In particular, Rana et al. reported a 100% sensitivity when fluorescence was used as an aid compared to 17% sensitivity with conventional oral examination alone (Farah, Dost, & Do, 2019). Similarly, Farah in 2012 and Bhatia in 2014 reported higher sensitivity scores using adjunctive fluorescence examination than COE alone (Bhatia, Matias, & Farah, 2014) (Farah, McIntosh, Georgiou, & McCullough, 2012).

However, although the sensitivity of the AF examination associated with COE is very high, both literature and the present study agrees to indicate a low specificity.

Values of specificity present in the literature are very heterogeneous depending on the characteristics of the studies. Ganga et al. in their review showed a mean specificity of the selected studies of 66.29% (95% CI: 58.76–73.24%) (Ganga, et al., 2017).

Recently, Shi et al. in their prospective study on 517 patients calculated sensitivity, specificity, positive prognostic value (PPV) and negative prognostic value (NPV) scores of VELscope examination for different outcomes (Giovannacci, et al., 2019). Regarding the detection of dysplasia and OSCC in oral suspicious lesions the scores of sensitivity,

PPV and NPV were from 40% to 75% (moderate) and specificity was < 40% (poor). Low PPV (< 20%) and specificity (< 40%) were detected in differential diagnosis of OSCC form oral suspicious lesions and differentiating high-risk lesions from low-risk lesions (Giovannacci, et al., 2019).

Low specificity score and low PPV are considered primary diagnostic limitation of VELscope examination.

In order to reduce the incidence of false positives, some indications have been proposed in literature such as: reassessment of the patient with COE and fluorescence examination 2 weeks after the initial evaluation. This is particularly indicated for lesions with suspicion of acute inflammatory origin or with a loss of autofluorescence not related to the clinical aspect (Bhatia, Matias, & Farah, 2014) (Rana, Zapf, Kuehle, Gellrich, & Eckardt, 2012). Farah et al in their study, of the 170 lesions analyzed 45.29% (n = 77) resolved (i.e. disappeared after reassessment), and 24.7% (n = 42) were confirmed as benign after 2-week reassessment (Farah, Dost, & Do, 2019).

Moreover, some Authors such as Bhatia and Farah described the diascopy technique: after applying pressure on the lesion LAF with negative blanching is to be considered indicative for dysplasia or malignancy (Bhatia, Matias, & Farah, 2014) (Rana, Zapf, Kuehle, Gellrich, & Eckardt, 2012).

The purpose of this perspective study was to evaluate the correlation between alteration of AF and specific variables (clinical appearance of the lesion, histological diagnosis and clinicopathological diagnosis).

Although both literature and the manufacturers of these devices consider the alteration of AF only as LAF, it is essential to consider also the hyper-fluorescence as possible alteration. Keratin is known as one of the main fluorophores of the oral mucosa and its alteration can produce an hyper-fluorescence in certain lesions such as PMDs with an increase of keratinization (e.g. leukoplakia), well-differentiated SCC with presence of keratin pearls and verrucous carcinoma (Giovannacci, et al., 2019).

As confirmation, 31 out of the 47 "white" lesions (66%) resulted hyperfluorescent versus only 1 out of the 21 "red" lesions (4.8%).

Regarding histological diagnosis, the percentage of cases in which the AF resulted altered (both hypo- and hyper-fluorescence) increased with the increase of the histological invasiveness of the lesion. AF resulted altered in 36% of lesions without dysplasia; in 75.9% of lesions with mild or moderate dysplasia and in the 100% of VC, in situ and invasive OSCC. In particular, looking at the typology of AF alteration, almost all VC (9 out of 10, 90%) were hyperfluorescent, while the majority of invasive SCC resulted hypo-fluorescent (23 out of 27, 85.2%). Also the majority of *in situ* OSCC were hypo-fluorescent, but the percentage was lower than invasive SCC (64,7% versus 85.2%).

Instead, taking a look to the lesions without dysplasia or with mild/moderate dysplasia, in the cases in which the AF was altered it was more frequently hyperfluorescent than hypo-fluorescent.

As a consequence, taking into account that a greater amount of keratin is more frequently detected in PMDs such as leukoplakia, in well-differentiated OSCC (e.g. presence of keratin pearls) and in VC (e.g. presence of keratin plugs) it is possible to speculate that hyper-fluorescence could mean an earlier stage of the malignant transformation process. On the contrary, oral malignant lesions with thin epithelial and/or keratin layers (or without keratin at all) are supposedly composed of cells far from their original developmental line (e.g. undifferentiated SCC) and probably related to a more advanced stage of the malignant transformation process (Meleti, et al., 2020).

Since both the clinical aspect of the lesion (red, white or mixed) and the histological diagnosis (absence of dysplasia, mild / moderate dysplasia, *in situ* carcinoma, invasive OSCC and VC) resulted statistically significant in determining the degree of AF, this study aimed to evaluate which one has more importance in determining the hypo-hyper or normal fluorescence.

Because the variables showed a strong correlation, the binomial logistic regression was performed separately and the diagnostic accuracy, sensitivity and specificity of prediction of the AF degree were calculated for each one. In particular, the “clinical aspect” of the lesion had an accuracy in determining the AF degree of 83.5% and the “histological diagnosis" of 78.8%.

In any case of *in situ* OSCC, invasive OSCC and VC the AF appeared normal. This means that, in accordance with the literature, the limit of this technique remains the presence of false positives. However, they can be drastically reduced by implementing the indications described.

Another great limitation of this technique is that the evaluation of the AF degree depends on the experience of the operator and that hypo-hyper- and normo-fluorescence is a qualitative scale. The introduction in the future of a quantitative evaluation of the degree of fluorescence may discriminate objectively and more precisely the various lesions and their histological stage.

4 Histopathological determinants of autofluorescence: a scientific study performed on 25 cases of oral carcinoma

4.1 Background

Oral squamous cell carcinoma (SCC) accounts for 2-4% of all human malignant neoplasms. Latest World Health Organization (WHO) data report an incidence of about 350000 new cases in 2018. Diagnosis usually occurs at a late stage.

OSCC development is, in most cases, associated to some risk factors, including tobacco use, alcohol abuse, several viral infections and the presence of oral potentially malignant disorders (PMD) (Warnakulasuriya, 2009).

Pathogenesis of OSCC is a multistage process based on the accumulation of alterations, which interfere with cells homeostasis, leading to uncontrolled proliferation, invasion of surrounding tissues and colonization of distant sites (Rivera & Venegas, 2014). Malignant transformation is thought to be the consequence of exposure to factors able to promote changes in the chromosomal pattern of a single cell, affecting both the structure of the genetic material and its genic expression (Gupta & Johnson, 2014).

OSCC may affect all oral subsites. Clinical manifestations are very heterogeneous, the most common being mucosal ulcerations. Other manifestations include nodules, erosion, exophytic lesions and white and/or red patches. Symptoms such as pain, burning sensation, bleeding are variously reported (Troeltzsch, Knösel, Eichinger, & al, 2014).

Overall 5-year survival-rate of patients with OSCC is less than 50% (Sciubba, 2001). Prognosis depends on stage at diagnosis, as defined through the Tumor-Node-Metastasis (TNM) staging system, which takes into account the size (T), involvement of regional lymph-nodes (N) and presence or absence of distant metastases (M) (Edge & Compton, 2010). Early diagnosis (Stage I) is associated to a 5-year survival rate of

approximately 80-90%, the cost of therapy being significantly lower in such cases (Sciubba, 2001).

Current gold standard for OSCC and PMD diagnosis is histopathologic analysis, usually performed on preoperative incisional biopsies. However, a comparison of the degree of dysplasia in the biopsies with that of the whole lesion demonstrated variation with concurrent diagnosis in 49% of the lesions (Holmstrup, Vedtofte, Reibel, & Stoltze, 2006). Several tools have been proposed in order to improve the diagnostic accuracy and to possibly help the identification of areas most suspicious of dysplastic or neoplastic alterations. However, the use of such diagnostic aids approaches is associated to somewhat low sensitivity and/or specificity (Giovannacci, Vescovi, Manfredi, & Meleti, 2016).

Biologic tissues (including oral mucosa) have the ability to absorb and re-emit specific light wavelengths, detectable through spectrophotometric devices. Such a phenomenon is known as "autofluorescence" (AF) (Croce & Bottiroli, 2014).

Despite a growing interest on oral AF, its biophysical and biochemical backgrounds are mostly unknown (Schantz, Savage, Sacks, & Alfano, 1997). Even though some specific human endogenous fluorophores (molecules responsible for AF) have been described in detail, there is a gap of knowledge on how changes in their structure and/or concentration may affect fluorescence. Fluorophores belong to a variety of categories, including, among others, proteins (e.g. collagen, elastin), amino acids (tryptophan), co-enzymes (NADH, NADPH and FAD) and organic compounds as porphyrin (Vedeswari, Jayachandran, & Ganesan, 2009) (Nazeer, Asish, Venugopal, Anita, & Gupta, 2014) (Gurushankar, Nazeer, Jayasree, & Krishnakumar, 2015) (Jayanthi, et al., 2009) (Lane, et al., 2006).

Several devices evaluating tissues AF have been developed and commercialized in the last two decades (Nazeer, Asish, Venugopal, Anita, & Gupta, 2014) (Jayanthi, et al., 2009) (Lane, et al., 2006) (Kikuta, Iwanaga, Todoroki, & al., 2018). Among these, the Velscope® system (LED Medical Diagnostics Inc., Barnaby, Canada) has been proposed

as visual diagnostic aid for PMD e malignant lesions of the oral mucosa (Morikawa, Kosugi, & Shibahara, 2019). However, rigorous data on diagnostic specificity and sensitivity of the Velscope® system are still lacking and controversial results on its usefulness have been drawn by different studies (Morikawa, Kosugi, & Shibahara, 2019) (Giovannacci, Vescovi, Manfredi, & Meleti, 2016).

According to some Authors, clinically healthy oral mucosa, evaluated through the Velscope® system, appears bright green (Ganga, et al., 2017). By contrast, specific alterations of the mucosal architecture (including presence of malignant lesions) may display a wide range of AF patterns, varying from hypo fluorescent (dark) to hyperfluorescent (very bright). A commonly reported observation is that oral tissues affected by dysplastic and/or neoplastic alterations lose the ability to emit AF, appearing darker than surrounding normal tissue, at Velscope® examination. Such a finding has been confirmed by some clinicopathological studies (Ganga, et al., 2017) (Yamamoto, et al., 2017) (Cicciù, et al., 2017). The usefulness of Velscope® a visual aid has however been somewhat criticized, as the loss of AF is not restricted to neoplastic lesions (Morikawa, Kosugi, & Shibahara, 2019). Benign ulcers, inflammatory disorders and physiologic conditions (e.g. fissured tongue) may well display some degree of loss of AF, making the use of the Velscope® system somewhat difficult, especially for dentists not trained in oral medicine. Moreover, contrarily to expectations, some malignant lesions may have an hyperfluorescent pattern. It is therefore evident a lack of knowledge on the specific histopathologic features associated to AF variations.

The present study has been designed in order to determine which are the main histopathological features possibly related to variations of AF patterns in a set of oral SCC and verrucous carcinoma (VC).

4.2 Material and methods

The present study was approved by the Ethical Committee of the Academic Hospital of Parma (n°46556/17).

Twenty-five oral lesions with histological diagnosis of SCC or VC, from 17 patients (males: 5; females: 12; mean age: 69 - min: 39, max: 90) were included in the present evaluation. All lesions were evaluated with regard to AF features before excisional or incisional biopsy.

4.2.1 Autofluorescence features

Target tissues were stimulated through irradiation with a blue-violet light (410-30 nm wavelength) and AF was recorded through the VELscope® system (LED Medical Diagnostics, Inc, Barnaby, BC, Canada).

AF was assessed as follows: 1. normofluorescence, when a lesion did not show fluorescence differences with regards to the surrounding tissues; 2. hypofluorescence, when a lesion displayed a darker aspect; 3. hyperfluorescence, when a lesion showed a white, shining appearance with regard to the green surrounding background.

4.2.2 Histopathological features

All specimens were stained with hematoxylin and eosin (H&E). Histopathological evaluation was performed by an oral pathologist unaware of the AF pattern of the lesion. An optical microscope (Nikon Eclipse 80i) associated to a digital camera (Nikon Digital Sight DS-2Mv) were used for specimens' analysis.

Eight histological categories were investigated, in order to identify which histopathological features are possibly related to the pattern of AF:

a) mean width of the entire epithelium (MWE);

b) mean width of the keratin layer (MWK);

c) mean width of the epithelium without taking into account the overlying keratin;

d) overall area of the epithelium (OAE);

e) mean depth of inflammatory infiltrate (MDI). For each specimen, severity of inflammatory infiltrate was taken into account (classified as “mild”, “moderate” and “severe”);

f) overall area of blood vessels (OAV);

g) mean area of blood vessels (MAV) and

h) mean diameter of blood vessels (MDV). Evaluations were performed through the Nikon NIS-Elements software® (3.06 version). All measures were taken at 4X magnification except for OAV, MAV and MDV which were taken at 10X magnification. Magnification does not influence measures (0.62 micron/pixel) when using the Nikon NIS-Elements software® (3.06 version).

1. MWE was measured in micrometers, taking into account the mean of 5 consecutive values: maximum, minimum and 3 random lengths of the epithelium, through the whole specimen. Maximum length was defined as the longer distance between the tip of epithelium (including keratin) and the neoplastic front of invasion in the connective tissue (Figure 4.1)
2. MWK was measured in micrometers, taking into account the mean of 5 consecutive values: maximum, minimum and 3 random lengths of the keratin, through the whole specimen (Figure 4.2).
3. MWE without keratin (micrometer): was obtained through subtraction of MWK from MWE.
4. OAE was measured in squared micrometers, taking into account the 3 (most representative) consecutive observational fields of dysplastic epithelium. Keratin was not included (Figure 4.3).
5. MDI, was measured in micrometers, taking into account the mean of 5 consecutive values: maximum, minimum and 3 random lengths of the inflammatory infiltrate around the tumor (Figure 4.4).

6. OAV and MAV were measured in squared micrometers and MDV in micrometers. We took in consideration the observation field with the highest density of blood vessel (Figure 4.5).

Specimens not fully evaluable with regard to one or more of the categories investigated were excluded.

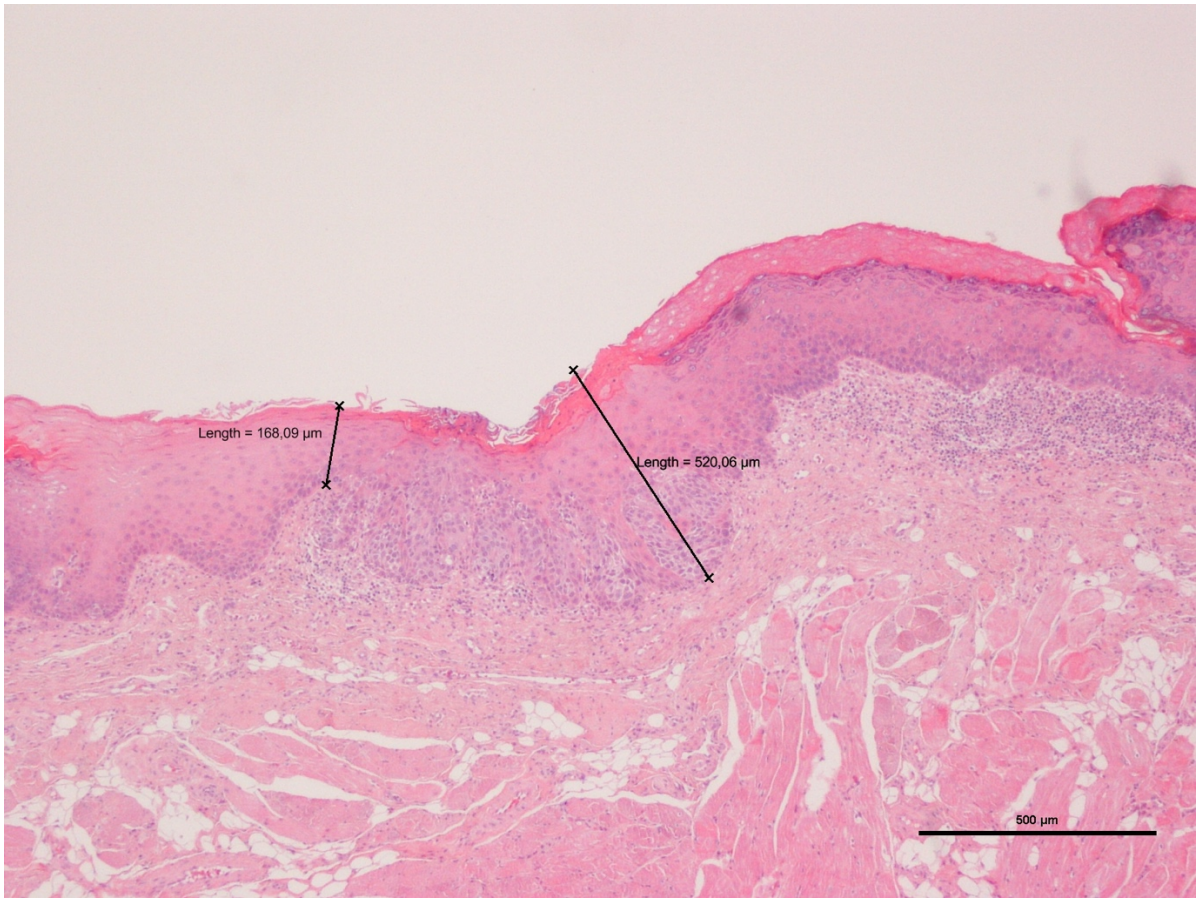

Figure 4.1 Maximum and minimum length of the epithelium (H&E staining, 4X magnification)

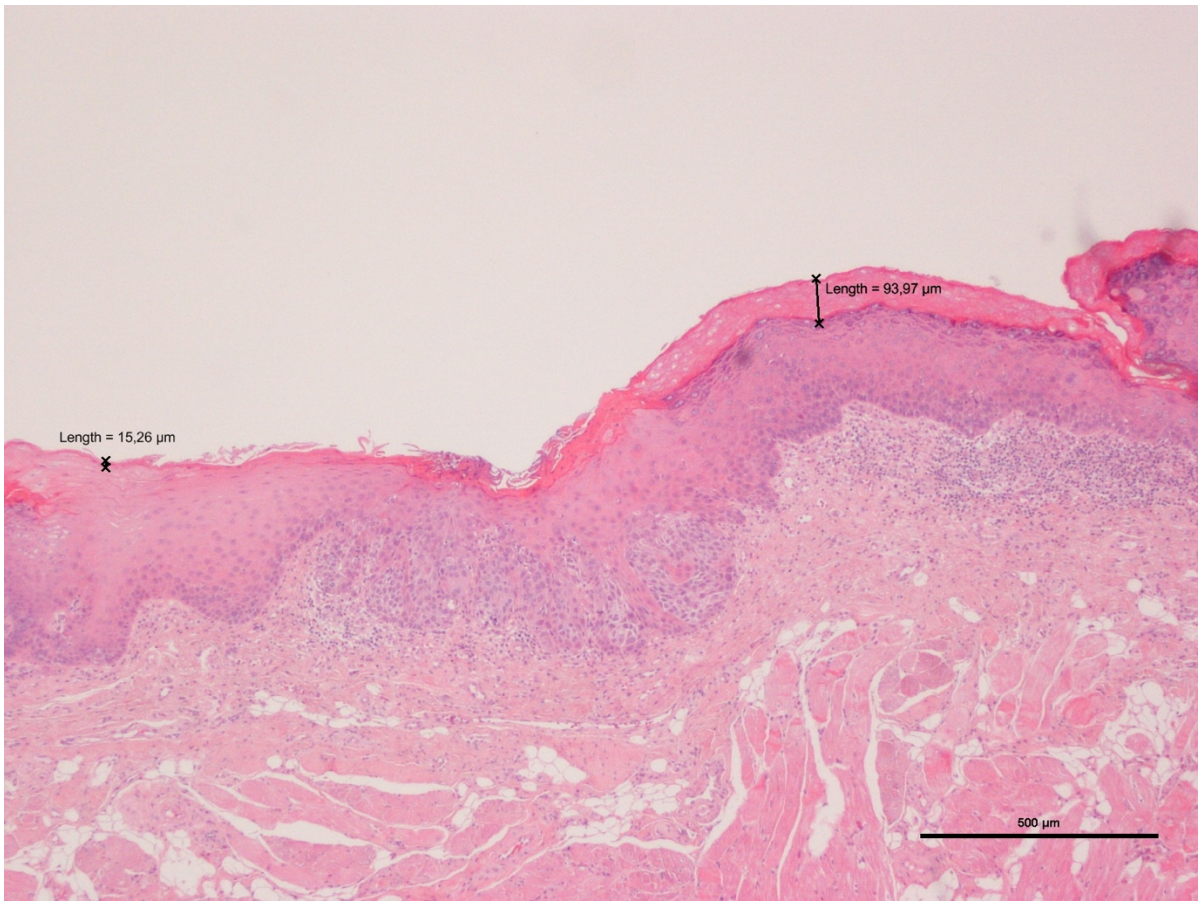

Figure 4.2 Maximum and minimum length of the keratin layer (H&E staining, 4X magnification)

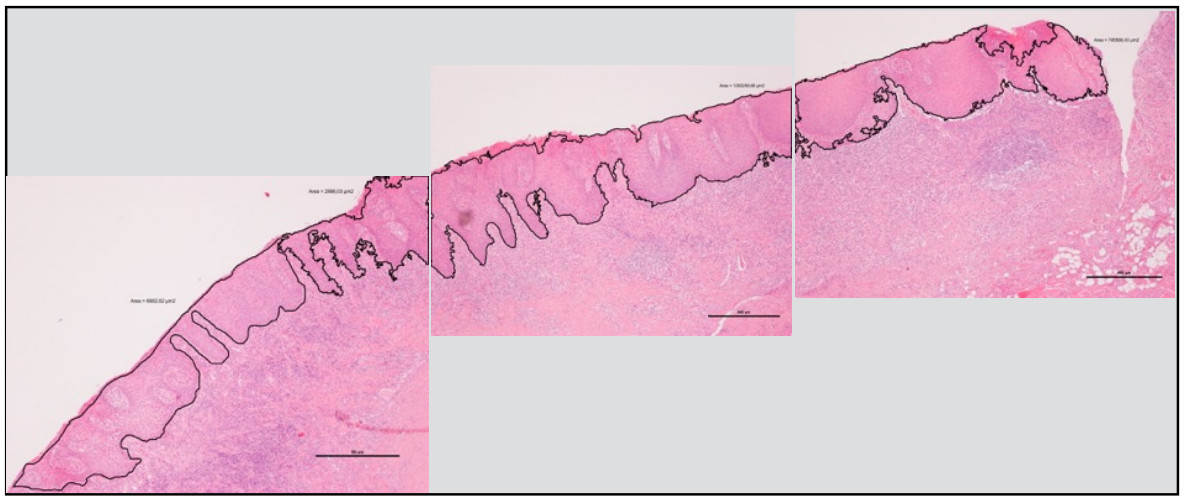

Figure 4.3 Overall area of the epithelium in 3 consecutive fields (H&E staining, 4X magnification)

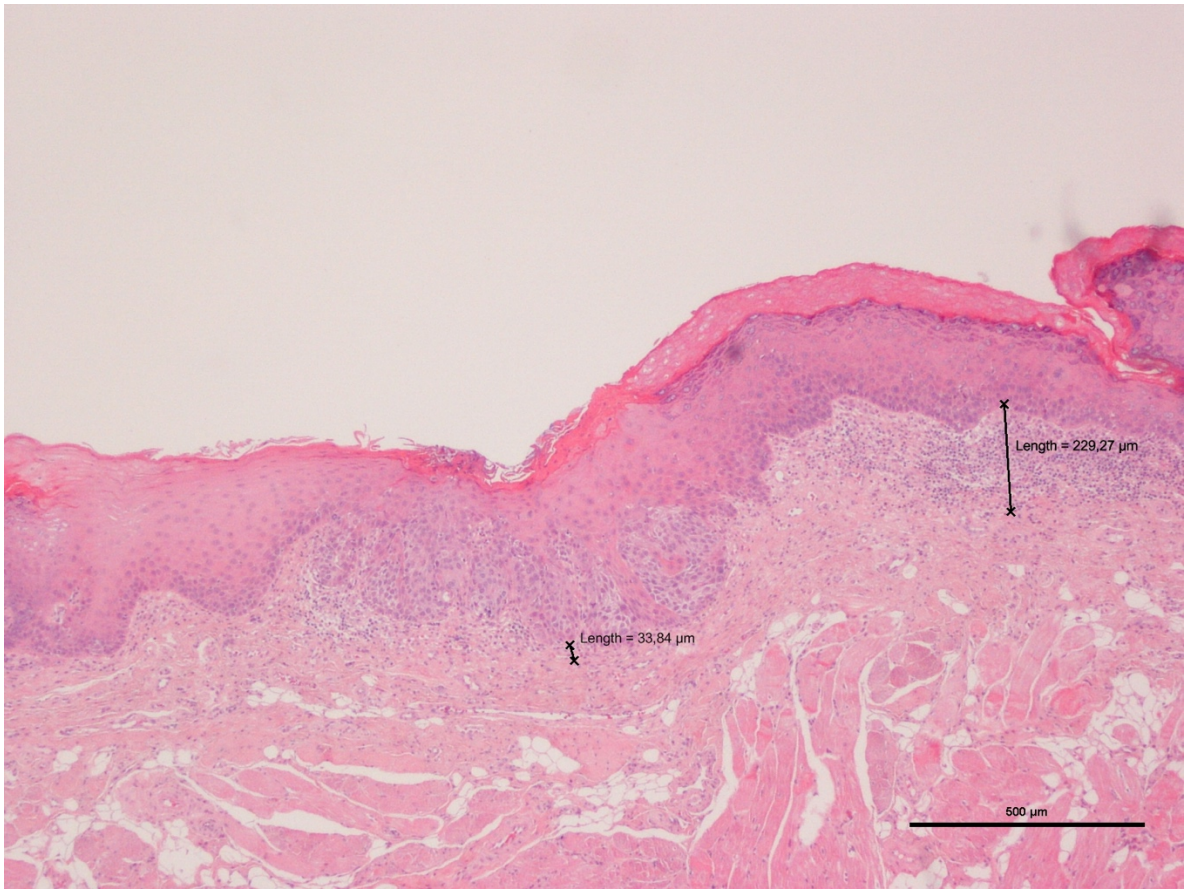

Figure 4.4 Maximum and minimum depth of inflammatory infiltration (H&E staining, 4X magnification)

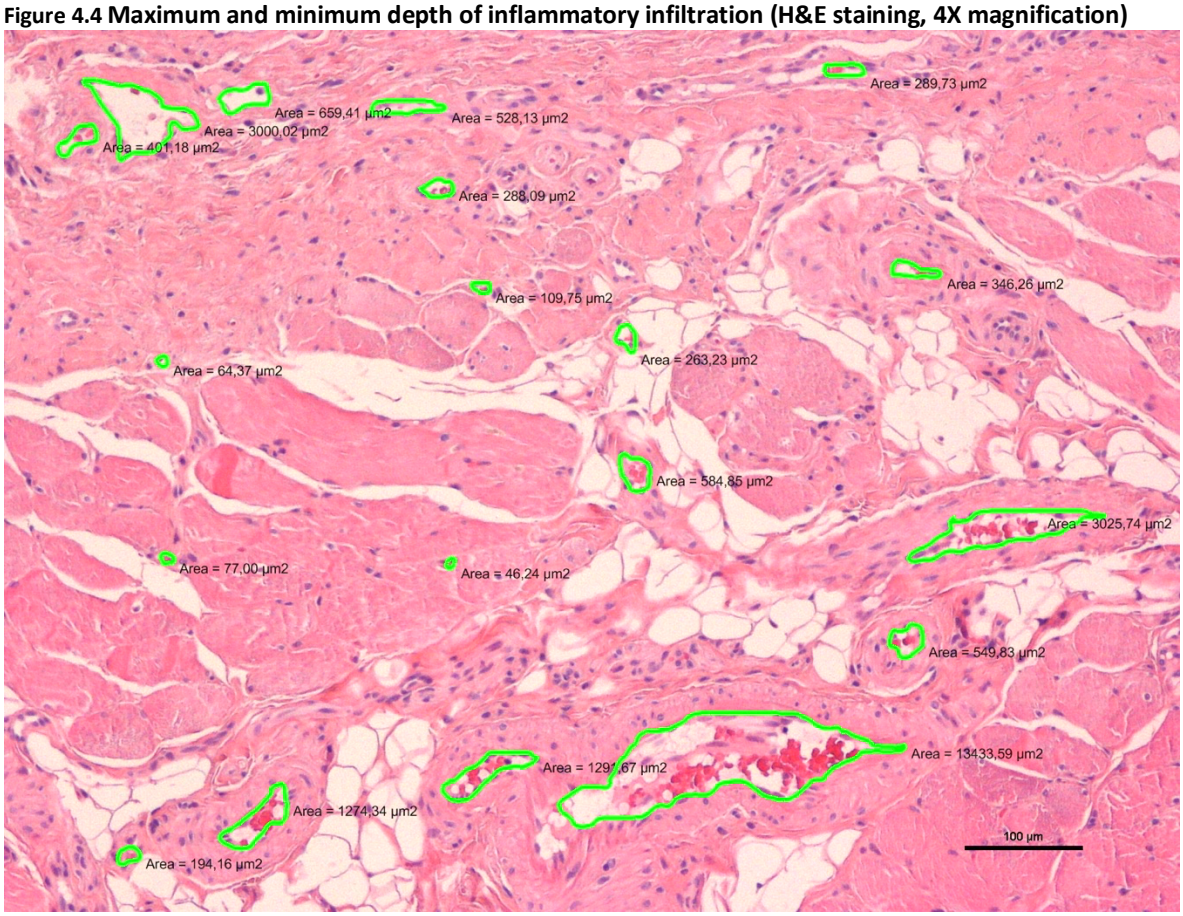

Figure 4.5 Overall area of blood vessel in one field of observation (H&E staining, 10X magnification)

4.2.3 Statistical analysis

Data analysis was performed using IBM-SPSS statistical package version 22.

Statistical analysis was obtained for the main descriptive indexes among which, mean, median, mode, 5% trimmed mean, variance, standard deviation, interquartile range, minimum, maximum, asymmetry, and kurtosis coefficients. Where relevant, standard errors and the corresponding 95% confidence intervals were also calculated. Qualitative characters have been reported in frequency tables and expressed as absolute frequencies, relative frequencies, cumulated frequencies and percentages. For the part of graphic analysis, histograms and box-plots were used. Histograms are useful to visualize the shape of the data distribution and to determine the presence of anomalous values, while the box-plots immediately make visible the differences in the central trend (median) between the different groups.

Both parametric tests (Student's t-test) and non-parametric tests (Mann-Whitney U-test) were used for groups comparisons between the continuous variables. The latter was preferred to the t-test when the data showed a clear deviation from the Normal distribution and therefore the validity of the t test was dubious.

Binary logistic regression was used to test the possible association between fluorescence expression (hyper, hypo) and the main covariates and factors. All the results were considered statistically significant for a p-value less than 5% ($p < 0.05$).

4.3 Results

Twenty specimens (2 VC and 18 SCC) from 15 patients (5 males and 10 females) were considered eligible for complete evaluation of all the histological categories. Data on oral subsite involved, clinical presentation, histopathologic diagnosis and AF are reported in Table 4.1. Twelve (60%) lesions were classified as hypofluorescent and 8 (40%) were hyperfluorescent.

Table 4.1 Clinical, histopathological and AF features of 20 cases of SCC and VC

Specimen	Oral site	Clinical presentation	AF pattern*	Histopathological diagnosis
1	cheek	non homogeneous white and red, harden	hypo-fluorescent	VC
2	cheek	non homogeneous red, harden	hypo-fluorescent	in situ OSCC
3	tongue	non homogeneous red, harden	hypo-fluorescent	in situ OSCC
4	tongue	non homogeneous red, ulcerated	hypo-fluorescent	infiltrative OSCC
5	tongue	homogeneous white, harden	hyper-fluorescent	in situ OSCC
6	gingiva	non homogeneous white and red, harden	hypo-fluorescent	in situ OSCC
7	tongue	non homogeneous white and red, harden	hyper-fluorescent	infiltrative OSCC
8	tongue	non homogeneous red, harden, ulcerated	hypo-fluorescent	in situ OSCC
9	hard palate	homogeneous red	hypo-fluorescent	in situ OSCC
10	gingiva	non homogeneous white and red, harden	hypo-fluorescent	infiltrative OSCC
11	tongue	non homogeneous red, ulcerated	hypo-fluorescent	infiltrative OSCC
12	tongue	non homogeneous red, ulcerated	hypo-fluorescent	in situ OSCC
13	tongue	non homogeneous white, ulcerated	hyper-fluorescent	VC
14	tongue	non homogeneous white and red, harden, ulcerated	hyper-fluorescent	infiltrative OSCC
15	tongue	non homogeneous white and red, harden, ulcerated	hypo-fluorescent	in situ OSCC
16	tongue	non homogeneous red, harden, ulcerated	hypo-fluorescent	infiltrative OSCC
17	tongue	non homogeneous white, harden	hyper-fluorescent	in situ OSCC
18	gingiva	non homogeneous white and red, harden, ulcerated	hyper-fluorescent	microinvasive OSCC
19	soft palate	non homogeneous white and red, harden, ulcerated	hyper-fluorescent	in situ OSCC
20	hard palate	non homogeneous white and red, harden, ulcerated	hyper-fluorescent	in situ OSCC

Legend:
* AF pattern is specifically referred to the site of where the biopsy was taken; VC: Verrucous Carcinoma; OSCC: Oral Squamocellular Carcinoma

4.3.1 Mean width of the epithelium

Mean MWE within the group of hypofluorescent lesions was 513 µm (SD: 264; SE: 72.2) while it was 790 µm (SD: 404; SE: 143) among hyperfluorescent lesions. MWE differences were not statistically significant among AF levels (t and Mann-Whitney U tests: p: 0.116 and 0.181, respectively), although we may guess that this negative result may be due to the limited sample size. Larger sample size could prove that hyperfluorescent carcinomas have indeed a thicker epithelium.

4.3.2 Mean width of the keratin

Among hypofluorescent lesions, mean MWK was 41.3 µm (SD: 34.4; SE: 9.93) while it was 197 µm (SD: 69.9; SE: 24.7) for hyperfluorescent cancers. Either parametric and non-parametric tests highlighted a strong statistical association between MWK and typology of AF ($p < 0.001$, for all tests). Particularly, hypofluorescent lesions have a decreased width of the keratin layer when compared to hyperfluorescent specimens.

4.3.3 Mean width of the epithelium without keratin

When MWK was subtracted to MWE, no statistically significant differences could be observed between the hypofluorescent and hyperfluorescent lesions with all the tests used. Particularly, mean values are very similar in the hypo and hyperfluorescent groups, being 496 µm (SD: 258; SE:74.4) and 463 µm (SD: 444; SE:157), respectively.

4.3.4 Overall area of epithelium

OAE was higher among hyperfluorescent lesions (3.37e+6 μm^2; SD: 2.37e+6; SE: 837481) than among hypofluorescent (2.51e+6 μm^2; SD: 1.38e+6; SE: 399328). All tests did not disclose statistically significant differences.

4.3.5 Mean depth of the inflammatory infiltration

Mean MDI within the group of hypofluorescent lesions was 248 µm (SD: 172; SE: 49.7) while it was 236 µm (SD: 148; SE: 52.4) among hyperfluorescent lesions. MDI was

not statistically different among the typology of AF. Severity of inflammatory infiltrate was homogeneously distributed among hypo fluorescent and hyperfluorescent cases ("mild": 3 in hypo and 3 in hyper; "moderate": 3 in hypo and 3 in hyper; "severe": 4 in hypo and 4 in hyper).

4.3.6 Blood vessels

Mean OAV were comparable among the two groups (hypofluorescent: 28641 μm^2, SD: 44682, SE: 1289; hyperfluorescent: 107418 μm^2; SD:152320; SE:53853) and not statistically different. Similarly, MDV did not significantly differ among the hypo and hyperfluorescent lesions (38.8 µm; SD: 14.1; SE: 4.08 *vs* 48.2 µm; SD: 27.9; SE :9.87. p: 0.328; 0.397; 0.792). On the other hand, a mild trend toward significance was observed when the MAV of the two groups was considered. In fact, mean MAV in hyperfluorescent lesions was 3755 μm^2 (SD: 3697, SE: 1307) and it was 1711 μm^2 (SD: 1352, SE: 390). Student's t-test resulted in a p-value of 0.094.

A tentative classification produced by a binomial logistic regression model including the predictors MWE, MWK, MAV, and OAV has shown a convergence to a solution only for a model with the variable MWK, with a prediction accuracy of 90% regarding the typology of fluorescence, sensitivity = 87.5% and specificity = 91.7% (Table 4.2, Figure 4.6 and 4.7). None of the other variables was statistically significant, very likely because of the low sample size. The model confirmed the relative importance of the variable MWK.

Table 4.2 Pearson's correlation coefficient and Spearman's rho values among the variables analyzed

Correlation Matrix									
		MWE	MWK	MWE without keratin	OAE	MDI	OAV	MAV	MDV
MWE	Pearson's r p value	- -	0.208 0.378	0.964 <0.001	0.790 <0.001	0.160 0.501	0.580 0.007	0.544 0.013	0.473 0.035
	Spearman's rho p value	- -	0.299 0.199	0.926 <0.001	0.689 0.001	0.426 0.063	0.329 0.156	0.362 0.117	0.319 0.171
MWK	Pearson's r p value		- -	-0.061 0.798	-0.022 0.926	-0.091 0.702	0.075 0.754	0.177 0.455	-0.043 0.857
	Spearman's rho p value		- -	-0.018 0.942	0.158 0.505	0.038 0.876	0.063 0.792	0.099 0.677	0.015 0.952
MWE without keratin	Pearson's r p value			- -	0.813 <0.001	0.188 0.427	0.572 0.008	0.507 0.022	0.494 0.027
	Spearman's rho p value			- -	0.731 <0.001	0.423 0.065	0.463 0.041	0.466 0.04	0.438 0.055
OAE	Pearson's r p value				- -	0.277 0.236	0.743 <0.001	0.684 <0.001	0.752 <0.001
	Spearman's rho p value				- -	0.332 0.152	0.684 0.001	0.66 0.002	0.687 0.001
MDI	Pearson's r p value					- -	0.145 0.542	-0.025 0.915	0.051 0.832
	Spearman's rho p value					- -	0.074 0.758	-0.008 0.977	-0.017 0.947
OAV	Pearson's r p value						- -	0.772 <0.001	0.757 <0.001
	Spearman's rho p value						- -	0.881 <0.001	0.859 <0.001
MAV	Pearson's r p value							- -	0.921 <0.001
	Spearman's rho p value							- -	- -
MDV	Pearson's r p value								- -
	Spearman's rho p value								- -

Omnibus Likelihood Ratio Tests

Predictor	χ^2	df	p
Mean width of the keratin layer (MWK)	22.56	1	< .001
Mean width of the entire ephitelium (MWE)	5.76e-10	1	1.000
Mean area of blood vessels (MAV)	3.64	1	0.056

Classification Table – fluo

	Predicted		
Observed	ipo	iper	% Correct
ipo	12	0	100
iper	0	8	100

Note. The cut-off value is set to 0.5

Model Coefficients

Predictor	Estimate	SE	Z	p	Odds ratio
Intercept	-181.2215	212217.2	-8.54e−4	0.999	1.98e-79
Mean width of the keratin layer (MWK)	0.7849	964.2	8.14e-4	0.999	2.19
Mean width of the entire ephitelium (MWE)	0.0471	111.0	4.25e-4	1.000	1.05
Mean area of blood vessels (MAV)	0.0159	24.2	6.59e-4	0.999	1.02

Note. Estimates represent the log odds of "fluo = iper" vs. "fluo = ipo"

Predictive Measures

Accuracy	Specificity	Sensitivity	AUC
1.00	1.00	1.00	1.00

Note. The cut-off value is set to 0.5

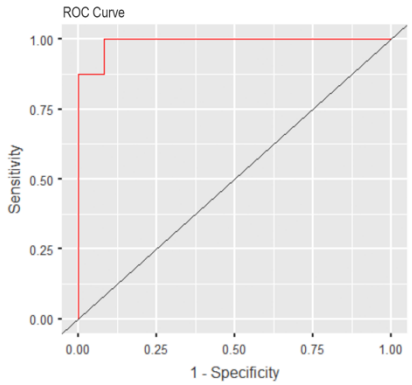

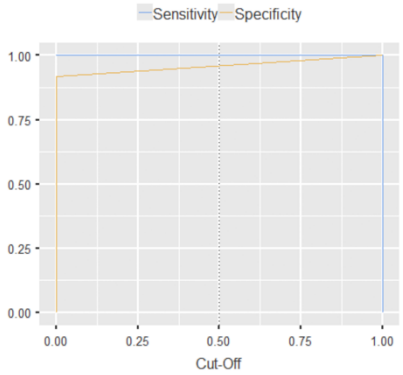

Figure 4.6 Binomial logistic regression model. Only the mean width of keratin shows convergence toward accuracy, specificity and sensitivity

Model Fit Measures

				Overall Model Test		
Model	Deviance	AIC	R^2McF	χ^2	df	p
1	2.31e-9	8.00	1.000	26.9	3	< .001

Figure 4.7 Model fit measures of binomial logistic regression.

4.4 Discussion

In the last 40 years, many researchers tried to develop new techniques potentially allowing early and non-invasive diagnosis of PMDs and malignant lesions. Proposed diagnostic aids, from time to time, included basic tools, such as vital staining (toluidine blue, Bengal rose, *etc*.), biochemical devices (e.g. chemiluminescence and 5-aminolevulinic acid induced protoporphyrin IX fluorescence) or more sophisticated technologies such as optical spectroscopies (including fluorescence, depth-sensitive optical, elastic scattering and Raman spectroscopy) (Petruzzi, Lucchese, Nardi, & al., 2014) (Pallagatti, Sheikh, Aggarwal, & al, 2013) (Mallia, et al., 2008) (Epstein, Silverman, Epstein, Lonky, & Bride, 2008) (Du, Li, Chen, & al., 2007) (Leunig, Betz, Mehlmann, & al., 2000).

Non-conventional approaches (such as salivary genomics, transcriptomics, proteomics and metabolomics) are still under research, their diffusion through commercially available tests being somewhat limited (Saxena, Sankhla, Sundaragiri, & Bhargava, 2017). Moreover, the specificity and sensibility of such tests are still not very high (Elashoff, Zhou, Reiss, & al., 2012). As a matter of fact, these methods did not show a higher diagnostic accuracy when compared to careful clinical inspection (particularly if performed by oral medicine specialists) followed by biopsy and histological evaluation of suspicious lesions (Patil, Arakeri, Alamir, & al., 2019).

Histological evaluation of specimens of (oral) lesions can sometime be misleading. In fact, it is well known that incisional biopsies may not reflect the histopathological severity of the whole lesion, thus leading to the risk of underestimating the diagnosis, as well as to incorrect therapies (Holmstrup, Vedtofte, Reibel, & Stoltze, 2006). The impossibility to identify with certainty mucosal areas with epithelial alterations is associated to other disadvantages such as the possible need for more invasive interventions (e.g. multiple biopsies or excisional biopsy) and the strong dependence

from operator skills and knowledge (Holmstrup, Vedtofte, Reibel, & Stoltze, 2006) (Giovannacci, Meleti, Merigo, & al., 2015).

AF is a fascinating phenomenon that has attracted the interest of both researchers and clinicians (Lane, et al., 2006) (Kikuta, Iwanaga, Todoroki, & al., 2018). The possibility to highlight alterations (dysplasia and malignancy), even confined within a small portion of tissue and/or in absence of clinically evident lesions, seems very promising. However, despite a presumptive ability of AF to highlight some histological alterations, the biochemical mechanism underlying such as physicochemical process is mostly unknown.

Several fluorophores have been described in detail (e.g. specific types of collagen, keratin, elastin or NADH and FAD) but their possible role and localization within dysplastic and malignant tissues have never clearly been demonstrated (Schantz, Savage, Sacks, & Alfano, 1997). The loss of AF is believed to reflect a complex mixture of alterations to intrinsic tissue fluorophore distribution (Poh, Zhang, Anderson, & al., 2006). There is evidence that some of the abovementioned molecules, in peculiar biochemical states (e.g. reduced NADH and oxidized FAD) are hypo-fluorescent (dark) (Croce & Bottiroli, 2014) (Gào & Schöttker, 2017). Moreover, it has been hypothesized that collagen alterations and a reduced width of the keratin layer might be associated to loss of fluorescence (Richards-Kortum & Sevick-Muraca, 1996). Therefore, some Authors tried to explain the typical dark appearance observed in some cases of oral dysplastic lesions/carcinomas on the basis of the possible presence of one or more of the described features (Burian, Schulz, Probst, & al., 2017). On the other hand, some rather unspecific molecules (e.g. hemoglobin), which are present, also in non-neoplastic, inflammatory lesions may be a confounding factor, which makes the understanding of AF mechanism very difficult (Ganga, et al., 2017).

The present study has been designed in order to try to shed some light on such a controversial issue. To the best of our knowledge, for the first time, we tried to find a

correlation between the clinical detectable pattern of AF and some definite histopathological features.

The model of oral carcinoma (either squamous and verrucous), seems to fit the purpose of the present research. In fact, rather than PMDs (and their dysplastic histological features), carcinomas harbor a series of alterations which are presumptively at high degrees of development.

The results of the present evaluation showed that the width of epithelium of oral mucosal malignant lesions (excluding the presence of the variable "keratin") does not significantly influence AF. However, it seems worthy to mention that hyperfluorescent bright lesions have a slightly thicker epithelium (790 µm) when compared to hypo-fluorescent lesions (513 µm). The absence of statistically significant differences may be due to the limited sample size. Larger sample size could prove that hyperfluorescent carcinomas have indeed a thicker epithelium. Such a finding seems to oppose the hypothesis that loss of AF depends on specific cellular features of dysplatic and/or malignant keratinocytes (e.g. hyperchromatism associated to higher nuclear/cytoplasm ratio and pleomorphism) (Poh, Zhang, Anderson, & al., 2006). If that was the case, thicker malignant epithelia (all in all containing higher quantity of nuclear material) should have a lower fluorescence than thinner ones, which is in contrast with the results of the present and previous studies (Kikuta, Iwanaga, Todoroki, & al., 2018) (Lohmann, Mussmann, Lohmann, & al, 1989).

When different epithelial compartments (cellular and keratin layers) are evaluated separately, it appears evident that keratin is, by far, the main portion of the whole oral epithelium that influences AF patterns. In the present research, epithelia from malignant lesions with thicker keratin layers are bright (hyper-fluorescent) whereas lesions with thinner keratin layers are dark (hypo-fluorescent).

Clinical implications of AF depending on epithelial and keratin widths are various. Taking into account that hyperplasia and increase of keratinization are more frequently observed in PMDs such as leukoplakia, in well-differentiated SCC (e.g. presence of

keratin pearls) and in verrucous carcinoma (e.g. presence of keratin plugs) it is possible to hypothesize that brighter lesions are presumptively at an early stage of the malignant developmental process. On the contrary, oral malignant lesions with thin epithelial and/or keratin layers (or without keratin at all) are supposedly composed of cells far from their original developmental line (e.g. undifferentiated SCC) and probably to a later stage of malignant development. Moreover, different AF patterns within the same lesion (e.g. inhomogeneous lesions with both increase and loss of AF) might guide the clinician in the choice of the site where to perform a biopsy, taking into account that hypo-fluorescent areas may supposedly correspond to a more advanced stage of malignant development or to a less differentiated group of cells.

The overall area of epithelium (without keratin) did not statistically differ between hypo- or hyperfluorescent lesions. Such a finding gives support to the mentioned hypothesis that keratin, more than the epithelium itself is the key variable influencing oral mucosa AF. On the other hand, it should be borne in mind that the present evaluation has been performed on three consecutive microscopic fields of observation and not on the whole epithelial tissue in the specimen. Such fields were obviously not always homogeneous with regard to histologic appearance and they included a range of alterations, in some cases varying from normal to hyperplastic to atrophic epithelium to invasive carcinoma.

According to some observations, oral lesions associated to inflammatory disorders (e.g. oral lichen planus, blistering diseases, *etc.*) show some degrees of AF alterations (Tiwari, Kujan, & Farah, 2019). It has been speculated that such alterations may depend on specific microscopic features directly related to inflammation (Kikuta, Iwanaga, Todoroki, & al., 2018). Among these, presence of inflammatory infiltrate (particularly accumulation of lymphocytes outside the blood and lymphatic vessels) and increased presence of blood (within pre-existing or newly-formed vessels), have been advocated by some Authors (Kikuta, Iwanaga, Todoroki, & al., 2018) (Tiwari, Kujan, & Farah, 2019). With regard to blood, the presence of the *heme* complex (within hemoglobin) is at the

basis of the well-known phenomenon of the Soret band, a peak of absorption corresponding to a wavelength of around 400 nm, in the blue region.

In the present evaluation, the inflammatory infiltrate as well as the area and the diameter of blood vessels were evaluated separately. The variables related to blood vessels were used as surrogates of the quantity of blood present in the specimens.

Depth and severity of inflammatory infiltrate were very similar between hypo- and hyperfluorescent lesions. The results of the present study did not show statistically significant associations between quantity of inflammatory cells (beneath and around malignant keratinocytes) and AF. However, it is not possible to exclude that the influence of inflammation on AF may be somewhat altered by the presence of epithelium and keratin. Such histological compartments, in fact, may well act as a shield, limiting the penetration of light in the superficial and/or deep stromal layers, thus preventing the influence of inflammatory cells on AF.

Overall area and mean diameter of blood vessels were not statistically associated to AF patterns. The mean area of blood vessels, in the portion of specimen where they were more represented, resulted not statistically significant (p-value of 0.094). However, blood vessels in hyperfluorescent lesions have a mean area greater than those in hypo-fluorescent lesions.

Taking into consideration that such a finding might merely be casual, it can be hypothesized that a higher quantity of relatively small blood vessels (e.g. phase of (neo)angiogenesis) can, altogether with other factors, be associated to the loss of AF. Even if not statistically significant, also the mean diameter of vessels is smaller in hypo-fluorescent lesions (38.8 µm *vs* 48.2 µm). Hypo-fluorescence could therefore be typical in stages of tumor development in which the formation of new, small, blood vessels occur. It should be borne in mind, however, that similarly to what hypothesized for the inflammatory infiltrate, also the influence of blood vessels (and, in last instance, of blood) on AF might be limited by the presence of the keratin and epithelium “shield”.

The binomial logistic regression model applied to the variables evaluated in the present study showed that MWK is the only histopathologic features that shows a prediction accuracy of 90% regarding the typology of fluorescence (sensitivity = 87.5% and specificity = 91.7%). It is possible therefore to state that the quantity of keratin in a tissue (either in the surface and in the deepest part of the epithelium of the oral mucosa) accounts for the fluorescence properties of the tissue.

4.5 Conclusion

Taking into account the possible bias of the study (e.g. limited sample size; histological measures possibly not reflecting the microscopic features of the whole specimen) it is possible to conclude that AF features of oral malignant lesions are strongly associated to the depth of their keratin layer. Even though also the area of blood vessels may play some role (lesions with smaller blood vessel appears more often hyperfluorescent) such a finding should be confirmed by further researches.

Autofluorescence evaluation seems to be a useful tool in differentiating hyperkeratinized from hypokeratinized lesions. Such a peculiarity might help clinicians by serving as a diagnostic aid, particularly with regard to where to perform a biopsy, in the context of non-homogeneous lesions.

5 Correlation between Autofluorescence intensity and histopathological features in Non-Melanoma Skin Cancer: an *ex vivo* study

5.1 Background

Non-Melanoma Skin Cancer (NMSC) represents the most common cancer in Caucasians, with continuing increase in incidence worldwide. Basal cell carcinoma (BCC) accounts for 75% of cases of NMSC, and squamous cell carcinoma (SCC) accounts for the remaining majority of NMSC cases. Whilst metastasis from BCC is extremely rare, metastasis from high-risk SCC may be fatal (Samarasinghe & Madan, 2012).

5.1.1 Basal cell carcinoma (BCC)

BCC is the most common malignancy in white population, accounting 15% of all tumours and 75% of all skin cancers. (Lai, Cranwell, & Sinclair, 2018) (Kim, Kus, & Ruiz, 2019) (Midgen, Chang, Dirix, & al., 2018) (Peris, Fargnoli, C, & al, 2019) (AIOM, 2018). The highest incidence rate has been reported in Australia, followed by USA and Europe. (Peris, Fargnoli, C, & al, 2019). In the USA, BCC is diagnosed in 2,8 million patients, while in Italy the incidence rate is 100/100.000 inhabitants (AIOM, 2018) (Midgen, Chang, Dirix, & al., 2018). In recent decades, however, in most European countries the incidence of NMSC has been rising rapidly and is almost approaching that in USA (Wild, Weiderpass, & Stewart, 2020), even if the true incidence of BCC may be significantly underestimated because in most cancer registers only the first histologically confirmed BCC per patient is recorded (Peris, Fargnoli, C, & al, 2019). Indeed, it is important to underline that BCC is prone to multiplicity, with a substantial risk of developing a subsequent BCC after an initial diagnosis of NMSC. Within 1 year, patients with one index BCC developed one new BCC in 33% of cases, two in 14% or three in 7% (Wild, Weiderpass, & Stewart, 2020) (Marzuka & Book, 2015). Despite the high incidence rate, locally advanced BCC (laBCC) is reported by a retrospective cohort US study to be

0,8% of BCC cases in the US population (Peris, Fargnoli, C, & al, 2019). Even metastatic BCC (mBCC), with histologically confirmed BCC metastases have a very low incidence rate of 0,0028%-0,55%. In a systematic review of 100 published mBCC cases, 50% of patients were reported to have regional metastases and 50% to have distant metastases. Patients with distant metastases were younger (mean age: 58 years) and with a shortened survival (median survival: 24 months) than patients with regional metastases (mean age: 66,3 years; median survival: 87 months)(McCusker, et al., 2014). The age-adjusted mortality rate is also very low: 0,12/100.000 (Kim, Kus, & Ruiz, 2019). The lifetime risk for the development of skin cancer is estimated to be the 20%, with more than 97% being NMSC (Marzuka & Book, 2015). For white-skinned individuals the risk to develop BCC is higher and reaches approximately the 30% (Peris, Fargnoli, C, & al, 2019). NMSCs primarily affect populations of European ancestry, occurring most frequently among the fair-skinned residents of Australia, New Zealand and low-latitude states of US. This shows that the incidence strongly correlates with sun exposure. Incidence also increases with age, even if BCCs tend to present at earlier ages than SCCs. The ratio between the two NMSCs (BCCs and SCCs), in fact, changes from 10:1 at age 40 years to 3:1 at age 60 years (Lomas, Leonardi-Bee, & Bath-Hextall, 2012)(Wild, Weiderpass, & Stewart, 2020). BCC is significantly more common in men than in woman, with a male/female ratio of 2:1 (Peris, Fargnoli, C, & al, 2019), but the incidence among Americans under 40 appears to be increasing especially among women (Marzuka & Book, 2015). The clinical diagnosis of BCC can be commonly performed by naked eye (sensitivity 66,9% - specificity 97,2%) or dermatoscopy (sensitivity 85% - specificity 98,2%; pooled data: sensitivity 91,2% - specificity 95%) (Reiter, et al., 2018). The parameters of sensitivity and specificity were higher for pigmented than non-pigmented BCCs, and the sensitivity increased if the dermatoscopy was performed by experts.

In diagnostic differentiation, dermatoscopy may be fundamental to distinguish BCC from melanoma, SCC (including Bowen's disease) and benign tumours (Peris, Fargnoli,

C, & al, 2019). Pigmented BCCs, in fact, can be a diagnostic challenge because they can show dermatoscopic features suggestive of melanocytic lesions, such as multiple brown-to-black dots/globules, blue/white veil-like structures and nonarborizing vessels (Marzuka & Book, 2015).

This diagnostic tool is also useful in the pre-operative classification of the BCC subtype and in the rating of tumour response to topical treatments (Peris, Fargnoli, C, & al, 2019).

Dermatoscopic diagnosis of BCC is mainly based on the identification of reliable and robust diagnostic parameters such as branching and linear vascular structures (arborizing and superficial telangiectasias), bluish-grey pigmented clods of variable size (ovoid nests and globules and focused dots), radial lines connected to a common base (leaf-like areas), radial lines converging to a central dot or clod (spoke-wheel areas), concentric structures, absence of brown reticular lines (areas of network associated with melanocytic lesions), and multiple erosions or ulceration.

The clinical subtypes are differentiated by the major presence of one of these characteristics: superficial BCC (sBCC) is often associated with multiple erosions, while aggressive subtypes like morpheiform (or sclerodermiform) and infiltrative BCCs are predicted by white scar-like zones with fine linear vessels. Morpheiform BCCs (from 5 to 10% out of BCC) are notorious for their subtlety and, because of a tendency to subclinical spread with the potential for extensive local destruction, are usually more aggressive.

Diagnosis by clinical examination without histopathological examination might be carried out for the small nodular subtype on typical locations (head, neck or trunk), for multiple BCCs in NBCCS and for the sBCC located on trunk and extremities (Peris, Fargnoli, C, & al, 2019).

In most patients, BCC can be effectively treated with standard procedures. However, a minority of patients mature advanced BCC, for which therapies can be challenging and outcomes are poorer (Midgen, Chang, Dirix, & al., 2018).

The category of “difficult-to-treat BCCs” includes common BCCs which specific management problems such as the technical difficulty of maintaining aesthetics and function due to the tumour size or location (eyes, nose, lip and ear); the slightly defined borders often associated with morpheiform subtype or prior recurrence; multiple prior recurrences on the face (requiring much larger excision); prior radiotherapy; patient’s unwillingness to accept the consequences of surgery and patient’s comorbidities interfering with surgery (Peris, Fargnoli, C, & al, 2019).

5.1.2 Squamous cell carcinoma (SCC)

Cutaneous squamous cell carcinoma (cSCC) is the second most common nonmelanoma skin cancer and is emerging as a public health problem, given its increasing incidence and potential for poor outcomes. (Waldman & Schmults, 2019) (Que, Zwald, & Schmults, 2018). The cSCC is typical of old age (6^{th} -7^{th} decade of life) and is predominant in males, while it is rare in subjects aged <45 years, although the incidence of cSCC seems to increase significantly in young subjects in the last few years.

The incidence rate of cSCC compared to melanoma doubles in Europe, and is up to 10 times higher in Australia, thus confirming that this tumor is more susceptible to UV radiation than melanoma, in particular to chronic UV exposure (Peris, et al., 2018).

In 2002, the overall incidence rate of cSCC in Australia - where the highest frequency of non-melanoma skin cancers (NMSC) was recorded - was estimated to be 387 cases per 100,000. (Que, Zwald, & Schmults, 2018).

Data from Australia suggest that most people who develop one lesion will develop more within 3 years; a small proportion will develop more than 20 cancers and this has important consequences for detection and control. (Pandeya, Olsen, & Whiteman, 2017)

The incidence of cSCC was higher in the southern and central United States, where the estimated mortality rate approximates that of renal and oropharyngeal carcinomas and melanoma. (Karia, Han, & Schmults, 2013)

European data show that the age-standardized incidence of cSCC ranges from 9 to 96 per 100,000 male inhabitants and 5 to 68 per 100,000 female inhabitants (2002-2007 estimates). (Que, Zwald, & Schmults, 2018)

No national incidence data for NMSCs are available in Italy. The estimated incidence of cSCC as reported by the single "Skin Cancer Registry" of the Trentino region was 29 per 100,000 inhabitants between 1993 and 1998. (Boi, Cristofolini, Micciolo, Polla, & Dalla, 2003)

According to the latest AIRTUM data, the incidence of SCC of the head and neck area, including skin variants, is 19.46 per 100,000 per year (AIRTUM Working Group, Mallone, Trama, Castaing, & al., 2016)

The data of the Italian Cancer Registries estimated that in 2018 approximately 19,000 new cases of cSCC would be diagnosed, with a higher incidence in males specially after 65 years and with a typical North-South gradient (I numeri del cancro in Italia, 2018).

Unlike basal cell carcinoma (BCC) that rarely metastasizes, cSCC can initially metastasize to regional lymph nodes and subsequently to anatomic sites that are distant from the primary cancer: the most frequent visceral localizations are the lungs, liver, central nervous system and bones. (Peris, et al., 2018). The metastatic overall rate is about 2%, but it is between 10% and 15% for lesions on the lips and ears. (Paolino, Donati, Didona, Mercuri, & Cantisani, 2017). The occurrence of distant metastases – despite their rarity - is associated with a poor prognosis and a median survival of less than 2 years (Que, Zwald, & Schmults, 2018).

The gold standard for the diagnosis of cSCC is histology. A biopsy or excision and histological confirmation should be performed in all clinically suspected cSCCs.

Two different surgical approach may be offered in patients with primary cSCC: conventional surgery with safety margins and micrographically controlled surgery (MCS). Safety excision margins should be adapted to the risk of subclinical extensions and recurrence, as defined by high-risk factors including clinical (tumor diameter > 2

cm, high-risk sites), histological (thickness >6 mm or invasion of subcutaneous fat, perineural invasion [PNI], poor differentiated, desmoplasia) and patient-related criteria (immunosuppression).

The European consensus group suggests a 5 mm margin for low-risk lesions and 6 to 10 mm range margin for cSCC with high-risk lesions although there is currently no unified recommendation for this case. It should be based on individual risk assessment and a constellation of tumor- and patient-related characteristics. In case of positive margins, a re-excision shall be done, for operable cases.

MCS is the collective term used for a surgical technique of removing skin cancer, processing skin tissue in horizontal sections and examining them under a microscope. Two techniques are being used in Europe: Moh's microsurgery (MMS) and 3D histology, the first one making use of frozen sections whereas the second one uses paraffin sections with diverse modifications of sectioning the tissue specimen. These time-consuming procedures are usually reserved for patients with high-risk tumors, in whom MCS provides the best guarantee for complete tumor resection, specially in the head and neck area, due to their conservative methodological approach.

The optimal management of NMSC is based on early and accurate diagnosis, appropriate treatment and monitoring of recurrence. The recent development in the field of optical imaging highlighted potential techniques for the non-invasive diagnosis (photodiagnosis) of NMSC, including the use of fluorescence, diffuse reflectance, Raman spectroscopy, confocal and multiphoton microscopy techniques (Dessinioti, Antoniou, & AJ, 2011) (Drakaki, et al., 2013) (Seidenari, et al., 2012).

In 2014 Drakaki et al. in their review of the literature on the use of fluorescence for the diagnosis and follow-up of BCC reported that AF appears to be a particularly promising technique for early diagnosis and demarcation of the BCC because of its high sensitivity, easy to use, real-time measurements and total non-invasiveness. (Drakaki, Dessinioti, Stratigos, Salavastru, & Antoniou, 2014)

Skin tissues under excitation with UV / blue light seem to show higher AF intensities in healthy skin than BCC, allowing their diagnostic differentiation.

The most accepted hypothesis is that in the malignant tissues, the spectral changes of the fluorescence are due to a decrease in collagen and elastin and a decrease in the levels of NADH, highly fluorescent, and parallel increase in the oxidized form less fluorescent NAD + in the malignant tissue.

Similar AF models have been shown for both superficial and nodular BCCs.

H. Zeng et al. in 1998 showed that the AF spectra of BCC lesions, excited with the HeCd laser at 442 nm showed a reduction in fluorescence intensity compared to the surrounding normal skin, a trend confirmed by the *in vivo* AF image of the lesions (Zeng, McLean, MacAulay, Palcic, & Lui, 1998).

In 2007 Q. He et al. reported that by irradiating with a blue laser light (442 nm) the cancerous regions, the epidermis showed a very weak fluorescence signal, while the stratum corneum showed fluorescence emissions exceeding 510 nm. They also reported that in the dermis, the basal cell islands and a band of surrounding areas showed a very weak fluorescence signal, while the dermis surrounding the basal cell island showed a greater fluorescence signal with different spectral shapes (He & al, 2007). In the conclusions of their review Drakaki et al. claim that the optical properties and the contribution of fluorophores in healthy skin and NMSC lesions are significantly different from each other and correlate well with tissue histology (Drakaki, Dessinioti, Stratigos, Salavastru, & Antoniou, 2014).

However, in the current state of literature there are no precise demonstrations of correlation between the histopathological features and the degree of fluorescence.

The primary objective of this study is to investigate the correlation between the intensity of cutaneous autofluorescence (AF) and the histopathological characteristics of malignant and potentially malignant lesions of the skin included the group of NMSC. This demonstration could lead to the introduction into clinical practice of a totally non-

invasive, real-time and simple to use technique both for first-level diagnosis, and for the demarcation of surgical margins, and for the follow-up of treated patients.

5.2 Materials and Methods

This is a mono-centric, pre-clinical *ex vivo* study approved by Area Vasta Emilia Nord ethical committee (COD. 1167.2018).

Inclusion criteria applied were:

- Patients of both sexes.
- Patients > 18 years old.
- Patients able to give their consent to participate in the study.
- Patients with clinical suspicion of epithelial carcinoma.
- Patients with clinical suspicion of actinic keratosis.
- Patients with previous histological diagnosis of epithelial carcinoma.
- Patients with previous histological diagnosis of actinic keratosis.

In patients who express their consent to participate in the study, the lesion was surgically removed as normal clinical practice.

The fluorescence spectra of the lesion were investigated on the excised specimen (*ex vivo*) in a point way. The number of points analyzed ranges from a minimum of 2 to a maximum of 5. For each lesion, a control point on clinically healthy skin must always be present. Each point analyzed with the spectrophotometer setup was marked with a suture point (landmark) and the histopathological analysis was carried out specifically in each landmark.

The spectrophotometric setup (Figure 5.1) has been assembled by combining the following items:

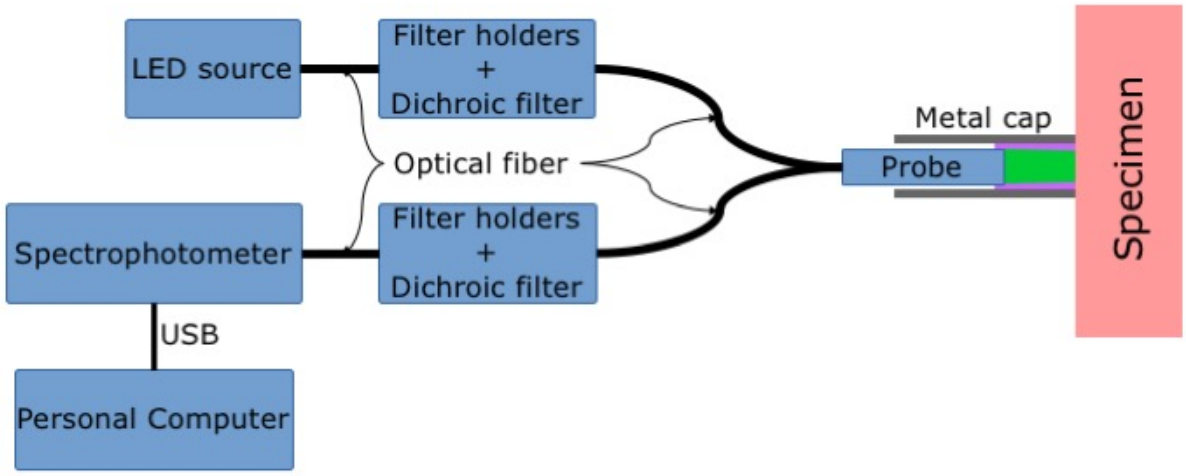

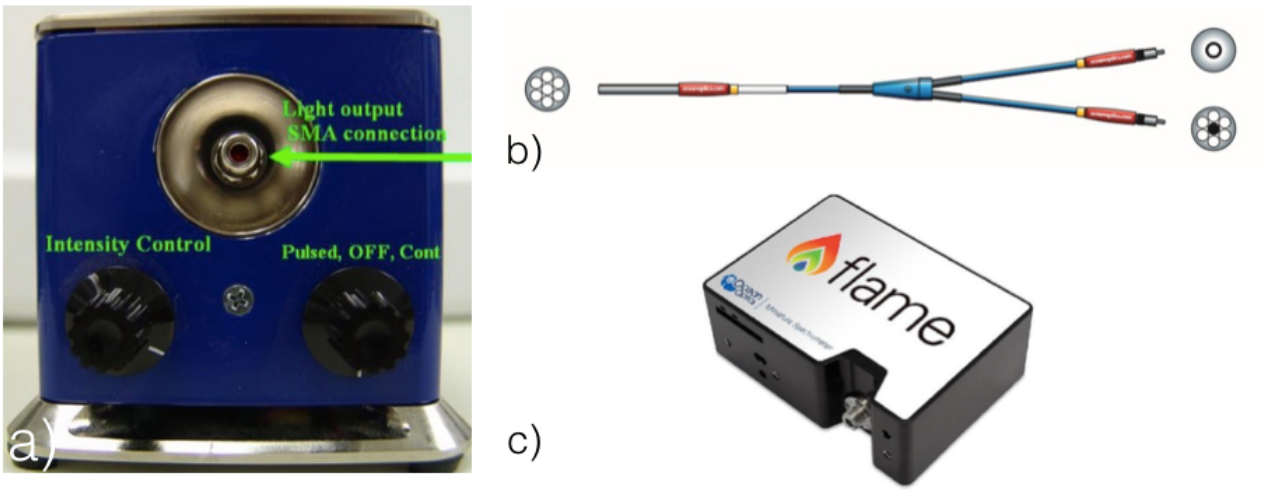

Figure 5.1 Spectrophotometric setup.

- A LED source (LLS, Ocean Optics), which emits a light in the violet spectrum (400-430nm), which is suitable to excite the autofluorescence of human tissues (Figure 5.1 a).

- Dichroic filters (Thorlabs) and filter holders (Mightex), which are suitable to remove the unwanted wavelengths from the excitation-light and from the collected emission-light.

- A bifurcated optical fiber probe (Ocean Optics), which is suitable to illuminate the tissue and to collect the emission-light (Figure 5.1 b).

- A spectrophotometer (Flame, Ocean Optics), which is suitable to measure the spectrum of the collected emission-light in the visible range above the excitation wavelengths (Figure 5.1 c).

- A personal computer (Linux operating system), used to control the spectrophotometer.

A software application (SW) has been developed (in C language) and integrated into the spectrophotometric setup (HW). The main features of the SW are the following:

- To acquire the autofluorescence spectra of the specimen.

- To process the acquired spectra.

- To save the processed spectra into a data-base (DB).

- To execute the post-processing analysis of the spectra that are saved in the DB.

- To plot the results of the post-processing analysis.

Emission spectra were recorded with a spectral resolution of 1 nm. Each spectrum is the result of a specified number of contiguous acquisitions, which are mathematically averaged, in order to reduce the signal noise. Each acquisition starts after a specified time period to guarantee the spectrometer stabilization and is obtained by integrating the incoming light signal for a specified number of micro-seconds.

The spectra are saved as numerical files (.csv format), which can be loaded by the SW during the post-processing. The ISO date-time format "yyyymmdd_hhmmss" is used to automatically define the unique identifier (ID) of each exam, in order to guarantee the maximum traceability in an anonymously way.

The spectra of each lesion are displayed both in absolute and in normalized mode (Figure 5.2). The absolute spectrum is useful to compare the intensities of the sampled areas, in order to highlight the hypo-fluorescence, normo-fluorescence and hyper-fluorescence (Figure 5.2 a). Instead, the normalized spectrum is useful to highlight the changes in the spectral shape of the sampled areas (qualitative analysis), in order to highlight the spatial distribution of the many involved fluorophores (Figure 5.2 b).

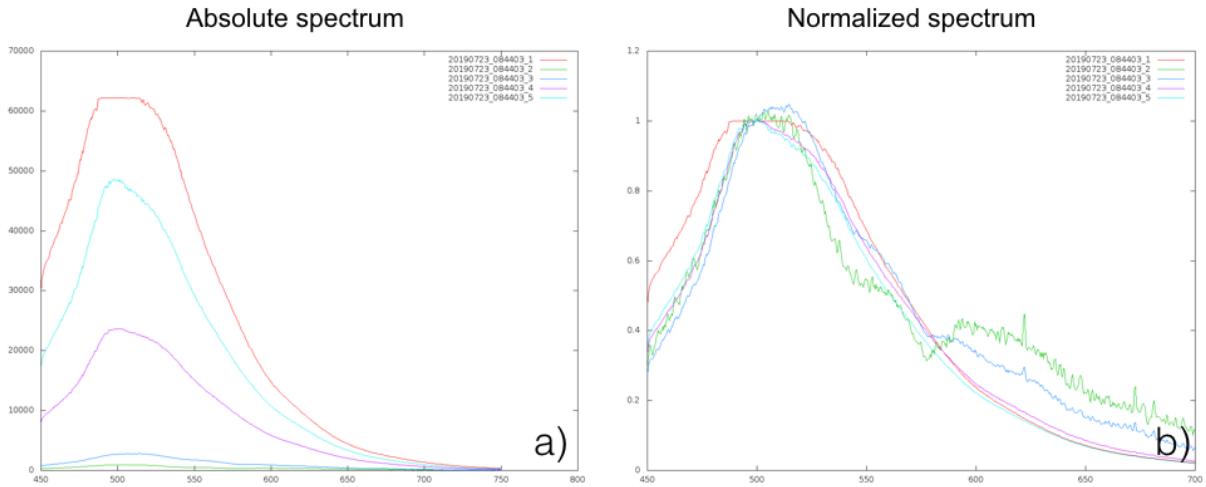

Figure 5.2 Absolute and normalized spectra relatives to lesion of Figure 5.3.

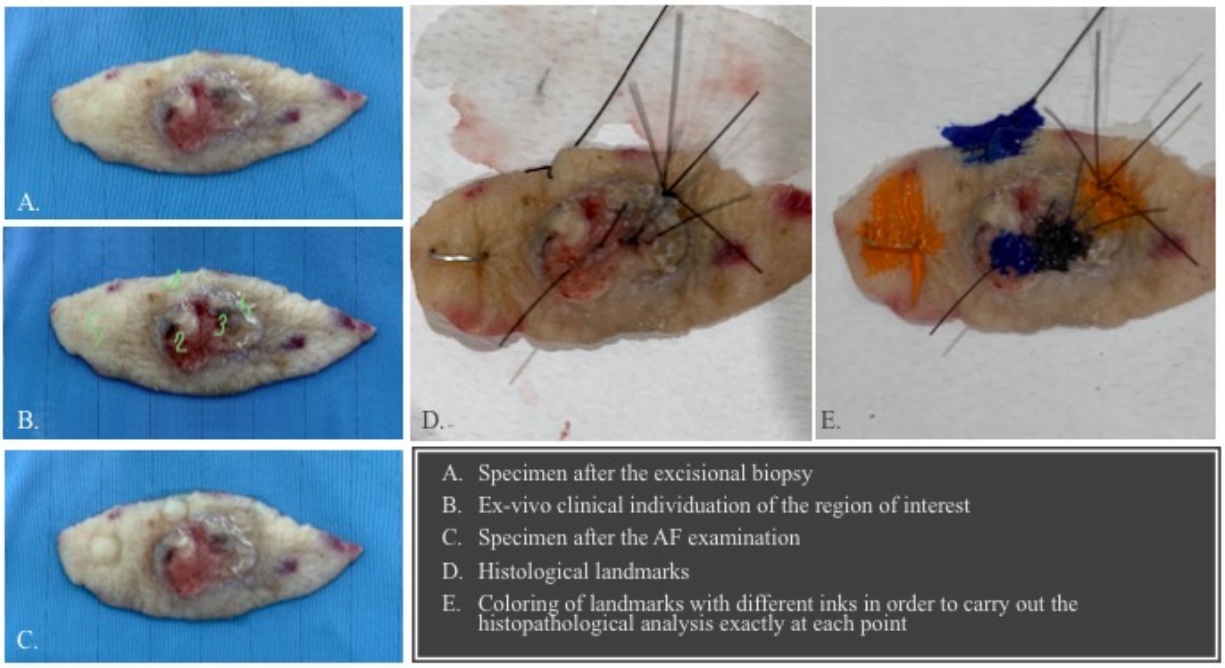

Figure 5.3 Procedure of marking the interest points on which the measurements using the spectrophotometer setup were made.

As shown in figure 5.3, the areas analyzed with the spectrophotometer setup and marked with different suture points were histologically analyzed one by one. To allow the differentiation of each point on the histological specimen, they have been marked with different color inks. The histological variables analyzed for each point were: diagnosis, hyperkeratosis, epithelial thickening, fibrosis, elastosis, neovascularization and cellular atypia.

Histopathological findings were compared with the characteristics of the spectrum of each point in order to investigate if there are correlations between specific histopathological characteristics and spectrum characteristics.

5.2.1 Statistical analysis

Data analysis was performed using the commercial package IBM-SPSS v.22© and the open source statistical system Jamovi v.1.2.22 which is based on the widespread open source statistical system R. Measures of central tendency, dispersion and shape were calculated for all the variables in the data set. Summaries included arithmetic

mean, median, standard deviation, interquartile range, minimum, maximum, asymmetry, kurtosis and the relevant standard errors and 95% confidence intervals. Normality of the data was tested by the Shapiro-Wilk test. Categorical data were reported in frequency tables and expressed as absolute, relative and cumulated frequencies and percentages.

Graphical analysis made use of histograms, scatter plots and box-plots. Histograms and boxplots are extremely useful to visualize the shape of the data, determine the presence of anomalous data (outliers) and make visible the differences in the central location between the different groups.

Univariate comparisons between continuous variables were performed using both parametric tests (Student's t-test, ANOVA) and non-parametric test (Mann-Whitney's U-test, Kruskal-Wallis test).

Comparisons between categorical variables in contingency tables were performed using the chi-square test and Fisher's exact test.

The combined effects of different predictors on outcome variables were tested by multiple linear regression. The results were considered statistically significant for a p-value less than 5% ($p < 0.05$).

5.3 Results

5.3.1 Sample description

The number of lesions included in the study was 98. One hundred and fifteen points on the lesions were analysed with the spectrophotometer setup and for each of these a control point was measured on clinically healthy skin. Each control point was analysed histologically and in 100% of cases the diagnosis of healthy skin was confirmed without any pathological alteration.

The patients included were 65% male (n=64) and 35% female (n=34), with an average age of 79 years (minimum: 42, maximum: 93).

The skin phototype was type II in 95% of cases (n = 93) and type III in 5% of cases (n = 5). Patients were smokers in 10.2% of cases (n = 10) and non-smokers in 87.8% of cases (n = 86). In 19.4% of cases (n = 19) patients were affected with diabetes, in 68.4% of cases (n = 67) with arterial hypertension, in 54% (n = 53) of cases they were under anticoagulant/antiplatelet therapy and in no case (n = 0) were affected with autoimmune diseases.

The localization of the lesions analyzed was in H-zone (high risk-zone: eyelids, eyebrow, periorbital region, nose, lip, chin, mandibular region, preauricular and retroauricular region, ear, temple, genitalia, hands and feet) in 43.9% of cases (n = 43), I-zone (intermediate risk-zone: cheeks, forehead, scalp, neck and pretibial region) in 30.6% of cases (n = 30) and in L-zone (low risk-zone: trunk and extremities) in 25.5% of cases (n = 25).

The diagnosis of the 115 spectrum points analyzed was in 51.3% of cases (n = 59) basal cell carcinoma (BCC), in 46.1% of cases squamous cell carcinoma (SCC) and in 2.6% of cases (n = 3) a different benign diagnosis.

The frequencies of diagnosis of BCC and SCC subtypes are shown in Figure 5.4.

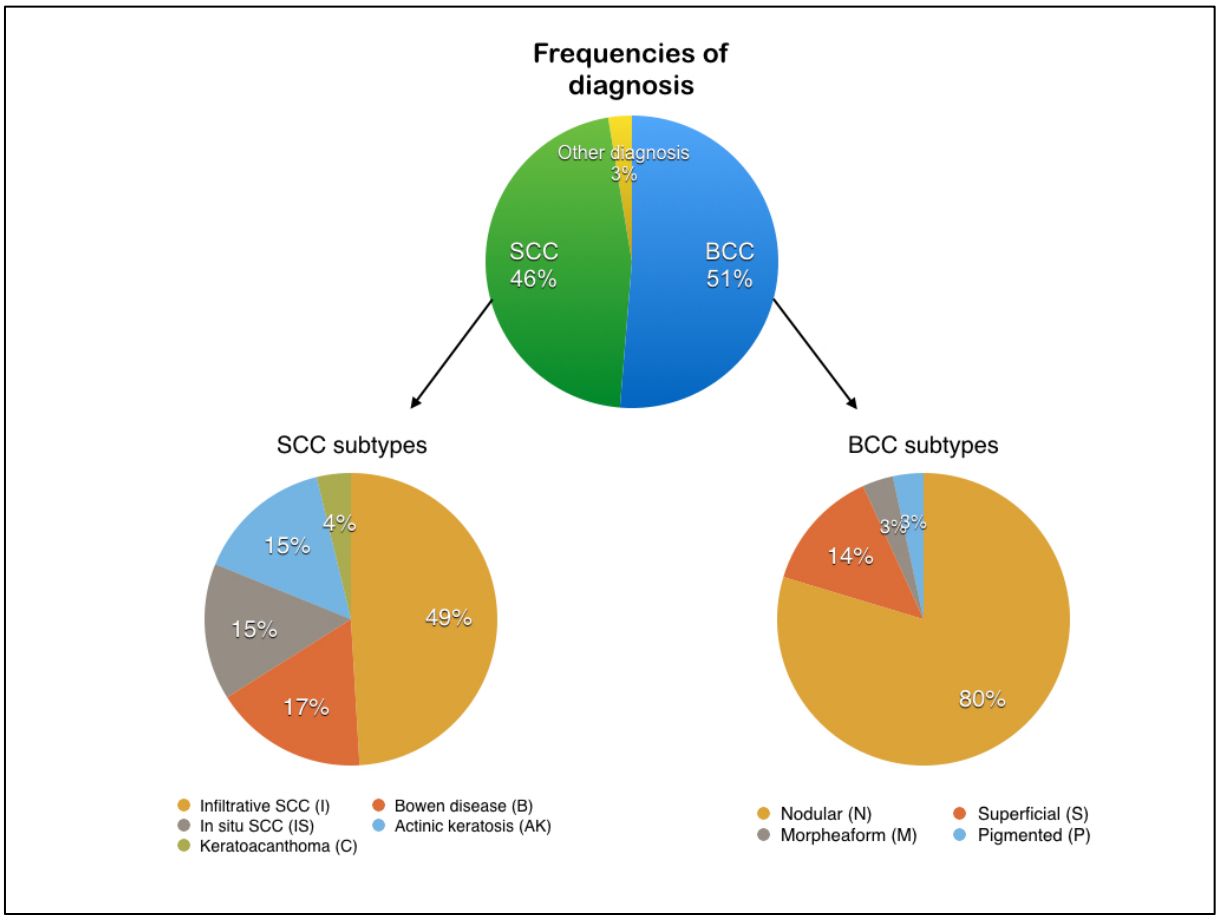

Figure 5.4 Frequencies of diagnosis of BCC and SCC subtypes.

5.3.2 Intensity ratio

The ratio between the emission intensity generated by healthy skin at 500 nm and the emission intensity generated by each pathological sample point at the same wavelength was calculated. This was named "*intensity ratio*".

The mean intensity ratio for BCC group was 4.5. This means that the fluorescence peak at 500 nm was more than 4 times lower (hypo-fluorescent) in BCCs than in healthy skin.

The mean intensity ratio for SCC group was 4.4, with a similar hypo-fluorescence for this group (Table 5.1 and Figure 5.5).

Table 5.2 shows that the emission intensity ratio at 500 nm between healthy control points and each of the pathological points has a strong statistical significance.

	BCC	SCC
N	59	53
Missing	0	0
Mean	4.489	4.371
Std. error mean	0.4663	0.5183
Median	3.295	3.033
Standard deviation	3.582	3.773
Minimum	1.354	0.4823
Maximum	16.10	18.02
Shapiro-Wilk W	0.7561	0.8198
Shapiro-Wilk p	< .001	< .001

Table 5.1 Descriptives of intensity ratio in BCC and SCC groups.

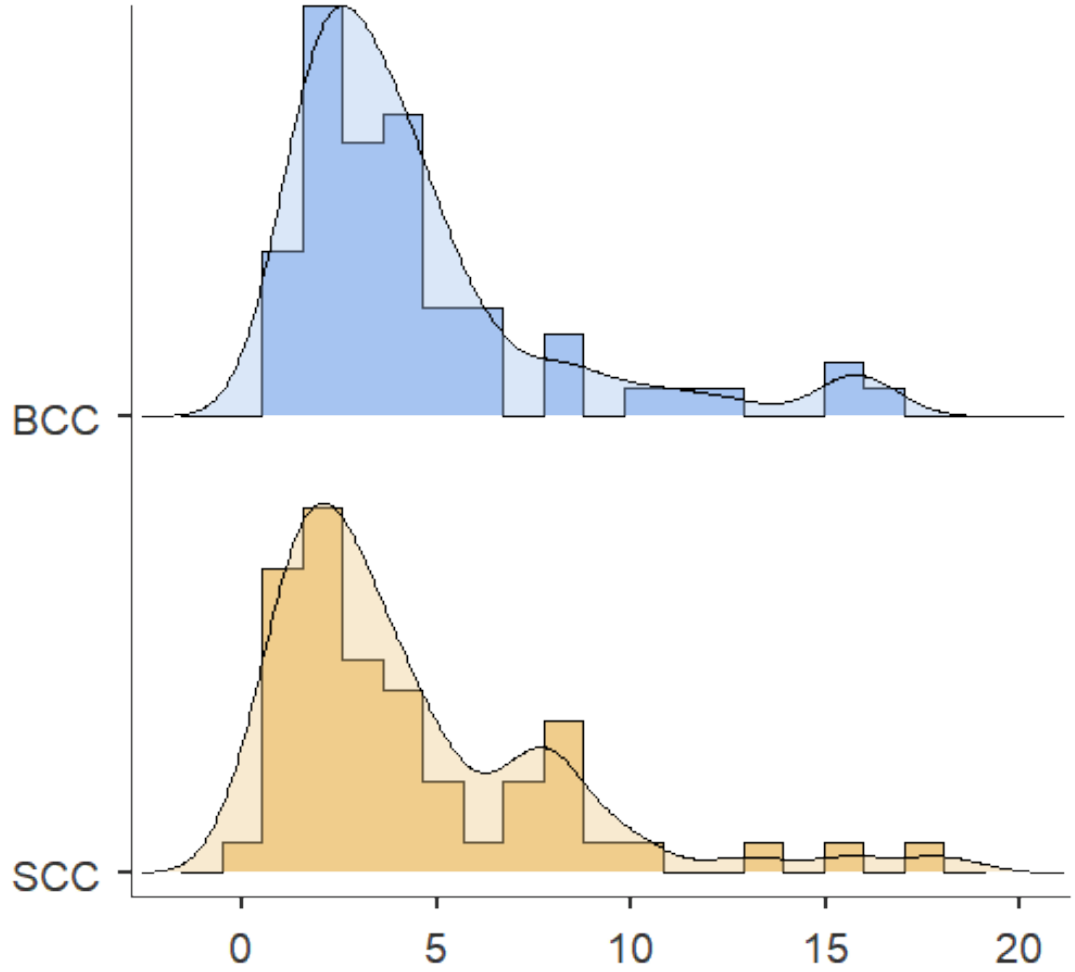

Figure 5.5 Distribution of intensity ratio in BCC and SCC groups

One Sample T-Test

		Statistic	df	p	Mean difference
Intensity ratio	Student's t	10.17	114.0	< .001	3.486
	Wilcoxon W	6638		< .001	2.759

Note. H_a population mean ≠ 1

Table 5.2 Demonstration that the emission intensity ratio between healthy control points and each of the pathological points has a strong statistical significance.

No statistically significant differences between the mean of intensity ratio in BCC and SCC groups were detected (Figure 5.6).

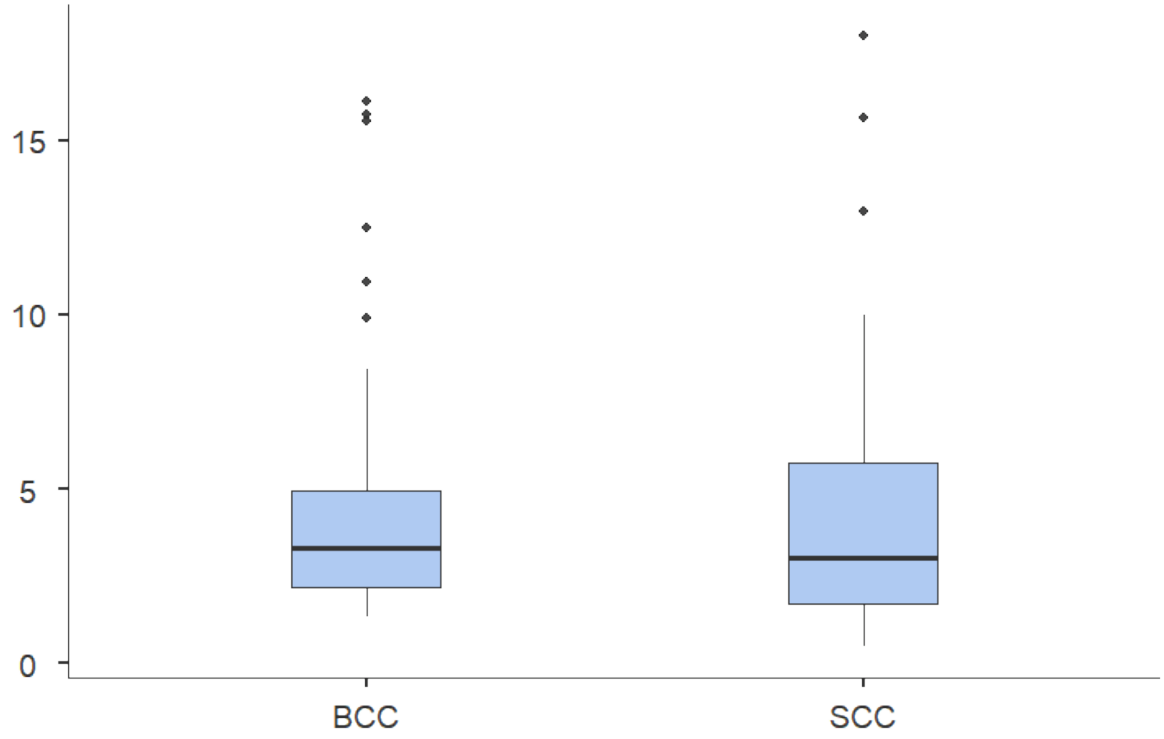

Figure 5.6 Box plot representing the mean of the intensity ratio in BCC and SCC groups.

The mean intensity ratio for BCC subtypes were the following (Figure 5.7):

- Superficial BCC: 2.6 (minimum: 1.435; maximum: 5.749; standard deviation: 1.358; standard error: 0.4802)
- Nodular BCC: 4.4 (minimum:1.354; maximum: 16.10; standard deviation: 3.437; standard error: 0.5014)
- Morpheiform BCC: 4.8 (minimum: 3.607; maximum: 6.082; standard deviation: 1.750; standard error: 1.237)
- Pigmented BCC: 12.8 (minimum: 9.908; maximum: 15.73; standard deviation: 4.120; standard error: 2.913)

The mean intensity ratio for SCC subtypes were (Figure 5.8):

- Keratoacanthoma: 1.8 (minimum: 1.296; maximum: 2.240; standard deviation: 0.6674; standard error: 0.4719)
- In situ SCC: 2.3 (minimum: 1.250; maximum: 3.286; standard deviation: 0.7685; standard error: 0.2717)
- Actinic keratosis: 4.1 (minimum: 0.4823; maximum: 18.02; standard deviation: 5.805; standard error: 2.052)
- Bowen disease: 5.0 (minimum: 1.342; maximum: 12.98; standard deviation: 4.173; standard error: 1.391)
- Infiltrative SCC: 5.1 (minimum: 0.5689; maximum: 15.63; standard deviation: 3.482; standard error: 0.6723)

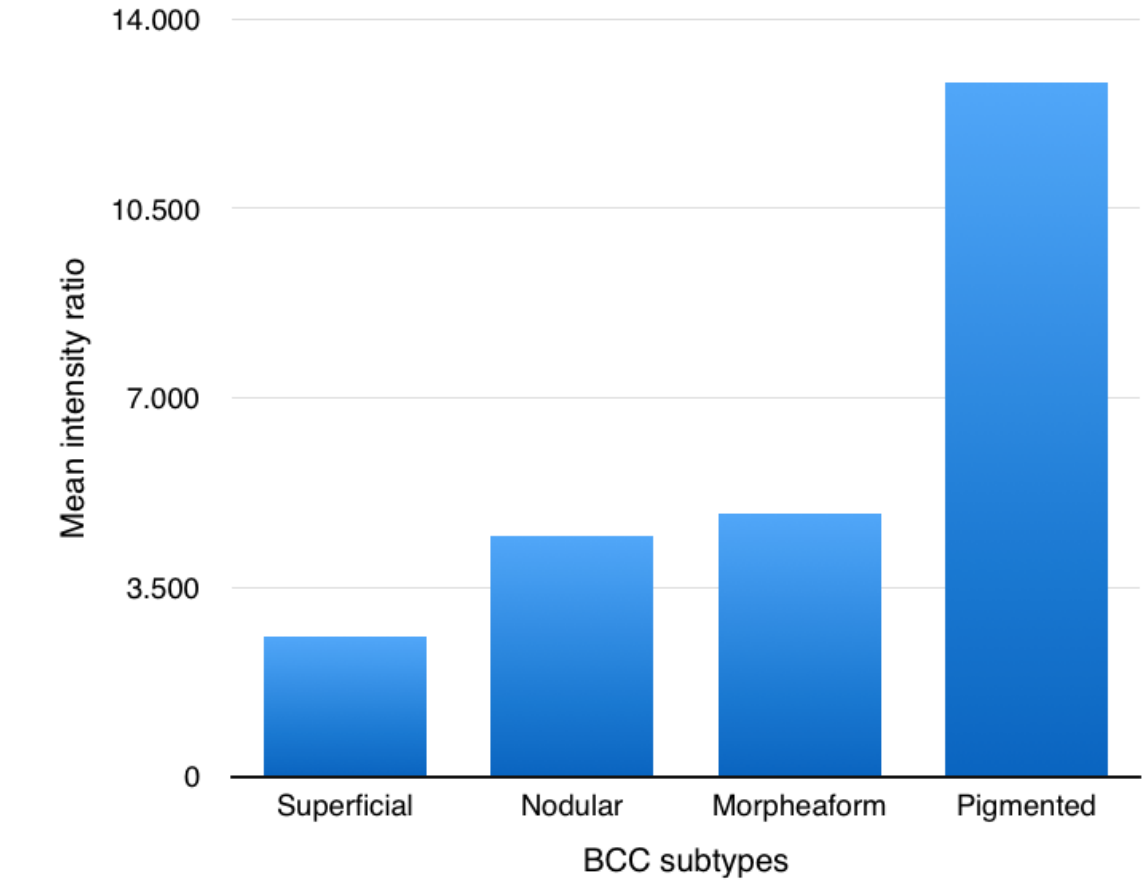

Figure 5.7 Mean intensity ratio in BCC subtypes

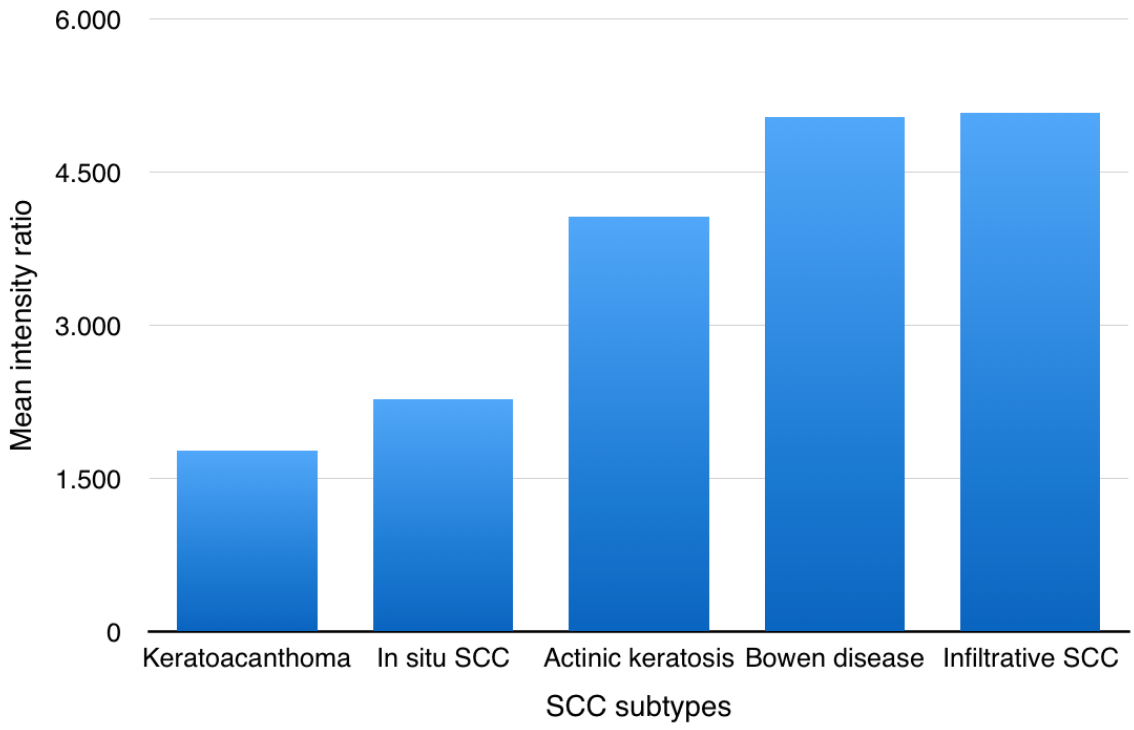

Figure 5.8 Mean intensity ratio in SCC subtypes

5.3.3 Histological variables

Six histological variables were compared with the healthy or pathological condition suggested by the intensity ratio.

5.3.3.1 Fibrosis and elastosis

The mean ratio in cases in which fibrosis was absent resulted 3.3 against a ratio of 4.7 in cases in which fibrosis were present. The difference was statistically significant with Mann-Whitney U test (p=0.047) (Table 5.3 and Figure 5.9).

The mean ratio in cases in which elastosis was absent resulted 4.2 against a ratio of 5.4 in cases in which elastosis were present. The difference was not statistically significant (p=0.563) (Table 5.4 and Figure 5.9).

It is interesting to evaluate how elastosis and fibrosis together influence the intensity ratio. In cases in which both fibrosis and elastosis were absent, the intensity ratio was 2.9, if only elastosis was present it was 3.4, if only fibrosis was present it was 4.3, but if both fibrosis and elastosis were present simultaneously, the intensity ratio rises to 7.7.

Group Descriptives (Fibrosis)

	Group	N	Mean	Median	SD	SE
Intensity ratio	absent	16	3.309	2.164	3.130	0.7825
	present	99	4.676	3.521	3.734	0.3753

Independent Samples T-Test (Fibrosis)

		Statistic	df	p
Intensity ratio	Student's t	-1.386	113.0	0.168
	Mann-Whitney U	546.0		**0.047**

Table 5.3 Descriptives and independent samples T-Test for "fibrosis" variable.

Group Descriptives (Elastosis)

	Group	N	Mean	Median	SD	SE
Intensity ratio	absent	89	4.230	3.295	3.322	0.3521
	present	26	5.361	3.054	4.659	0.9138

Independent Samples T-Test (Elastosis)

		Statistic		df	p
Intensity ratio	Student's t	-1.386	[a]	113.0	0.169
	Mann-Whitney U	1070			0.563

[a] Levene's test is significant ($p < .05$), suggesting a violation of the assumption of equal variances

Table 5.4 Descriptives and independent samples T-Test for "elastosis" variable.

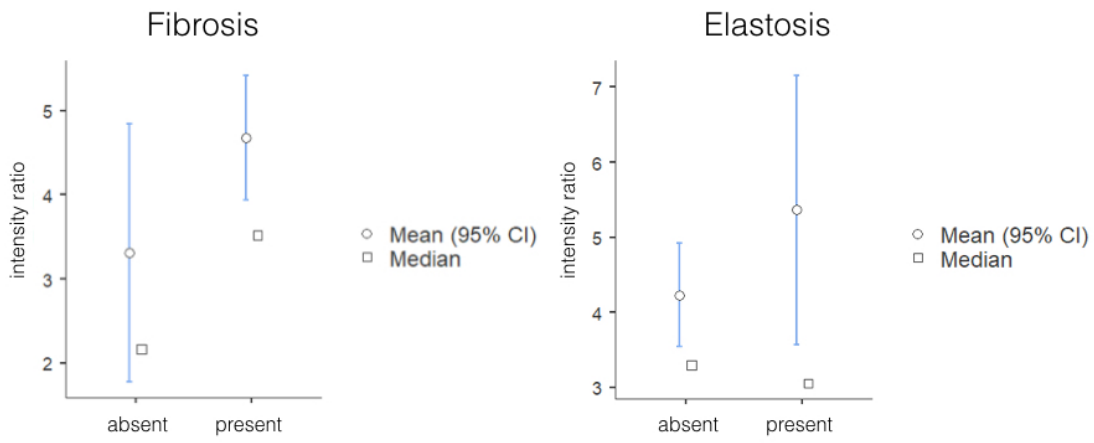

Figure 5.9 Plots representing differences in intensity ratio when fibrosis or elastosis were present.

5.3.3.2 *Hyperkeratosis*

Hyperkeratosis was classified as absent (grade 0) or present with grade 1, 2 and 3. In case in which hyperkeratosis was absent the intensity ratio resulted 4.8, with a grade 1 hyperkeratosis resulted 4.4, with a grade 2 resulted 4.5 and with a grade 3 hyperkeratosis resulted 1.5. One-Way ANOVA (Non-parametric) test resulted statistically significant (p=0.034). Pairwise comparisons revealed that the statistically significant comparison was that between absent hyperkeratosis and grade 3 hyperkeratosis (p = 0.016) (Table 5.5).

One-Way ANOVA (Non-parametric) - **Hyperkeratosis**			
Kruskal-Wallis			
	χ^2	**df**	**p**
Intensity ratio	8.686	3	**0.034**

Dwass-Steel-Critchlow-Fligner pairwise comparisons – intensity ratio			
		W	**p**
0	1	-0.27054	0.998
0	2	-0.01111	1.000
0	3	-4.18994	**0.016**
1	2	0.04837	1.000
1	3	-3.22125	0.103
2	3	-3.63054	0.050

Table 5.5 One-Way ANOVA and pairwise comparisons for "hyperkeratosis" variable.

5.3.3.3 Epithelial thickening

Epithelial thickening was classified as absent (grade 0) and present with grade 1, 2, 3 or 4. In case in which epithelial thickening was absent the intensity ratio resulted 4.2, with a grade 1 resulted 3.9, with a grade 2 was 4.0, with a grade 3 was 2.4 and with a grade 4 resulted 6.5. One-Way ANOVA (Non-parametric) test resulted statistically significant (p=0.038). Pairwise comparisons revealed that the statistically significant comparison was that between absent epithelial thickening and grade 4 epithelial thickening (p = 0.056) (Table 5.6).

One-Way ANOVA (Non-parametric) – **Epithelial thickening**			
Kruskal-Wallis			
	χ^2	**df**	**p**
Intensity ratio	10.16	4	**0.038**

Dwass-Steel-Critchlow-Fligner pairwise comparisons – intensity ratio			
		W	**p**
0	1	-0.99385	0.956
0	2	-0.04026	1.000
0	3	-0.96425	0.961
0	4	3.79521	**0.056**
1	2	0.70088	0.988
1	3	-1.00000	0.955
1	4	3.20000	0.157
2	3	-0.70548	0.988
2	4	3.63763	0.076
3	4	2.42272	0.426

Table 5.6 One-Way ANOVA and pairwise comparisons for "epithelial thickening" variable.

5.3.3.4 *Neovascularization*

Neovascularization was classified as absent (grade 0) and present with grade 1, 2 or 3. In case in which neovascularization was absent the intensity ratio resulted 2.1, with a grade 1 resulted 4.6, with a grade 2 was 6.4 and with a grade 3 resulted 4.8. One-Way ANOVA (Non-parametric) test resulted statistically significant (p=0.019). Pairwise comparisons revealed that the statistically significant comparisons were that between absent neovascularization and grade 1 neovascularization (p = 0.016) and border-line comparison between absent neovascularization and grade 2 neovascularization (p = 0.099) (Table 5.6).

One-Way ANOVA (Non-parametric) – **Neovascularization**			
Kruskal-Wallis			
	χ^2	**df**	**p**
Intensity ratio	9.989	3	**0.019**

Dwass-Steel-Critchlow-Fligner pairwise comparisons – intensity ratio			
		W	**p**
0	1	4.1995	**0.016**
0	2	3.2451	**0.099**
0	3	2.7520	0.209
1	2	1.6459	0.650
1	3	-0.7508	0.952
2	3	-1.3799	0.763

Table 5.7 One-Way ANOVA and pairwise comparisons for "neovascularization" variable.

5.3.3.5 *Cellular atypia*

Cellular atypia was classified as absent (grade 0) and present with grade 1, 2 or 3. In case in which cellular atypia was absent the intensity ratio resulted 4.5, with a grade 1 resulted 3.8, with a grade 2 was 5.8 and with a grade 3 resulted 4.4. One-Way ANOVA (Non-parametric) test resulted not statistically significant (p=0.334). Therefore, pairwise comparisons were not performed.

One-Way ANOVA (Non-parametric) – **Cellular atypia**

Kruskal-Wallis

	χ^2	df	p
Intensity ratio	3.396	3	0.334

Table 5.8 One-Way ANOVA for "cellular atypia" variable.

5.3.4 Linear regression

A linear regression including all the histological variables analysed was carried out in order to evaluate which, considered all together, were significant in influencing the intensity ratio between the emission stemming from healthy skin and from the lesions.

In table 5.9 is shown the model fit measures of linear regression and in table 5.10 are shown the results. The histological variables that were significant are fibrosis and elastosis (present vs absent); neovascularization (absent versus grade 1, 2 and 3) and hyperkeratosis (absent versus grade 3). Epithelial thickening and cellular atypia are not statistically significant in the regression.

Model Fit Measures

Model	R	Adjusted R^2
1	0.4778	0.1114

Table 5.9 Model fit measures of linear regression

Model Coefficients – intensity ratio

Predictor	Estimate	SE	t	p
Intercept [a]	-1.36559	1.633	-0.83614	0.405
1) **Fibrosis**:				
present – absent	2.95274	1.331	2.21771	**0.029**
2) **Elastosis**:				
present – absent	2.67802	1.071	2.50069	**0.014**
3) **Neovascularization**:				
1 – 0	2.69778	1.098	2.45708	**0.016**
2 – 0	4.17302	1.539	2.71197	**0.008**
3 – 0	3.00542	1.339	2.24429	**0.027**
4) **Epithelial thickening**:				
1 – 0	-0.28104	1.332	-0.21107	0.833
2 – 0	-0.50670	1.298	-0.39037	0.697
3 – 0	-1.04651	2.774	-0.37731	0.707
4 – 0	0.97872	1.033	0.94719	0.346
5) **Hyperkeratosis**:				
1 – 0	-0.04351	1.260	-0.03454	0.973
2 – 0	-0.63988	1.015	-0.63038	0.530
3 – 0	-3.42011	1.714	-1.99522	**0.049**
6) **Cellular atypia**:				
1 – 0	1.06353	1.178	0.90300	0.369
2 – 0	1.46131	1.174	1.24451	0.216
3 – 0	0.71902	1.455	0.49424	0.622

[a] Represents reference level

Table 5.10 Results of linear regression including all histological variables analysed.

5.3.5 Systemic and behavioural variables

No variables between smoking, diabetes, hypertension, autoimmune diseases and anticoagulant/antiplatelet therapy influenced the logistic regression and all were not statistically significant in influencing the intensity ratio.

However, a statistically significant correlation between the presence of hypertension and elastosis was highlighted (p=0.021) (Table 5.11). Table 5.12 is the contingency table containing the frequencies of the two variables. In particular, both hypertension and elastosis were detected in 84.91% of patients.

χ^2 Tests

	Value	df	p
χ^2	5.342	1	0.021
N	115		

Table 5.11 Statistical correlation between hypertension and elastosis.

Contingency Tables

		Hypertension		
Elastosis		**absent**	**present**	**Total**
absent	Observed	21	41	62
	% within row	33.87 %	66.13 %	100.00 %
present	Observed	8	45	53
	% within row	15.09 %	84.91 %	100.00 %
Total	Observed	29	86	115
	% within row	25.22 %	74.78 %	100.00 %

Table 5.12 Contingency table containing the frequencies of "hypertension" and "elastosis" variables.

5.4 Discussion

Cutaneous squamous cell carcinoma (SCC) and basal cell carcinoma (BCC), commonly named “nonmelanoma skin cancer” (NMSC) or “epithelial skin cancers”, are the most common cancers in white-skinned populations. Despite its low mortality rate, BCC may cause considerable morbidity as it may occasionally grow aggressively causing extensive local tissue destruction or recurrences after treatment. Skin SCC, is associated with a 0.5% to 5% risk of metastasis in the general population, and often displays a more aggressive and difficult-to-treat course (Drakaki E. , et al., 2013).

Therefore, early diagnosis and accurate removal of the lesion is essential in the management of these diseases. This can be tricky in patients with multiple lesions, with particularly destructive lesions in aesthetic areas, or lesions with margins difficult to define intraoperatively such as SCC or morpheiform BCC.

For this reason, in recent years there emerged in literature a great interest in optical imaging technologies that may provide the possibility of real-time non-invasive, high-resolution analysis of the skin.

Several of these technologies have been studied, including light-induced fluorescence (LIF) and diffused reflectance spectroscopy (DRS), optical coherence tomography (OCT), near-infrared and Raman spectroscopy, multispectral fluorescence polarization imaging, and reflectance or fluorescence confocal microscopy (Astner, et al., 2008) (Drakaki E. , et al., 2013).

In particular, fluorescence spectroscopy is a very attractive potential diagnostic technique for early diagnosis and demarcation of skin cancer due to its high sensitivity, easy-to-use methodology for real-time measurements, and non-invasiveness. Fluorescence emission from malignant skin tissue is usually excited using an irradiation source such as a laser, a LED, a xenon, or halogen lamp.

In the field of fluorescence, AF imaging is an attractive potential tool due to lack of need for application of exogenous agents on the tissue under investigation. It allows differentiation on the base of differences between health and pathological status in

biochemical content and metabolic state of the fluorophores. After illumination of the tissue with an appropriate light source, the photons diffuse in the tissue and fluorescence is re-emitted, enabling not invasive spectroscopic measurements and the “optical biopsy” approach (Drakaki E. , et al., 2013) (Drakaki, Dessinioti, Stratigos, Salavastru, & Antoniou, 2014).

AF has been proposed for detection of malignant and premalignant tissues in a variety of organ systems such as oral mucosa, lung, esophagus, colon, and cervix (Lam, 1993) (Panjehpour, et al., 1995) (Cothren, et al., 1996) (Ramanujam, et al., 1996).

The purpose of this study is to perform a precise correlation between the spectrum of specific points of the lesion and the histopathological characteristics of these points. Besides the emission spectrum of each pathological sample point, a control spectrum was measured on healthy skin of the same patient. Control points were also analyzed histologically and confirmed as healthy. The evaluation was performed on a large sample, with a total of 115 spectra from pathological points analyzed and compared each with its own control point.

The wavelength of 500 nm (where the skin has the maximum emission) was chosen as the reference to evaluate and compare the intensity of each spectrum.

Consequently, for each analyzed point the ratio between the emission intensity generated by healthy skin at 500 nm and the emission intensity generated by each pathological sample point at the same wavelength was calculated. This ratio was called "intensity ratio".

The first important result highlighted was that the intensity ratio was significantly higher than 1 in the NMSCs. A higher intensity ratio means having a lower fluorescence (hypo-fluorescence) in the pathological point compared to the relative healthy control point. In particular, both BCCs and SCCs are significantly (more than 4 times) less fluorescent than healthy skin.

This result agrees with those already present in the literature. In 2002, Panjehour et al. highlighted that normal skin exhibited a stronger fluorescence emission than BCC

and SCC with 410 nm excitation (Panjehpour, Julius, Phan, Vo-Dinh, & & Overholt, 2002).

Lower fluorescence signal in BCC tumours was reported for different excitation wavelengths, in comparison with normal skin fluorescence, by different Authors such as Na et al., Zeng et al., Borisova et al. and Drakaki et al. (Drakaki E. , et al., 2013). Differently, in 2001 Brancaleon et al., observed a higher fluorescence intensity in NMSCs versus normal skin, using UV excitation. This difference can be explained by the different excitation wavelength. Using an UV light the tryptophan fluorophore is stimulated and it increases in the tumour site as a consequence of the thickening of the epidermis (Brancaleon, et al., 2001).

Instead, using a wavelength from 350 to 450 nm, the higher fluorescence intensity shown in the normal tissues is due primarily to a conversion of collagen (emission around 390 to 405 nm) and elastin (emission around 400 to 410 nm) from normal to malignant tissues and a decrease in NADH (emission around 440 to 460 nm) levels in the malignant tissues (Drakaki E. , et al., 2013).

Moreover, some more considerations can be made by evaluating the subtypes of BCCs and SCCs.

With regard to BCCs, the lower intensity ratio was highlighted in superficial BCCs with a mean value of 2.6 (this means having a fluorescence 2.6 times less intense than in healthy skin). These are followed by nodular BCCs with a hypo-fluorescence of 4.4 with respect to healthy skin and morpheiform BCCs with a hypo-fluorescence of 4.8 with respect to healthy skin. The highest intensity ratio (strongeste quenching of emission) was observed for pigmented BCCs, with a mean value of 12.8.

This result can be explained by the histological conformation of the subtypes of the lesions. In fact, the superficial BCC is the typology in which there are fewer variations of the main fluorophores involved in the modification process of the AF such as collagen and elastin. The basaloid cells proliferate along an axis parallel to the

epidermal surface, but no more deeply than papillary dermis and only a retraction of palisade basal cell from the subjacent stroma may be observed.

Otherwise, nodular (both infiltrating and non-infiltrating) and morpheiform BCCs detected a much more marked hypo-fluorescence because in both cases there is an invasion of the dermis with consequent disintegration of one of the main fluorophores which is collagen. In particular, nodular BCC subtype grows as large nests of basaloid cells in the papillary or reticular dermis followed by peritumoral retraction from the stroma and peripheral palisading. The pattern of morpheiform BCC subtype is characterized by strands of basaloid cells, one to five cells thick, extending between dense collagen bundle. The tumour is slightly demarcated and may present widespread invasion of the reticular dermis or even the infiltration of subcutaneous fat.

Finally, the major hypo-fluorescence was highlighted for pigmented BCCs, because they contain melanin. Being a dark pigment, it completely captures the light and avoids normal fluorescence release.

Regarding SCCs subtypes, the lower intensity ratio was shown for keratoacanthoma, with a mean value of 1.7, so slightly hypo-fluorescent compared to normal skin. This is followed by in situ SCCs with an intensity ratio of 2.3. The major hypo-fluorescence was highlighted for Bowen diseases and infiltrative SCCs, with values of 5.0 and 5.1 respectively.

In SCC group several factors seem to contribute to hypo-fluorescence such as epithelial thickening due to the proliferation of altered keratinocytes, the breakdown of collagen and elastin, the neovascularization and the presence of cellular atypia.

The mean intensity ratio detected for actinic keratoses was about 4, but the values were extremely variable; they range from a strong hypo-fluorescence (intensity ratio: 18) to a hyper-fluorescence (intensity ratio 0.4, with a lesion fluorescence greater than fluorescence of the normal skin).

This great difference within the group of actinic keratoses can be explained by the presence or absence of hyperkeratosis. In cases where there is no hyperkeratosis, the average intensity ratio is 5.4, meaning a 5-times less intense emission than in healthy skin. In cases with hyperkeratosis the average intensity ratio is 1.8 and when the hyperkeratosis is of a high degree (grade 3) the intensity ratio decreases to 0.4 (hyper-fluorescence with respect to the control skin).

In fact, the keratin is an important fluorophore of the skin and when hyper-expressed it generates an increase in the intensity of the fluorescence of the lesion.

To the best of our knowledge, this is the first study in the literature that analyzes the variation of fluorescence intensity in relation to a series of histological variables specifically studied for each point of the lesion analyzed with the spectrophotometer.

The hyperkeratosis is one of the histological variables analyzed and an increase in the intensity ratio with an increasing in the degree of hyperkeratosis was highlighted. In particular, the statistical analysis showed a significant variation in the fluorescence intensity between the grade 0 (absent hyperkeratosis) and the grade 3 (maximum hyperkeratosis).

As previously demonstrated by clinical and histological studies conducted on the oral mucosa (*cf.* chapters 3 and 4), among the main fluorophores stimulated by excitation wavelength, there are collagen and elastin. Both in case of fibrosis and elastosis there was a quenching of fluorescence compared to healthy skin, because these conditions reduce the contribution of AF from collagen and elastin respectively. If fibrosis and elastosis coexist simultaneously the fluorescence is quenched even more strongly (intensity ratio of about 8).

However, only fibrosis, and not elastosis, resulted statistically significant in influencing the intensity of fluorescence.

With regard to epithelial thickening, the comparison between absent and grade 4 thickening was statistically significant, with a higher intensity ratio (therefore greater quenching) with maximum thickening. This can be explained by the fact that a high

epithelial thickening removes light from important fluorophores such as collagen and elastin, stimulated by wavelengths such as 400-460 nm. On the other hand, if the excitation wavelength were shorter (UV zone), as described by Brancaleon et al., there would probably be an increase in fluorescence with the increasing of epithelial thickening because tryptophan would be stimulated (Brancaleon, et al., 2001).

The last histopathological variable that resulted statistically significant in influencing the intensity ratio of the lesion was the neovascularization. The presence of neovascularization was associated with a more pronounced hypo-fluorescence compared to the absence.

However, a growing trend was not observed with increasing of degree of neovascularization.

A multivariate analysis model with logistic regression was carried out in which all the analyzed histological variables were inserted together. It emerged that, when considered together, the variables significant in varying the intensity ratio resulted: the presence/absence of fibrosis, the presence/absence of elastosis, the presence of neovascularization of any degree compared to absence and the presence of hyperkeratosis of maximum degree compared to absence.

Systemic and behavioral variables were also included in the regression, but none of these (smoking, diabetes, hypertension, autoimmune diseases and anticoagulant therapy) was significant in influencing the degree of fluorescence of the lesion. A statistically significant correlation emerged between hypertension and elastosis, because 85% of patients had both hypertension and elastosis.

However, this is probably a random correlation due to the fact that in a sample with an average age of 79, hypertension is very common, and elastosis is also present in almost all patients as a result of photo-exposure.

Another consideration regards the phototype of the skin. Previous studies showed that the effectiveness of fluorescence is better with clear phototypes. In particular, Panjehpour et al., in their study demonstrated that BCCs and SCCs were classified

correctly in 93, 89, and 78% of patients with skin types I, II, and III, respectively. Normal tissues were classified correctly in 93, 88, and 50% of patients with skin types I, II, and III, respectively. In the present study the sample resulted extremely homogeneous with a phototype II in almost all cases (95%) and only 5% of patients with phototype III. This is because the incidence of NMSC is more widespread in light phototypes like I and II.

It is important to highlight that all the results of this study were obtained in relation to the fluorescence (photon count) of the lesion compared to healthy skin. Moreover, it is interesting to consider also a qualitative analysis of the spectra in order to evaluate whether, in addition to changes in intensity, there are also shape modifications. To carry out this evaluation, all the spectra were normalized at 500 nm and grouped according to the diagnosis. From a first analysis, in the BCCs group the intensity variation seems to prevail, while no significant shape variation could be appreciated. On the other hand, in SCCs group, in addition to intensity variations, shape modifications are also appreciated.

However, further studies are needed in order to extrapolate the shape variations from spectra in a standardized way.

5.5 Conclusion

The results of the present study suggest that the analysis fluorescence spectra seem to be an extremely effective tool in highlighting NMSCs in a non-invasive, rapid and real-time way.

These characteristics make it a technique potentially suitable for both early diagnosis and intra-operative use for the precise demarcation of surgical margins.

In fact, during surgery the margins of the lesion may not be clinically defined and complex and time-consuming procedures such as extemporaneous freezer examination or Mohs micrographic surgery must be necessary.

However, in order to validate the technique, in vivo studies with large patient cohorts are required.

5.6 Case of nodular BCC

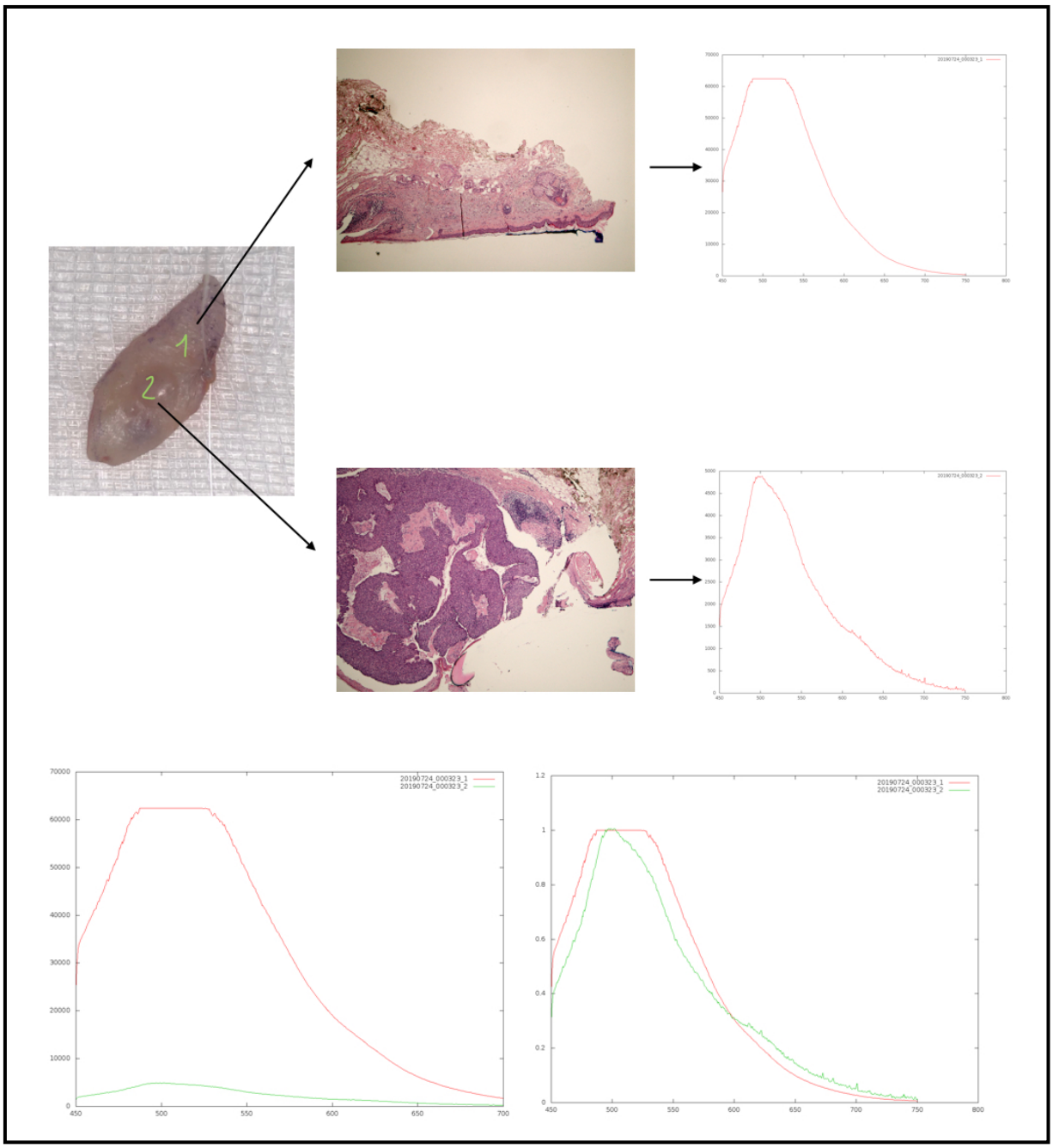

Figure 5.10 Clinical, histological and spectral representation of a case of nodular BCC.

In Figure 5.10 is presented a case of nodular BCC. Point 1 corresponds to an area of clinically healthy skin histologically confirmed. Point 2 corresponds to the central area of the lesion, diagnosed by histological examination as a nodular BCC. The spectra related to points 1 and 2 are shown both in absolute form and in normalized at 500 nm form.

5.7 Case of infiltrating BCC

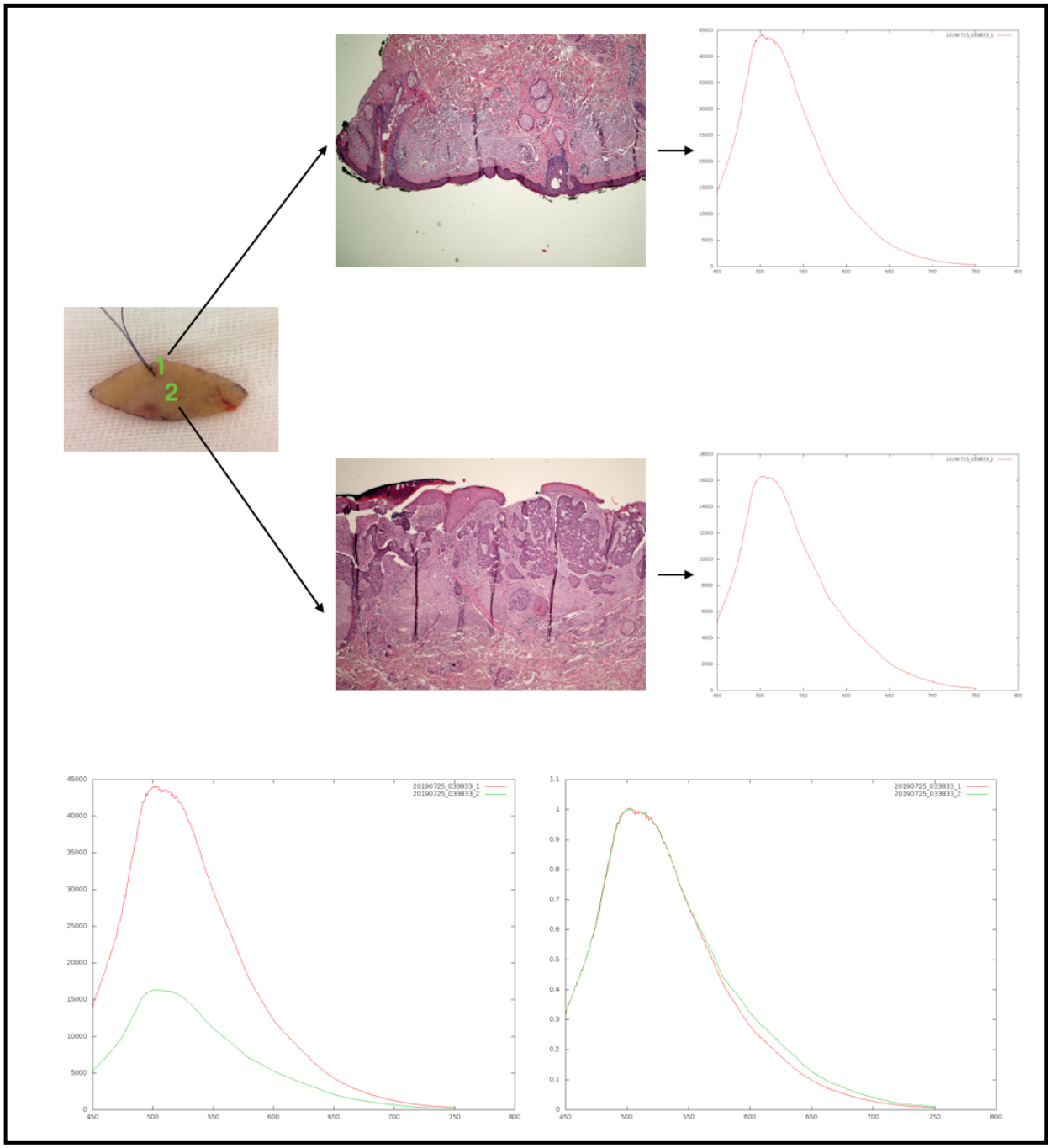

Figure 5.11 Clinical, histological and spectral representation of a case of infiltrating BCC.

In Figure 5.11 is presented a case of infiltrating BCC. Point 1 corresponds to an area of clinically healthy skin histologically confirmed. Point 2 corresponds to the central area of the lesion, diagnosed by histological examination as an infiltrating BCC. The spectra related to points 1 and 2 are shown both in absolute form and in normalized at 500 nm form.

5.8 Case of poorly differentiated SCC

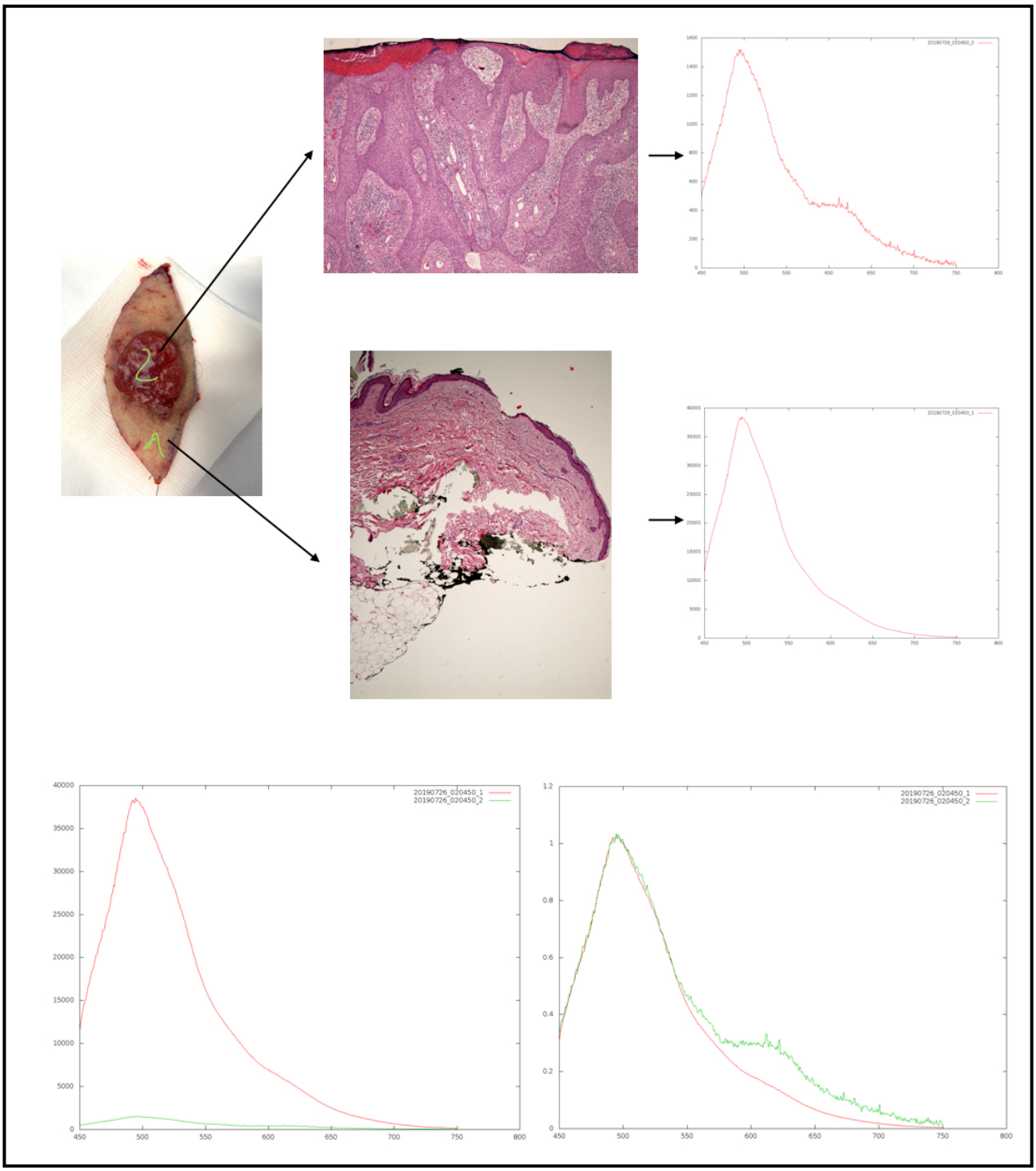

Figure 5.12 Clinical, histological and spectral representation of a case of poorly differentiated SCC.

In Figure 5.12 is presented a case of poorly differentiated SCC. Point 1 corresponds to an area of clinically healthy skin histologically confirmed. Point 2 corresponds to the central area of the lesion, diagnosed by histological examination as a poorly differentiated SCC. The spectra related to points 1 and 2 are shown both in absolute form and in normalized at 500 nm form.

5.9 Case of moderately differentiated SCC

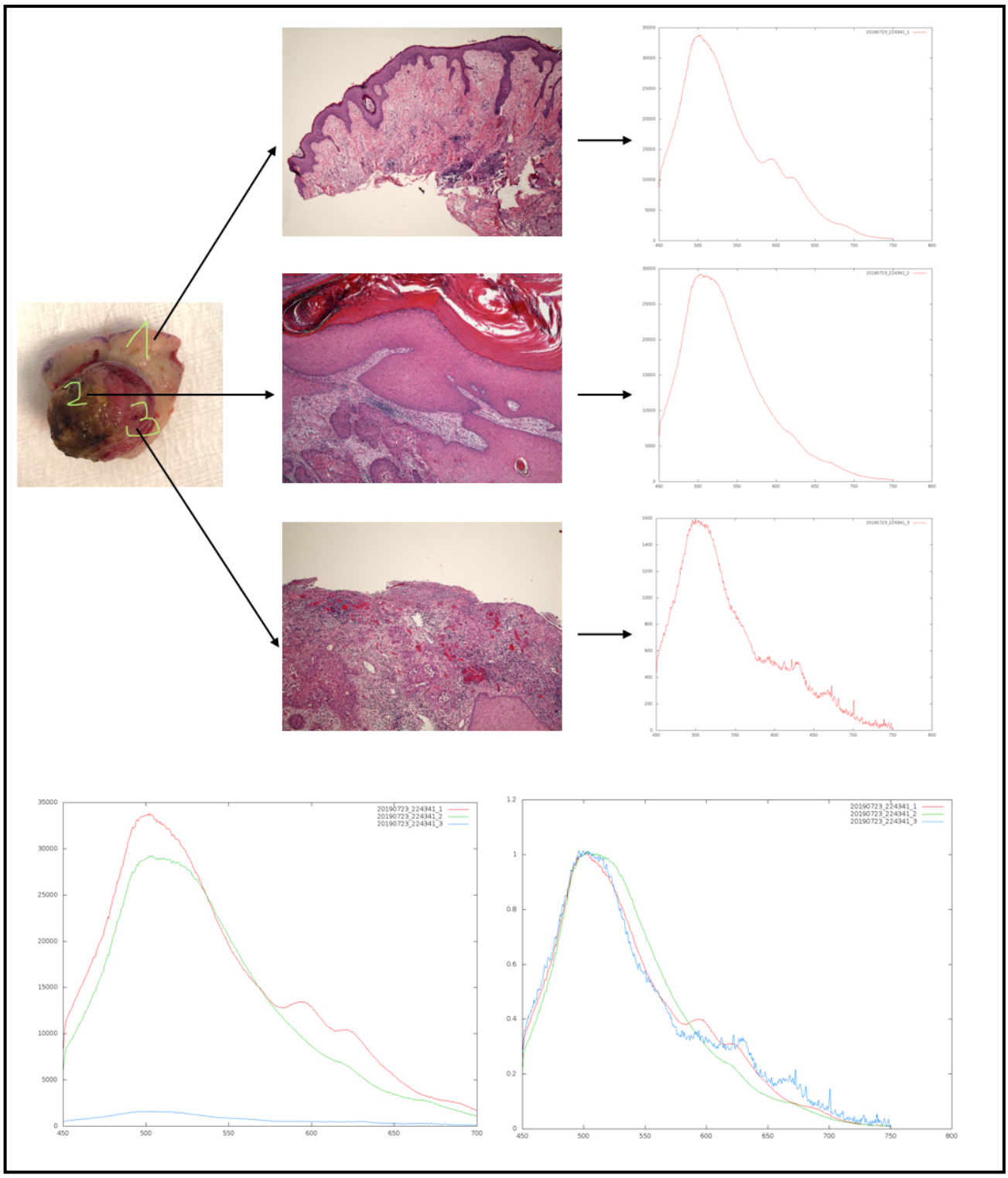

Figure 5.13 Clinical, histological and spectral representation of a case of moderately differentiated SCC.

In Figure 5.13 is presented a case of moderately differentiated SCC. Point 1 corresponds to an area of clinically healthy skin histologically confirmed. Point 2 and 3 correspond to the central area of the lesion, diagnosed by histological examination as a moderately differentiated SCC. In particular, point 2 was measured on the area with the scrub and point 3 on the ulcerated area. The spectra related to points 1, 2 and 3 are shown both in absolute form and in normalized at 500 nm form.

6 Summary and future perspectives

The studies exposed in the previous chapters are the result of a research program that aims to analyse the fluorescence of the oral mucosa and the skin.

The most important evolution of this path was the transition from the qualitative study of fluorescence to the quantitative study of that.

The qualitative studies were carried out with the Velscope system which allows the real-time visualization of the image of the tissues fluorescence. The evaluation is therefore subjective and allows to classify the lesion as normo-fluorescent hypo-fluorescent or hyper-fluorescent in comparison to the surrounding healthy tissues.

In the last study, performed *ex vivo* on the NMSCs, an experimental setup was developed in order to evaluate the tissue fluorescence in a quantitative and objective way.

The quantitative study of fluorescence was organised with an integrated clinical and histopathological approach. In particular, potentially healthy and diseased areas were clinically identified; then quantitative measurement of autofluorescence and histopathological examination were carried out on these in parallel. The statistical analysis highlighted the most important variables capable of influencing the tissue fluorescence and performing a multivariate linear regression, a model of variables which established the histopathological basis of skin fluorescence was identified.

Among the future perspectives, the first objective of this research program will be the quantitative study of fluorescence *in vivo* on malignant and pre-malignant lesions of both the oral mucosa and the skin.

This could lead to a validation of the technique, resulting in the possibility to realize an autofluorescence-guided clinical mapping of the lesions, in the use for early diagnosis and in the intra-operative use for real-time evaluation of cancer margins.

Acknowledgement

Firstly, I would like to express my gratitude to my supervisor, Professor Cristina Magnoni, for all the time she dedicated to me in these years. Every day she instills me a great passion and skills both towards clinical and research activities. She will always be a source of inspiration and admiration for me.

I would also like to thank Professor Marco Meleti, co-tutor of this PhD thesis, for the support that he constantly shows me. He has followed my research activities with extreme dedication and passion from the beginning of my career and I thank him infinitely for everything.

I thank Professor Giuseppe Biagini, coordinator of the doctoral school, for his constant availability and for his support for this research project.

A special thanks goes to Professor Giuseppe Pedrazzi, who carried out the statistical analysis of all the studies exposed in this thesis.

I would like to thank Dr. Annamaria Cesinaro for the collaboration in the histopathological analysis of the *ex vivo* study exposed in chapter 5 of this thesis.

I thank all the team of Pathology and Oral Surgery of the Parma Hospital for their collaboration in carrying out the studies on the oral mucosa.

Last but not the least, I would like to thank my husband and my son Francesco, who was born during these PhD years. They support every day of my life and each of my efforts and sacrifices would not make sense without them.

Bibliography

AIOM. (2018). *I numeri del cancro in Italia.* Brescia: Intermedia Editore.

AIRTUM Working Group, B. S., Mallone, S., Trama, A., Castaing, M., & al., e. (2016). Italian cancer figures--Report 2015: The burden of rare cancers in Italy. *Epidemiol Prev, 40*(Suppl 2), 33-37.

Astner, S., Dietterle, S., Otberg, N., Röwert-Huber, H., Stockfleth, E., & Lademann, J. (2008). Clinical applicability of in vivo fluorescence confocal microscopy for noninvasive diagnosis and therapeutic monitoring of nonmelanoma skin cancer. *Journal of Biomedical Optics, 13*(1), 014003.

Bagri-Manjrekar, K., Chaudhary, M., Sridharan, G., Tekade, S., Gadbail, A., & Khot, K. (2018). n vivo autofluorescence of oral squamous cell carcinoma correlated to cell proliferation rate. *Journal of Cancer Research and Therapeutics, 14*(3), 553-558.

Barnes, D., Aggarwal, S., Thomsen, S., Fitzmaurice, M., & Richards-Kortum, R. (1992). A characterization of the fluorescent properties of circulating human eosinophils. *Photochemistry and Photobiology, 52*, 297-303.

Becquerel, E. (1867). *La Lumière. Ses Causes et ses Effets.* Paris: Firmin Didot.

Bhatia, N., Matias, M., & Farah, C. (2014). Assessment of a decision making protocol to improve the efficacy of VELscopeTM in general dental practice: A prospective evaluation. *Oral Oncology, 50*(10), 1012-9.

Boi, S., Cristofolini, M., Micciolo, R., Polla, E., & Dalla, D. P. (2003). Epidemiology of Skin Tumors: Data from the Cutaneous Cancer Registry in Trentino, Italy. *Journal of Cutaneous Medicine and Surgery*, 300-305.

Brancaleon, L., Durkin, A., Tu, J., Menaker, G., Fallon, J., & & Kollias, N. (2001). In vivo fluorescence spectroscopy of nonmelanoma skin cancer. *Photochemistry and photobiology, 73*(2), 178–183.

Breunig, H., Studier, H., & König, K. (2010). Multiphoton excitation characteristics of cellular fluorophores of human skin in vivo. *Optics Express Journal, 18*(8), 7857- 71.

Brewster, D. (1834). *On the colours of natural bodies* (Vol. 12). Edinburgh: Trans Royal Soc.

Burian, E., Schulz, C., Probst, F., & al., e. (2017). Fluorescence based characterization of early oral squamous cell carcinoma using the Visually Enhanced Light Scope technique. *J Craniomaxillofac Surg, 45*(9), 1526-1530.

Chernomyrdin, N. V., Lesnichaya, A. D., Yakovlev, E. V., Kudrin, K. G., Cherkasova, O. P., Rimskaya, E. N., . . . Zaytsev, K. I. (2019). Differentiation of basal cell carcinoma and healthy skin using multispectral modulation autofluorescence imaging: A pilot study. *Journal of Biomedical Photonics & Engineering*.

Cicciù, M., Herford, A., Cervino, G., Troiano, G., Lauritano, F., & Laino, L. (2017). Tissue Fluorescence Imaging (VELscope) for Quick Non-Invasive Diagnosis in Oral Pathology. *J Craniofac Surg, 28*(2), e112-e115.

Clarke, E. (1819). *Account of a newly discovered variety of green flour spar, of very uncommon beauty and with remarkable properties of colour and phosphorescence* (Vol. 14). Ann Philos.

Cothren, R., Sivak Jr, M., Van Dam, J., Petras, R., Fitzmaurice, M., Crawford, J. & Feld, M. (1996). Detection of dysplasia at colonoscopy using laser-induced fluorescence: a blinded study. *Gastrointestinal endoscopy, 44*(2), 168–176.

Croce, A., & Bottiroli, G. (2014). Autofluorescence spectroscopy and imaging: a tool for biomedical research and diagnosis. *European Journal of Histochemistry, 58*(4), 2461.

Croce, A., Santamaria, G., De Simone, U., Lucchini, F., Freitas, I., & Bottiroli, G. (2011). Naturally-occurring porphyrins in a spontaneous-tumour bearing mouse model. *Photochemical & Photobiological Sciences, 10*(7), 1189-95.

Dessinioti, C., Antoniou, C., & AJ, S. (2011). New targeted approaches for the treatment and prevention of nonmelanoma skin cancer. *Expert review dermatology, 6*(6), 625-634.

Díaz-García, M., & Badía-Laíño, R. (2019). *Encyclopedia of Analytical Science (Third Edition).* Spain: Paul Worsfold, Colin Poole, Alan Townshend, Manuel Miró.

Dimitrow, E., Riemann, I., Ehlers, A., Koehler, M., Norgauer, J., Elsner, P., & al., e. (2009). Spectral fluorescence lifetime detection and selective melanin imaging by mul- tiphoton laser tomography for melanoma diagnosis. *Experimental Dermatology, 18*(6), 509-15.

Dimitrow, E., Ziemer, M., Koehler, M., Norgauer, J., König, K., Elsner, P., & al., e. (2009). Sensitivity and specificity of multiphoton laser tomography for in vivo and ex vivo diagnosis of malignant melanoma. *Journal of Investigative Dermatology, 129*(7), 1752-8.

D'Orazio, J., Jarrett, S., Amaro-Ortiz, A., & Scott, T. (2013). UV Radiation and the Skin. *International Journal of Molecular Sciences, 14*(6), 12222–12248.

Dissanayaka, W., Pitiyage, G., Kumarasiri, P., Liyanage, R., Dias, K., & Tilakaratne, W. (2012). Clinical and histopathologic parameters in survival of oral squamous cell carcinoma. *Oral Surg Oral Med Oral Pathol Oral Radiol, 113*(4), 518-25.

Drakaki, E., Dessinioti, C., Stratigos, A., Salavastru, C., & Antoniou, C. (2014). Laser-induced fluorescence made simple: implications for the diagnosis and follow-up monitoring of basal cell carcinoma. *Journal of Biomedical Optics, 19*(3), 30901.

Drakaki, E., Vergou, T., Dessinioti, C., Stratigos, A. J., Salavastru, C., & Antonioua, C. (2013). Spectroscopic methods for the photodiagnosis of nonmelanoma skin cancer. *Journal of Biomedical Optics*.

Du, G., Li, C., Chen, H., & al., e. (2007). Rose bengal staining in detection of oral precancerous and malignant lesions with colorimetric evaluation: a pilot study. *Int J Cancer, 120*(9), 1958-63.

Edge, S., & Compton, C. (2010). The American Joint Committee on Cancer: the 7th edition of the AJCC cancer staging manual and the future of TNM. *Ann Surg Oncol, 17*(6), 1471-4.

Elashoff, D., Zhou, H., Reiss, J., & al., e. (2012). Prevalidation of salivary biomarkers for oral cancer detection. *Cancer Epidemiol Biomarkers Prev, 21*(4), 664-72.

Eny, K., Orchard, T., Miller, R., Maynard, J., Grant, D., Costacou, T., . . . Group, D. R. (2015). Caffeine Consumption Contributes to Skin Intrinsic Fluorescence in Type 1 Diabetes. *Diabetes Technology & Therapeutics, 17*(10), 726-34.

Epstein, J., Silverman, S. J., Epstein, J., Lonky, S., & Bride, M. (2008). Analysis of oral lesion biopsies identi ed and evaluated by visual examination, chemiluminescence and toluidine blue. *Oral Oncology, 44*(6), 538-44.

Ericson, M., Simonsson, C., Guldbrand, S., Ljungblad, C., Paoli, J., & Smedh, M. (2008). Two-photon laser-scanning fluorescence microscopy applied for studies of human skin. *Journal of Biophotonics, 1*(4), 320-30.

Farah, C., Dost, F., & Do, L. (2019). Usefulness of optical fluorescence imaging in identification and triaging of oral potentially malignant disorders: A study of VELscope in the LESIONS programme. *J Oral Pathol Med, 48*(7), 581-587.

Farah, C., McIntosh, L., Georgiou, A., & McCullough, M. (2012). Efficacy of tissue autofluorescence imaging (VELScope) in the visualization of oral mucosal lesions. *Head Neck, 34*(6), 856-62.

Gào, X., & Schöttker, B. (2017). Reduction–oxidation pathways involved in cancer development: a systematic review of literature reviews. *Oncotarget, 8*(31), 51888– 51906.

Ganga, R., Gundre, D., Bansal, S., Shirsat, P., Prasad, P., & Desai, R. (2017). Evaluation of the diagnostic efficacy and spectrum of autofluorescence of benign, dysplastic and malignant lesions of the oral cavity using VELscope. *Oral Oncology, 75*, 67-74.

Gillies, R., Zonios, G., Anderson, R., & Kollias, N. (2000). Fluorescence excitation spectroscopy provides information about human skin in vivo. *Journal of Investigative Dermatology, 115*(4), 704-7.

Giovannacci, I., Magnoni, C., Vescovi, P., Painelli, A., Tarentini, E., & Meleti, M. (2019). Which are the main fluorophores in skin and oral mucosa? A review with emphasis on clinical applications of tissue autofluorescence. *Archivies of Oral Biology, 105*, 89-98.

Giovannacci, I., Meleti, M., Merigo, E., & al., e. (2015). Erratum to: Advantages of new technologies in oral mucosal surgery: an intraoperative comparison among Nd:YAG laser, quantic molecular resonance scalpel, and cold blade. *Lasers Med Sci, 30*(7), 1911.

Giovannacci, I., Vescovi, P., Manfredi, M., & Meleti, M. (2016). Non-invasive visual tools for diagnosis of oral cancer and dysplasia: A systematic review. *Medicina Oral, Patología Oral y Cirugía Bucal, 21*(3), e305-15.

Grossi, C., & Zaccheo, D. (1963). Sulla fluorescenza delle granulazioni specifiche dei leucociti eosinofili. *Bollettino Società Italiana Biologia Sperimentale, 39*, 421-3.

Gupta, B., & Johnson, N. (2014). Emerging and established global life-style risk factors for cancer of the upper aero-digestive tract. *Asian Pac J Cancer Prev, 15*(15), 5983-91.

Gurushankar, K., Nazeer, S., Jayasree, R., & Krishnakumar, N. (2015). Evaluation of Antitumor Activity of Hesperetin-Loaded Nanoparticles Against DMBA-Induced Oral Carcinogenesis Based on Tissue Autofluorescence Spectroscopy and Multi- variate Analysis. *Journal of Fluorescence, 25*(4), 931-9.

He, Q., & al, e. (2007). Microscopic fluorescence spectral analysis of basal cell carcinomas. *Proc. SPIE*(6534), 653414.

Herschel, J. (1845). *On a Case of Superficial Colour Presented by a Homogeneous Liquid Internally Colourless* (Vol. 135). London: Philos. Trans.

Ho, P., Wang, W., Huang, Y., & Yang, Y. (2019). Finding an oral potentially malignant disorder in screening program is related to early diagnosis of oral cavity cancer - Experience from real world evidence. *Oral Oncology, 89*, 107–14.

Hoffmann, K., Stucker, M., Altmeyer, P., Teuchner, K., & Leupold, D. (2001). Selective femtosecond pulse-excitation of melanin fluorescence in tissue. *Journal of Inves- tigative Dermatology, 116*, 629–630.

Holmstrup, P., Vedtofte, P., Reibel, J., & Stoltze, K. (2006). Long-term treatment outcome of oral premalignant lesions. *Oral Oncology, 42*, 461-474.

Huang, T., Huang, J., Wang, Y., Chen, K., Wong, T., Chen, Y., & al, e. (2017). Novel quantitative analysis of autofluorescence images for oral cancer screening. *Oral Oncology, 68*, 20-26.

Inaguma, M., & Hashimoto, K. (1999). Porphyrin-like fluorescence in oral cancer: In vivo fluorescence spectral characterization of lesions by use of a near-ultraviolet excited autofluorescence diagnosis system and separation of fluorescent extracts by capillary electrophoresis. *Cancer, 86*(11), 2201-11.

Jayanthi, J., Mallia, R., Shiny, S., Baiju, K., Mathews, A., Kumar, R., & al., e. (2009). Discriminant analysis of autofluorescence spectra for classification of oral lesions in vivo. *Lasers in Surgery and Medicine, 41*(5), 345-52.

Jayanthi, J., Subhash, N., Stephen, M., Philip, E., & Beena, V. (2011). Comparative evaluation of the diagnostic performance of autofluorescence and diffuse reflectance in oral cancer detection: a clinical study. *Journal of Biophotonics, 4*(10), 696- 706.

Karia, P., Han, J., & Schmults, C. (2013, June). Cutaneous squamous cell carcinoma: Estimated incidence of disease, nodal metastasis, and deaths from disease in the United States. *Journal of the American Academy of Dermatology, 68*(6), 957-966.

Kikuta, S., Iwanaga, J., Todoroki, K., & al., e. (2018). Clinical Application of the IllumiScan Fluorescence Visualization Device in Detecting Oral Mucosal Lesions. *Cureus, 10*(8), e3111.

Kim, D. P., Kus, K. J., & Ruiz, E. (2019). Basal Cell Carcinoma Review. *Hematology/Oncology Clinics of North America* , 13-24 .

Koenig, K., & Riemann, I. (2003). High-resolution multiphoton tomography of human skin with subcellular spatial resolution and picosecond time resolution. *Journal of Biomedical Optics, 8*, 432–439.

Krasieva, T., Stringari, C., Liu, F., Sun, C., Kong, Y., Balu, M., & al., e. (2013). Two-photon excited fluorescence lifetime imaging and spectroscopy of melanins in vitro and in vivo. *Journal of Biomedical Opticst, 18*(3), 31107.

Kunz, W. (1986). Spectral properties of fluorescent flavoproteins of isolated rat liver mitochondria. *FEBS Letters, 195*, 92-6.

Kunz, W., & Kunz, W. (1985). Contribution of different enzymes to flavoproteins fluorescence of isolated rat liver mitochondria. *Biochimica et Biophysica Acta, 841*, 237-46.

Lai, V., Cranwell, W., & Sinclair, R. (2018). Epidemiology of skin cancer in the mature patient. *Clinics in Dermatology*, 167–176.

Laiho, L., Pelet, S., Hancewicz, T., Kaplan, P., & So, P. (2005). Two-photon 3-D mapping of ex vivo human skin endogenous fluorescence species based on fluorescence emission spectra. *Journal of Biomedical Opticst, 10*(2), 024016.

Lakowicz, J. (1999). *Principles Of Fluorescence Spectroscopy.* New York: Kluwer Academic/Plenum.

Lam, S. M. (1993). Detection of dysplasia and carcinoma in situ with a lung imaging fluorescence endoscope device. *The Journal of thoracic and cardiovascular surgery, 105*(6), 1035–1040.

Lane, P., Gilhuly, T., Whitehead, P., Zeng, H., Poh, C., Ng, S., & al., e. (2006). Simple device for the direct visualization of oral-cavity tissue fluorescence. *Journal of Bi- omedical Opticst, 11*(2), 024006.

Leunig, A., Betz, C., Mehlmann, M., & al., e. (2000). Detection of squamous cell carcinoma of the oral cavity by imaging 5-aminolevulinic acid-induced protoporphyrin IX fluorescence. *Laryngoscope, 110*(1), 78-83.

Leupold, D., Scholz, M., Stankovic, G., Reda, J., Buder, S., Eichhorn, R., & al., e. (2011). The stepwise two-photon excited melanin fluorescence is a unique diagnostic tool for the detection of malignant transformation in melanocytes. *Pigment Cell & Melanoma Research, 24*(3), 438-45.

Lohmann, W., Mussmann, J., Lohmann, C., & al, e. (1989). Native fluorescence of the cervix uteri as a marker for dysplasia and invasive carcinoma. *Eur J Obstet Gynecol Reprod Biol, 31*(3), 249-53.

Lomas, A., Leonardi-Bee, J., & Bath-Hextall, F. (2012). A systematic review of worldwide incidence of nonmelanoma skin cancer. *Br J Dermatol*, 1069-1080.

Mallia, R., Thomas, S., Mathews, A., Kumar, R., Sebastian, P., Madhavan, J., & al., e. (2008). Laser-induced autofluorescence spectral ratio reference standard for early discrimination of oral cancer. *Cancer, 112*, 1503-1512.

Marzuka, A. G., & Book, S. E. (2015). Basal Cell Carcinoma: Pathogenesis, Epidemiology, Clinical Features, Diagnosis, Histopathology, and Management. *YALE JOURNAL OF BIOLOGY AND MEDICINE*, 167-179.

Mascitti, M., Orsini, G., Tosco, V., Monterubbianesi, R., Balercia, A., Putignano, A., & al., e. (2018). An overview on current non-invasive diagnostic devices in oral oncology. *Front Physiol, 9*, 1510.

Mayeno, A., Hamann, K., & Gleich, G. (1992). Granule-associated flavin adenine dinucleotide (FAD) is responsible for eosinophil autofluorescence. *Journal of Leukocyte Biology, 51*, 172-5.

McCusker, M., Basset-Seguin, N., R., D., K., L., D., S., A., S., & al., e. (2014). Metastatic basal cell carcinoma: prognosis dependent on anatomic site and spread of disease. *Eur J Cancer*, 774-783.

McMullen, R., Chen, S., & Moore, D. (2012). Spectrofluorescence of skin and hair. *International Journal of Cosmetic Science, 34*(3), 246-56.

Meleti, M., Giovannacci, I., Vescovi, P., Pedrazzi, G., Govoni, P., & Magnoni, C. (2020). Histopathological determinants of autofluorescence patterns in oral carcinoma. *Oral Disease*, 10.1111/odi.13304. Advance online publication. .

Midgen, M. R., Chang, A. L., Dirix, L., & al., e. (2018). Emerging trends in the treatment of advanced basal cell carcinoma. *Cancer Treatment Reviews*, 1-10.

Miyamoto, K., & Kudoh, H. (2013). Quantification and visualization of cellular NAD(P)H in young and aged female facial skin with in vivo two-photon tomography. *British Journal of Dermatology, 169*(Suppl 2), 25-31.

Moher, D., Liberati, A., Tetzlaff, J., & Altman, D. (2009). Preferred reporting items for systematic reviews and meta-analyses: the PRISMA State- ment. *PLoS Medicine*.

Monici, M. (2005). Cell and tissue autofluorescence research and diagnostic applications. *Biotechnology Annual Review, 11*, 227-56.

Morikawa, T., Kosugi, A., & Shibahara, T. (2019). The Utility of Optical Instrument "ORALOOK®" in the Early Detection of High-risk Oral Mucosal Lesions. *Anticancer Research, 39*(5), 2519-2525.

Na, R., Stender, I., Henriksen, M., & Wulf, H. (2011). Autofluorescence of human skin is age-related after correction for skin pigmentation and redness. *Journal of Investigative Dermatology, 116*(4), 536-40.

Nazeer, S., Asish, R., Venugopal, C., Anita, B., & Gupta, A. (2014). Noninvasive as- sessment of the risk of tobacco abuse in oral mucosa using fluorescence spec- troscopy: a clinical approach. *Journal of Biomedical Opticst, 19*(5), 057013.

Pallagatti, S., Sheikh, S., Aggarwal, A., & al, e. (2013). Toluidine blue staining as an adjunctive tool for early diagnosis of dysplastic changes in the oral mucosa. *J Clin Exp Dent, 5*(4), e187-91.

Pandeya, N., Olsen, C., & Whiteman, D. (2017, Oct 16). The incidence and multiplicity rates of keratinocyte cancers in Australia. *Med Journal, 207*(8), 339-43.

Panjehpour, M., Julius, C., Phan, M., Vo-Dinh, T., & & Overholt, S. (2002). Laser-induced fluorescence spectroscopy for in vivo diagnosis of non-melanoma skin cancers. *Lasers in surgery and medicine, 31*(5), 367–373.

Panjehpour, M., Overholt, B., Schmidhammer, J., Farris, C., Buckley, P., & & Vo-Dinh, T. (1995). Spectroscopic diagnosis of esophageal cancer: new classification model, improved measurement system. *Gastrointestinal endoscopy, 41*(6), 577–581.

Paolino, G., Donati, M., Didona, D., Mercuri, S., & Cantisani, C. (2017, Dec 20). Histology of Non-Melanoma Skin Cancers: An Update. *Biomedicines, 5*(71).

Patalay, R., Talbot, C., Alexandrov, Y., Munro I, N. M., König, K., & al., e. (2011). Quan- tification of cellular autofluorescence of human skin using multiphoton tomography and fluorescence lifetime imaging in two spectral detection channels. *Biomedical Optics Express Journal, 2*(12), 3295-308.

Patil, S., Arakeri, G., Alamir, A., & al., e. (2019). Role of salivary transcriptomics as potential biomarkers in oral cancer: a systematic review. *J Oral Pathol Med*, [Epub ahead of print].

Penzer, G. (1980). Molecular emission spectroscopy (Fluorescence and Phos- phorescence). In An Introduction to spectroscopy for biochemists. *Academic Press, London*, 70-114.

Peris, K., Alaibac, M., Argenziano, G., Di Stefani, A., Fargnoli, M., Frascione, P., Calzavara Pinton, P. (2018, Jun). Cutaneous Squamous Cell Carcinoma - Italian Guidelines by SIDeMaST adapted to and updating EADO/EDF/EORTC guidelines. *Giornale Italiano di Dermatologia e Venereologia*.

Peris, K., Fargnoli, M., C, G., & al, e. (2019). Diagnosis and treatment of basal cell carcinoma: European consensusebased interdisciplinary guidelines. *European Journal of Cancer*, 10-34.

Perrin, F. (1929). *La fluorescence des solutions* (Vol. 12). Paris: Ann . Phys.

Petruzzi, M., Lucchese, A., Nardi, G., & al., e. (2014). Evaluation of auto fluorescence and toluidine blue in the differentiation of oral dysplastic and neoplastic lesions from non dysplastic and neoplastic lesions: a cross-sectional study. *J Biomed Opt, 19*(7), 76003.

Poh, C., Zhang, L., Anderson, D., & al., e. (2006). Fluorescence visualization detection of field alterations in tumor margins of oral cancer patients. *Clinical Cancer Research, 12*(22), 6716-22.

Que, S. K., Zwald, F. O., & Schmults, C. D. (2018, Feb). Cutaneous squamous cell carcinoma. *Journal of the Academy of Dermatology, 78*(2), 237-247.

Ramanujam, N., Mitchell, M., Mahadevan-Jansen, A., Thomsen, S., Staerkel, G., Malpica, A. & Richards-Kortum, R. (1996). Cervical precancer detection using a multivariate statistical algorithm based on laser-induced fluorescence spectra at multiple excitation wavelengths. *Photochemistry and photobiology, 64*(4), 720–735.

Rana, M., Zapf, A., Kuehle, M., Gellrich, N., & Eckardt, A. (2012). Clinical evaluation of an autofluorescence diagnostic device for oral cancer detection: A prospective randomized diagnostic study. *Eur J Cancer Prev, 21*(5), 460-6.

Rashid, A., & Warnakulasuriya, S. (2015). The use of light-based (optical) detection systems as adjuncts in the detection of oral cancer and oral potentially malignant disorders: a systematic review. *J Oral Pathol Med, 44*(5), 307-328.

Reiter, O., Mimouni, I., Gdalevich, M., Marghoob, A., Levi, A., Hodak, E., & al., e. (2018). The diagnostic accuracy of dermoscopy for basal cell carcinoma: a systematic review and meta-analysis. *Journal of the American Academy of Dermatology*, 1380-88.

Richards-Kortum, R., & Sevick-Muraca, E. (1996). Quantitative optical spectroscopy for tissue diagnosis. *Annu Rev Phys Chem, 47*, 555-606.

Richter, C., Trojahn, C., Dobos, G., Blume-Peytavi, U., & Kottner, J. (2016). Follicular fluorescence quantity to characterize acne severity: a validation study. *Skin Research and Technology, 22*(4), 451-459.

Rivera, C., & Venegas, B. (2014). Histological and molecular aspects of oral squamous cell carcinoma (Review). *Oncology Letter, 8*(1), 7-11.

Salmon, J., Kohen, E., Viallet, P., Hirschberg, J., Wouters, A., & Kohen, C. (1982). Microspectrofluorometric approach to the study of free/bound NAD(P)H ratio as metabolic indicator in various cell types. *Photochemistry and Photobiology, 36*, 585-93.

Samarasinghe, V., & Madan, V. (2012). Nonmelanoma skin cancer. *Journal of cutaneous and aesthetic surgery, 5*(1), 3-10.

Sandby-Møller, J., Thieden, E., Philipsen, P., Heydenreich, J., & Wulf, H. (2004). Skin autofluorescence as a biological UVR dosimeter. *Photodermatology, Photoimmunology & Photomedicine, 20*(1), 33-40.

Saxena, S., Sankhla, B., Sundaragiri, K., & Bhargava, A. (2017). A Review of Salivary Biomarker: A Tool for Early Oral Cancer Diagnosis. *Adv Biomed Res, 28*, 6:90.

Schantz, S., Savage, H., Sacks, P., & Alfano, R. (1997). Native cellular fluorescence and its application to cancer prevention. *Environmental Health Perspectives, 105 Suppl 4*, 941-4.

Sciubba, J. (2001). Oral cancer. The importance of early diagnosis and treatment. *Am J Clin Dermatol, 2*, 239-51.

Seidenari, S., Arginelli, F., Bassoli, S., Cautela, J., French, P., & Guanti, M. (2012). Multiphoton laser microscopy and fluorescence life-time imaging for the evaluation of the skin. *Dermatology Research and Practice*(2012), 810749.

Shi, L., Li, C., Shen, X., Zhou, Z., Liu, W., & Tang, G. (2019). Potential role of autofluorescence imaging in determining biopsy of oral potentially malignant disorders: A large prospective diagnostic study. *Oral Oncology, 98*, 176-179.

Simon, J., Peles, D., Wakamatsu, K., & Ito, S. (2009). Currentchallengesinunderstanding melanogenesis: bridging chemistry, biological control, morphology, and function. *Pigment Cell & Melanoma Research, 22*(5), 563-79.

Skala, M., Riching, K., Bird, D., Fitzpatrick, A., Eickhoff, J., Eliceiri, K., Ramanujam, N. (2007). In vivo multiphoton fluorescence lifetime imaging of protein-bound and free nicotinamide adenine dinucleotide in normal and precancerous epithelia. *Journal of Biomedical Opticst, 12*, 024014.

Speight, P., Khurram, S., & Kujan, O. (2018). Oral potentially malignant disorders: risk of progression to malignancy. *Oral Surg Oral Med Oral Pathol Oral Radiol, 125*(6), 612–27.

Stirban, A., Nandrean, S., Negrean, M., Koschinsky, T., & Tschoepe, D. (2008). Skin autofluorescence increases postprandially in human subjects. *Diabetes Technology & Therapeutics, 10*(3), 200-5.

Stokes, G. (1852). *On the change of refrangibility of light* (Vol. 142). Lond: Philos Trans R Soc.

Teuchner K, F. W., Volkmer, A., Birch, D., Altmeyer, P., & al., e. (1999). Femtosecond two-photon excited fluorescence of melanin. *Photochemistry and Photobiology, 70*, 146–151.

Tiwari, L., Kujan, O., & Farah, C. (2019). Optical fluorescence imaging in oral cancer and potentially malignant disorders: A systematic review. *Oral Disease*, 10.1111/odi.13071. Advance online publication. .

Troeltzsch, M., Knösel, T., Eichinger, C., & al, e. (2014). Clinicopathologic features of oral squamous cell carcinoma: do they vary in different age groups? *J Oral Maxillofac Surg, 72*(7), 1291-300.

Valeur, B., & Berberan-Santos, M. (2011). A Brief History of Fluorescence and Phosphorescence before the Emergence of Quantum Theory. *Journal of Chemical Education, 88*(6), 731-738.

Vedeswari, C., Jayachandran, S., & Ganesan, S. (2009). In vivo autofluorescence characteristics of pre- and post-treated oral submucous fibrosis: a pilot study. *Indian Journal of Dental Research, 20*(3), 261-7.

Waldman, A., & Schmults, C. (2019). Cutaneous Squamous Cell Carcinoma. *Hematology/Oncology Clinics of North America, 33*(1), 1-12.

Warnakulasuriya, S. (2009). Causes of oral cancer - an appraisal of controversies. *British Dental Journal, 207*(10), 471-5.

Warnakulasuriya, S., & Ariyawardana, A. (2016). Malignant transformation of oral leukoplakia: a systematic review of observational studies. *J Oral Pathol Med, 45*, 155-166.

Warnakulasuriya, S., Reibel, J., Bouquot, J., & Dabelsteen, E. (2008). Oral epithelial dysplasia classification systems: predictive value, utility, weaknesses and scope for improvement. *J Oral Pathol Med, 3*, 127-133.

Wild, C., Weiderpass, E., & Stewart, B. (2020). *World Cancer Report: Cancer Research for Cancer Prevention (IARC, WHO).* Lyon.

Wolfbeiss, O. (1985). *The fluorescence of organic natural products. In:Schulman GS (ed) Molecular luminescence spectrometry: methods and applications — part 1.* New York,: Wiley.

Yamamoto, N., Kawaguchi, K., Fujihara, H., Hasebe, M., Kishi, Y., Yasukawa, M., & al, e. (2017). Detection accuracy for epithelial dysplasia using an objective autofluorescence visualization method based on the luminance ratio. *Int J Oral Sci, 10*(9), e2.

Yaroslavsky, A., Neel, V., & Anderson, R. (2004). Fluorescencepolarizationimaging for delineating nonmelanoma skin cancers. *Optics Letters, 29*(17), 2010-2.

Yu, Y., Lee, A., Wang, H., Tang, S., Zhao, J., Lui, H., & al., e. (2012). Imaging-guided two- photon excitation-emission-matrix measurements of human skin tissues. *Journal of Biomedical Opticst, 17*(7), 077004.

Zeng, H., MacAulay, C., McLean, D., & Palcic, B. (1995). Spectroscopic and microscopic characteristics of human skin autofluorescence emission. *Photochemistry and Photobiology, 61*, 39–645.

Zeng, H., McLean, D., MacAulay, C., Palcic, B., & Lui, H. (1998). Autofluorescence of basal cell carcinoma. *Proc. SPIE*(3245), 314–317.

Zhao, H., Chen, Y., Zhao, H., Tan, Z., Zhang, C., Fu, X., & al., e. (2016). Autofluorescence of eccrine sweat glands. *Skin Research and Technology, 22*(1), 98-103.